Macroscale Hydrological Modelling and Impact of landcover change on streamflows of the Mahanadi River Basin

Thesis submitted to Andhra University
in partial fulfillment of the requirements for the award of

Master of Technology in Remote Sensing and Geographical Information System

ANDHRA UNIVERSITY

By

Nidhi Mishra

Supervised By

Dr. S. P. Aggarwal
Scientist/Engineer"SE",
Water Resources Division,
IIRS, Dehradun

Dr. V. K. Dadhwal
Dean, IIRS
Dehradun

iirs

Indian Institute of Remote Sensing
(National Remote Sensing Agency)
Dept. of Space, Govt. of India,
(March, 2008)

Dedicated

To my Parents

CERTIFICATE

This is to certify that **Ms. Nidhi Mishra** has carried out the dissertation entitled "Macroscale Hydrological Modelling and Impact of landcover change on Streamflow of the Mahanadi River Basin**"** for the partial fulfillment of the requirement of M.Tech in **'Remote Sensing and Geographical Information System'**. This work has been carried out at Water Resources Division, Indian Institute of Remote Sensing, Dehradun, India.

Dr. V. Hari Prasad
In-charge, WRD
Scientist/Engineer 'SF'

Dr. S.P. Aggarwal
Project Supervisor
Scientist/Engineer 'SE'

Dr. V.K. Dadhwal
Dean, IIRS

ACKNOWLEDGEMENT

First of all, I express my sincere gratitude to Dr. V.K. Dadhwal, Dean IIRS, Dehradun for providing me the opportunity to join this course at IIRS. I also acknowledge him for providing timely suggestions, critical evaluation and encouragement as a supervisor without which the work would not have been carried out successfully. I acknowledge Andhra University for evaluating our work and awarding the M. Tech. degree.

I express my deep sense of gratitude to Dr. S.P. Aggarwal, Scientist/ Engr. 'SE', Water Resources Division, IIRS, for his constant guidance, impeccable advises and all possible help that enabled me to bring this research work to a successful completion.

I extend my sincere and heartfelt thanks to Dr. V. Hari prasad, Incharge, Water Resources Division, Er. Praveen Thakur, Scientist 'SC', Er. Ashutosh Bhardwaj Scientist 'SD', Dr. A. K. Mishra 'M. Tech. course coordinator', IIRS Dehradun for their constant help and support throughout the studies.

I express my gratitude to Ms. Neha Goyal for helping me in the programming part. I extend my sincere thanks to Mr. Shraddhanand Shukla from University of Washington for providing valuable and timely help which was vital for my work. During my project work I had been greatly supported and helped by my friends, Mrs. Anshu Gupta, Ms. Vidya. A, Smita, Ambika, Rupinder, Deepthi, Pranav, Saurabh, Aditi, Nihar, Hrushikesh. I thank them for their immense cooperation and support to deal with the work pressures. I thank the IIRS staff Mr. M. L. Batra, Mr. Kailash, Mr. Paramjeet and Mr. Bhaskar.

I owe a lot to my parents Shri O. P. Mishra and Smt. Manoj Kiran Mishra, younger brother and sister for their constant encouragement enabling me to achieve this goal. I express my deep love for the Institute in which I have carried out my work and record my gratefulness to all the faculties who imparted me each and every bit of their valuable knowledge.

Date: 25/04/08 (Nidhi Mishra)

ABSTRACT

The Mahanadi river, rising in the state of Chattisgarh is an important river specially in the state of Orissa. Upstream of the basin (Chattisgarh plain) experiences periodic droughts in contrast with the regular flood events in downstream (delta region of Orrisa). Frequent occurrence of these events indicates a shift in the hydrological response of the basin attributed to anthropogenic activities causing significant landcover changes. The landcover mapping of Mahanadi basin was attempted using remotely sensed images of LANDSAT MSS for 1972, NOAA AVHRR for 1985, and AWiFs for 2003. Analysis of the landcover changes revealed that the total forest cover area has been reduced by 5.71% from 1972 to 2003. A reduction in barren land (0.64%) is followed by an increase in areas of surface water bodies (0.47%), built up land (0.22%), river bed (0.11%) and most prominently agriculture (5.55%). Major changes were from forest and barren land to agriculture, built up and water bodies.

A physically based distributed Variable Infiltration Capacity hydrological model was used to simulate the hydrology of Mahanadi river basin and analysis were carried out of the impact of landcover changes on streamflow pattern. The meteorological forcing, vegetation parameters and soil parameters were derived using remote sensing based products and other ancillary information. VIC model performance was found good and a close agreement between the observed and simulated values was obtained with the Nash-Sutcliffe coefficient of 0.821 and relative error of 0.085 at the main Mundali outlet. Model performance was also found good for Kantamal, Simga and Sundergarh sub-basins.

Streamflows were simulated for year 1972, 1985 and 2003 to look for the changes that have taken place due to change in landcover. Only the vegetation related parameters were changed during simulation, forcing was kept same to remove the effects of climate change. An increase by 4.53% (3514.2 million cubic meters) in the annual streamflow is predicted at Mundali outlet of the Mahanadi basin from 1972 to 2003. It may be concluded that a decrease in forest cover by 5.71% in the Mahanadi river basin has caused the river flow to increase by 4.53%. Kantamal sub-basin characterized by dense moist deciduous forest and intensive irrigated agriculture, has seen a rise by 4.54% where a significant forest cover in the upstream sub-basin was lost for cultivation. A rise in flow by 3.06% and 3.47% was observed in Baminidihi and Sundergarh sub-basins. The relative percentage increase in streamflows was found high in the months of May and November in all sub-basins.

CONTENTS

LIST OF TABLES

LIST OF FIGURES

CHAPTER 1 - INTRODUCTION

1.1 **Background**

Water influences every sphere of the environment supporting life on earth. Its varying availability in time and space is a matter of concern to the mankind since fresh water is not a ubiquitous resource. Its assessment, monitoring and management thus become important for judicious use. Water resources management requires a systems approach that includes not only all of the hydrological components, but also the links, relations, interactions, consequences, and implications among these components. Human modifications of the environment, including land cover change, irrigation, and flow regulation, now occur on scales that significantly affect seasonal and yearly hydrologic variations. A thorough knowledge and understanding of the different hydrological phenomena and hydrological cycle as a whole is required in studying the implications of these changes.

1.2 **Hydrological cycle and its Importance**

The Earth system may be subdivided into two subsystems—the physical climate system and biogeochemical cycles—that are linked by the global hydrologic cycle as shown in figure 1.1 (Asrar and Dozier, 1994). The physical climate subsystem is sensitive to fluctuations in the Earth's radiation balance. Human activities have caused changes to the planet's radiative heating mechanism that exceed natural change. The Earth's biogeochemical cycles have also been changed by man. Atmospheric carbon dioxide has increased by 30% since 1859, methane by more than 100%. The hydrologic cycle links the physical climate and biogeochemical cycles. The phase change of water between its gaseous, liquid and solid states involves storage and release of latent heat, so it influences atmospheric circulation and globally redistributes both water and heat (Asrar and Dozier, 1994). The hydrologic cycle is the integrating process for the fluxes of water, energy, and chemical elements among components of the Earth system. Significant changes in the external forcing functions and human activities can have a dramatic impact on the physical climate system, biogeochemical cycles, and the global hydrologic cycle. Examination of these subsystems and their linkages defines the critical questions that the remote sensing based Earth Observing Systems and Global Circulation Models are attempting to answer.

Apart from role that water plays in the Earth's ecosystem and cycles, at the land surface it is a vital resource for human needs. Society's growing water resource needs include hazard mitigation (floods, droughts, and landslides), agriculture and food production, human health, municipal and industrial supply, environmental quality, and sustainable development in a changing global environment. It thus becomes necessary to understand

and quantify various hydrological components of the catchment for efficient resource management.

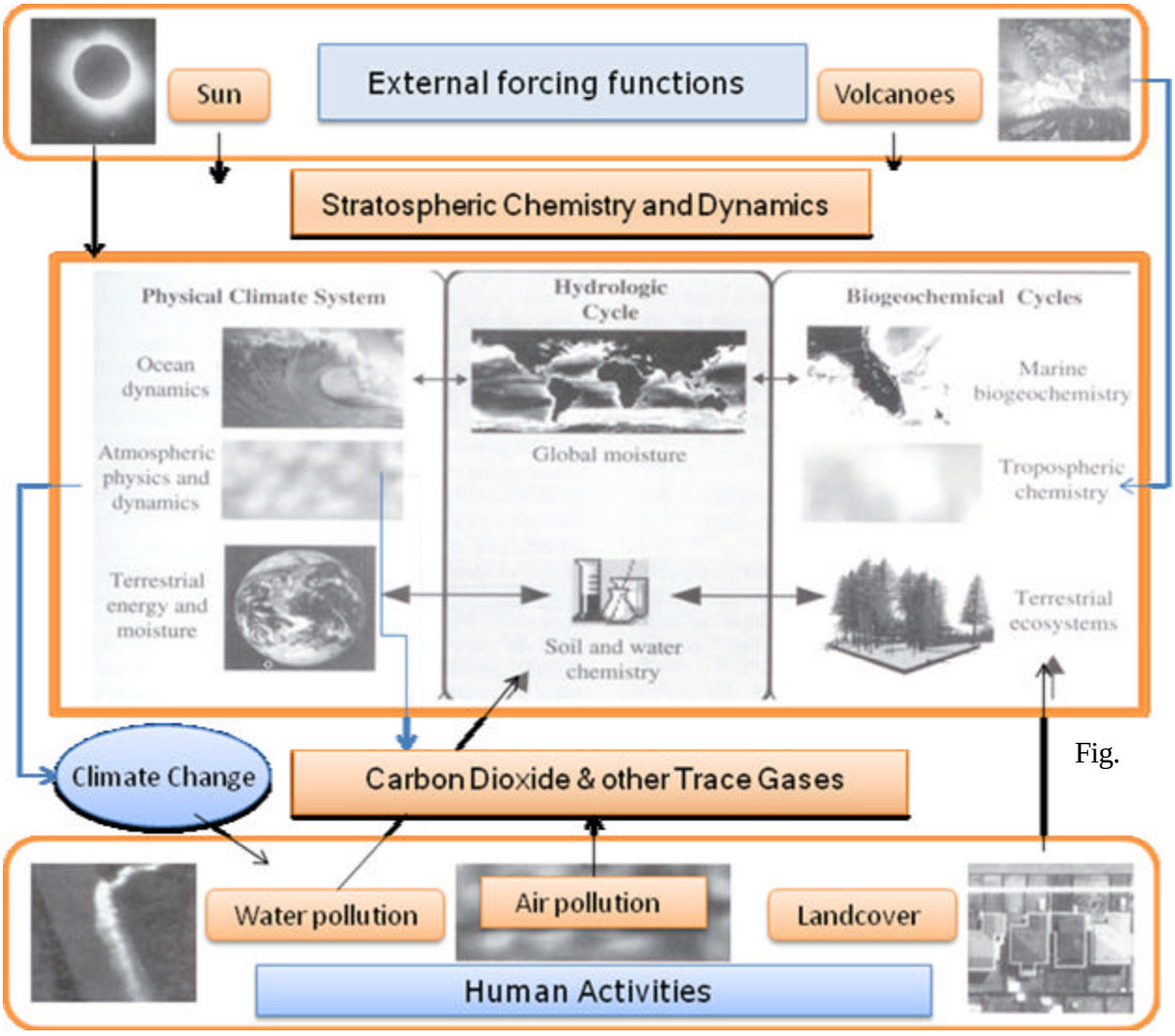

Fig.

1.1 Components of Earth's System
(Source: J. R. Jenson, 2000)

Knowledge of precipitation is required in estimating runoff, planning erosion control measures, planning for irrigation, removal of excess water and conserving water in low rainfall regions. Knowledge of runoff is required in designing structures and channels that will handle natural flows of water. Data about infiltration, evaporation and transpiration are required in planning irrigation and drainage systems, moisture conservation practices, etc. The watershed at the ap

propriate scale is generally the most logical geographical unit of streamflow analysis and water resources management.

Runoff representing the response of a catchment to precipitation reflects the integrated effects of a wide range of landcover, soil, topography, climate and precipitation characteristics of the area. Hence, if we have to study the impact of changes in climate and landcover on basin hydrology, altering streamflow pattern is an important component to look for. Quantification of runoff and other hydrological components can be done in many ways; Hydrological modeling is one efficient way for consistent long term behavioral studies.

1.3 **Hydrological modeling:**

Hydrological modelling is a mathematical representation of natural processes that influence primarily the energy and water balances of a watershed. Broadly two types of models exist: Conceptual and Physically based hydrologic models. **Conceptual-lumped models** rely on simple arrangement of a relatively small number of interlinked conceptual elements and may be thought of as one which averages inputs/outputs over an area and integrates several hydrological processes and their spatial variability. They are catchment oriented, use relatively simple input because they lump spatial/ temporal heterogeneity, data requirement is less, easily applicable and interfaced with GIS. These models may be too general in applicability or too site specific.

Physically based-distributed models contain equations that describe the physical interaction of different components of the water and energy balance. Model parameters relate these abstract physical laws (or scale-dependant approximations of these laws) to the specific basin at hand. They take an explicit account of spatial variability of processes, input, boundary conditions, and system (watershed) characteristics such as topography, vegetation, land use, soil characteristics, rainfall, and evaporation etc. From their physical basis such models can simulate the complete runoff regime, providing multiple outputs. In these models transfer of mass, momentum and energy are calculated directly from the governing partial differential equations which are solved using numerical methods, for example the St. Venant equations for surface flow, the Richards equation for unsaturated zone flow and the Boussinesq equation for ground water flow. As the input data and computational requirements are enormous, the use of these models for real-time forecasting has not reached the 'production stage' so far, particularly for data availability situations prevalent in developing countries like India.

Inevitably, all models are imperfect representations of reality; each is a different perspective on a system. Many parameters are observable (e.g. basin area, slope, elevation, vegetation type) although some parameters are unobservable conceptualizations of basin characteristics. One of the major problems in distributed

modeling is parameter identifiability, owing to a mismatch between model complexity and the level of data which is available to parameterize, initialize, and calibrate such models (Troch et.al, 2003). AVSWAT (ArcView Soil and Water Assessment Tool), MIKE-SHE, Variable infiltration Capacity model, HEC-HMS (Hydrologic Engineering Centre-Hydrologic Modelling System) are some of the physically based distributed hydrologic models. In the present study the Variable Infiltration Capacity (VIC) land surface hydrologic model has been used for modeling the river flow regime.

The fundamental objective of hydrological modeling is to gain an understanding of the hydrological system in order to provide reliable information for managing water resources in a sustained manner. Its value lies in its ability, when correctly chosen and adjusted, to extract the maximum amount of information from the available data, so as to aid in decision making process. Models are increasingly used in hydrology to simulate changes in catchment management, to extend data sets and to evaluate the impacts of external influences (such as climate change and landcover change). They can be used to estimate river flows at ungauged sites, fill gaps in broken records or extend flow records with respect to longer records of rainfall. Powerful spatially-distributed models are based on physical principles governing the movement of water within a catchment area, but they need detailed high-quality data to be used effectively. There are many simulation models in use; the skill is in selecting the right model for the job and balancing data requirements against the cost of model implementation.

1.4 **Remote Sensing in Hydrological modelling:**

The use of remote sensing and GIS facilitates hydrologists to deal with large scale, complex and spatially distributed hydrological processes. Remote sensing has held a great deal of promise for hydrology, mainly because of the potential to observe areas and entire river basins rather than merely points. For land surface hydrologic applications, the existing large amounts of multi-angle visible, microwave and thermal spectral measurements have proven very valuable for hydrologic applications. These measurements have been used to estimate surface incident radiation, surface temperature, spectral albedo, land cover type, canopy structure features, and a number of other variables relevant to the derivation of energy and moisture fluxes at the land surface (Entekhabi et al., 1999). The land cover maps derived by remote sensing are the basis of deriving hydrologic response units for modelling.

For an understanding of the hydrology of areas with little available data, a better insight into the distribution of the physical characteristics of the catchments is provided by image processing techniques. Some of the new measurement methods (photographic systems, active and passive radar systems etc.) could yield to some extent reliable areal totals or averages of hydrologic variable such as precipitation, evapotranspiration and soil

moisture. Current remote sensing techniques have the capability of providing relatively reliable information on land cover type and LAI. Therefore, incorporating such new remote sensing information (e.g., new spatial vegetation information with high resolution to allow multiple land cover types to coexist within a model computational grid cell) into land surface models may lead to significant improvement in evapotranspiration estimations, which would then lead to improvement in calculations of other components in the land surface models. Some other hydrological application areas of remote sensing are:

- Deriving spatial rainfall patterns (using active & passive microwave technique)
- Evapotranspiration and soil moisture estimation
- Snow cover mapping and studying dynamics
- Groundwater targeting, exploration and modelling
- Deriving topography (Digital Elevation Models) using Stereo and Satellite Photogrammetry.
- Surface water mapping and Derivation of bio-physical parameters etc.

1.5 **GIS in Hydrological Modeling:**

GIS has evolved as a highly sophisticated data management system to put together and store the voluminous data typically required for hydrological studies. GIS provides representations of spatial features of the Earth, while hydrologic modeling is concerned with the flow of water and its constituents over the land surface and in the subsurface environment.

Since GIS does not directly land itself to time varying studies, its features are utilised in hydrological studies by coupling it with hydrological models. The possibility of rapidly combining data of different types in a GIS has led to significant increase in its use in hydrological applications. It also provides the opportunities to combine a data from different sources and different types. One of the typical applications is use of a digital terrain model (DTM) for extraction of hydrologic catchment properties such as elevation matrix, basin boundary delineation, flow direction matrix, flow accumulation matrix, slope, aspect etc. GIS is a valuable tool for use in parameterization for large scale physically based distributed models. Significant developments in this area are taking place which would result in corresponding increase in operational use of such models. It is probably true that the factor most limiting hydrologic modeling is not the ability to characterize hydrologic processes mathematically, or to solve the resulting equations, but rather the ability to specify values of the model parameters representing the flow environment accurately. GIS will help overcome this limitation.

1.6 **Relevance of the Study undertaken:**

Human activity can dramatically alter landcover characteristics and subsequently hydrological and watershed processes in the long run. The effects of changes in landcover on catchment hydrological responses have been extensively carried out at watershed and river basin scales (Hibbert, 1967; Bosch and Hewlett, 1982; Stednick, 1996, Matheussen et. al., 2000). Studies concluded that forest cover strongly affects evapotranspiration, snow accumulation and snowmelt processes relative to other classes of landcover (Bosch and Hewlett, 1982). Removal of forest cover is known to increase streamflow as a result of reduced evapotranspiration and to increase peak flows as a result of higher water tables.

The Mahanadi river basin covering major portions of Chattisgarh and Orissa has been repetitively facing the adverse hydro-meteorological conditions such as floods, droughts and cyclones in the recent times. The river has often been referred to as the 'Sorrow of Orissa'. The inhabited inner basin Chhattisgarh plain is suffering from frequent droughts whereas the fertile deltaic area has been wrecked by repeated floods despite of operation of dams and barrages to control them. The watershed hydrology has changed considerably due to the increased anthropogenic activities, producing disasters. Frequent occurrence of these events indicates a shift in the hydrological response of the basin because of which the upstream of Hirakud is unable to retain sufficient moisture resulting in drought and the downstream river is unable to handle large streamflows resulting in floods. The reason for such changes in hydrological regime could be attributed to the long term climate and landcover changes in the region. The landcover change impact assessment on hydrology more specifically streamflows can be best handled through simulation of the hydrological conditions that shall prevail under the projected weather conditions in an area. Such a treatment is essential because of the fact that the hydrological response is a highly complex process governed by a large number of variables such as terrain, landuse, soil characteristics and the state of the moisture in the soil.

In the present study, an attempt has been made to model and evaluate the changes in streamflows attributable to changes in landcover throughout the Mahanadi basin. Ideally, such an investigation could be based on evaluation of long term streamflow records; however, this was not possible for two reasons. First, the unavailability of long term flow records and inadequacy to provide the level of spatial detail that is required to resolve the effects of multiple landuse changes. Second, almost all long term stream gauges have been extensively affected by water management activities, especially the construction of number of reservoirs which affect streamflows. For these reasons, an alternative, model based approach was used to simulate streamflow scenarios that would have occurred under historical (1972) and current (2003) vegetation cover conditions. Only the

vegetation cover and related parameters were changed in the simulations; the model meteorological forcings were same for both the current and historical scenarios. In this way, the effects of vegetation change on basin hydrology were isolated from the effects of climate variability.

The model used for simulation was Variable Infiltration Capacity land surface hydrologic model (Liang et. al, 1994) primarily developed for Global Circulation models and to study long term climate and landuse changes on hydrology. It is a physically based, macroscale hydrological model which represents the partitioning of incoming (solar and long wave) radiation at the land surface into latent and sensible heat, and the partitioning of precipitation (or snowmelt) into direct runoff and infiltration. VIC explicitly represents vegetation, and simultaneously solves the surface energy and water balances. A river routing model when coupled with VIC permits comparisons between the model-derived discharge and observations at gauging stations.

1.7 **Present study was taken up with the following main objective:**

Application of VIC-2L land surface hydrologic model to simulate streamflows for assessment of landcover change impact on hydrology of Mahanadi river basin. This required:

- Spatio-temporal data collection, database preparation using Remote Sensing / GIS and their integration for model input
- Modelling hydrological components of the Mahanadi river basin using Variable Infiltration Capacity model
- Routing the runoff component at various river outlets using the routing model.
- Calibration and validation of the hydrological model with respect to observed streamflows.
- Studying the Landcover changes in the basin and their impact on streamflows.

1.8 **Research Questions:**

- Is VIC suitable to model the hydrology of semi-humid regions like Mahanadi river basin?
- How far global remote sensing datasets can be utilised to derive Macroscale hydrological model input with reasonable accuracy?
- Can VIC simulate the hydrological response to landcover changes over large areas and long time frames?

CHAPTER 2 - LITERATURE REVIEW

This chapter provides an overview of Hydrological cycle, its importance, hydrological modelling, types of hydrological models and role of remote sensing/GIS in modelling hydrology. Previous works on methods and applications of Variable Infiltration Capacity model have been reviewed extensively. Special attention is directed towards impact of climate and landcover change on basin hydrology.

2.1 Hydrological cycle and its importance:

Hydrological cycle, which links Earth's subsystems, is a conceptual model, which describes how water moves around and between the earth and the atmosphere in different states such as gas, liquid, or solid (David R Maidment, 1992). From a global perspective, the hydrological cycle comprises of three major systems: the ocean as the major source of water, the atmosphere as the deliverer of water, and the land as the user of water. Precipitation, surface runoff, groundwater flow, infiltration, evapotranspiration, soil moisture, interception, depression, and detention storage are major components in land surface hydrology. The mathematical statement of hydrological cycle within a given time frame incorporating principles of mass and energy continuity is termed as the water budget or water balance. In its simplest form it is expressed as,

$$P - Q - ET - G = ? S$$

Where P is precipitation,
Q is surface runoff,
G is subsurface runoff,
ET is evapotranspiration,
And S is storage in the control volume.
Figure 2.1 shows the components of a hydrological cycle and their mutual interaction.

Physically, chemically and biologically interacting with the environment, water has an enormous impact on many aspects of life. The physical structure of the earth is altered as water moves through the landscape. Biological communities live, adjust and die depending on the water cycle. Human economies are strongly dependent on the movement, or lack of movement, of water.

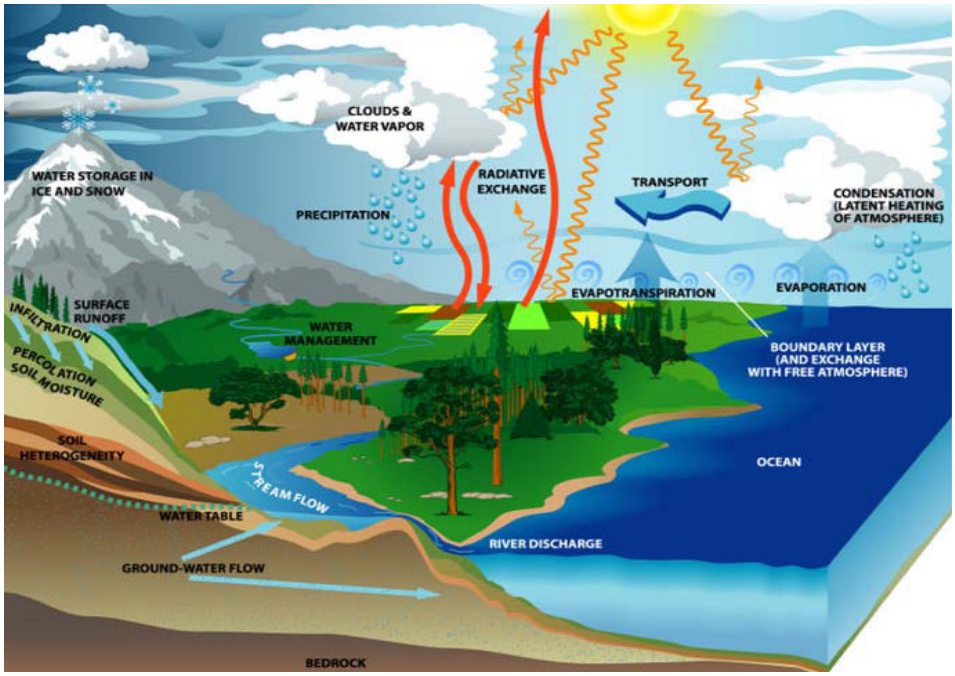

Fig 2.1 Hydrological cycle & its Components

Floods and droughts can cause havoc for human societies. Conflict and tension over water resources has a long history (Gleick 2002). Recent fears of climate change have implications for the hydrologic cycle, and the biologic communities that depend on the current nature of the water cycle.

2.2 Hydrological modelling and types of hydrological models:

"Prior to the advent of the unit hydrograph by Sherman (1932), hydrologic modeling was mostly empirical and based on limited data. In those days, graphs, tables, and simple analytical solution were the standard models, and hand calculations, in conjunction with slide rule, reflected computing prowess" (Singh and Fiorentino, 1996). Since the advent of the hydrograph, hydrologic modeling has developed into data intensive, computer software driven science. Today, there are models covering every facet of water's interaction with the environment. This sub-section is meant to provide some background to hydrologic modelling, focusing on physically-based watershed modelling. Fig 2.2 (Chow *et al.* 1988) presents one classification of hydrological models.

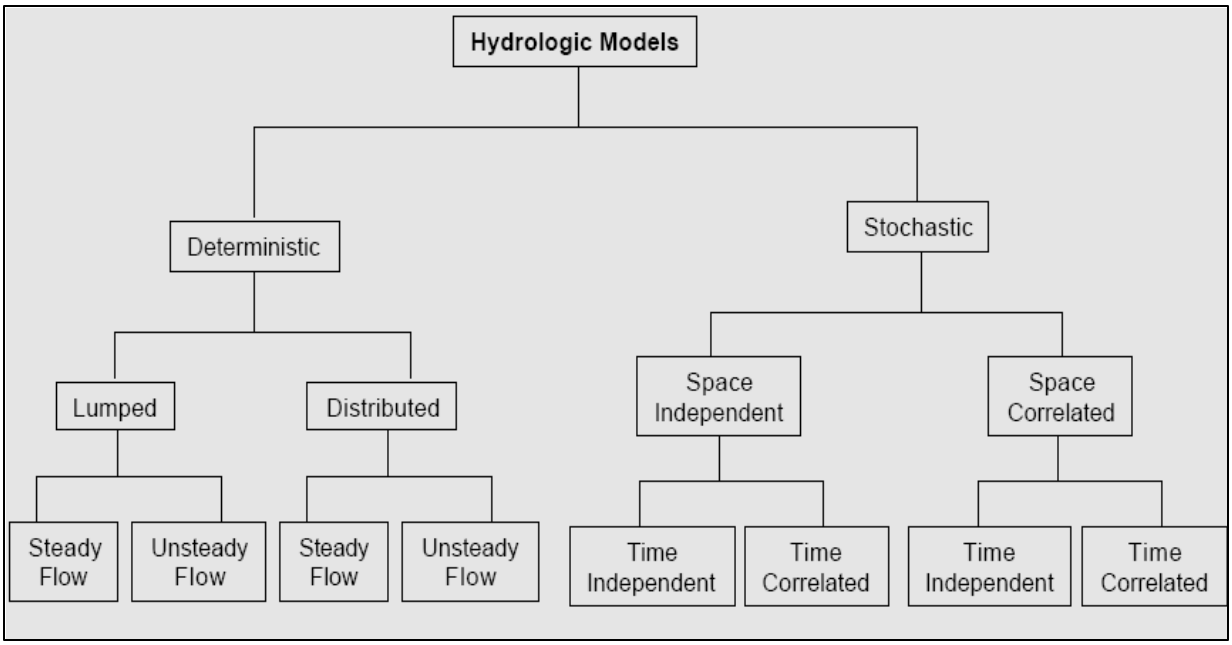

Fig 2.2: A Classification of Watershed Hydrologic Models

The first level of separation between the watershed models depends on whether or not the model includes randomness in its calculations. A given deterministic model will always produce the same output given a particular input. Stochastic models, however, incorporate the statistical nature of hydrology in their analysis. The second level of separation splits the models based on their ability to handle spatial variation. Lumped models spatially average the variables while distributed models consider the spatial distribution of the variables. The third level of separation considers the handling of time variation within a model. Deterministic watershed models consider whether the flow changes with time (unsteady) or not (steady). Stochastic model output always varies with time, but time-dependent models consider that one event is correlated with the nearby events (temporally speaking), while time-independent models do not make such a consideration. In the field of deterministic modelling, recent efforts are focused towards developing physically-based models, which try to mimic natural processes as closely as possible.

Lumped Models

Lumped hydrologic models are those models that commonly ignore spatial variations of precipitation, water flow, and other related processes, focusing instead on spatially averaged inputs, outputs, and parameter values. Lumped models are limited in their ability to achieve the physically-based goal because of this spatial averaging necessary for the variables. They are unable to account for the complexities of hydrologic processes and systems. Lumped models therefore are usually limited to those catchments where spatial variability does not dictate the outcome of an event (Muszik, 1996).

Distributed Models

"A truly distributed model of a process is possible only if the process can be described by an equation having an analytical solution" (Muszik, 1996). These types of models are physically based; meaning they are based on observed parameters rather than estimations. While the majority of distributed models require some degree of lumping, their objective is to account for spatial variations of hydrologic processes and parameters. Previously, limitations of distributed models came from computing the vast amount of data required to run the model. However, due to advancements in computers and modeling software, the current limitation for distributed modeling is the lack of available distributed hydrologic data (Muszik, 1996). In most of the distributed hydrologic models, HRU's (Hydrologic Response Units) are delineated by combining topography, soil properties, land use and other pertinent properties. Distributed models are especially useful, for example, when impacts of land use change are to be studied or for analyzing spatially varying flood responses.

A brief review of some popular hydrologic models being used is presented:

HEC-HMS (Hydrologic Modeling System)

HMS is a comprehensive hydrologic model developed by Hydrologic Engineering Center (HEC) of United States Army Corps of Engineers (USACE). It is an event – based overall lumped model (HEC, 2000). HMS offers several options to model various physical processes occurring in a watershed system. One such process is the direct runoff computations. Most of runoff models available with HMS are lumped in nature except for two which are distributed. Most of the lumped runoff models derive their roots from the Unit Hydrograph (UH) concept. This model provides a lumped model option called Clark's UH. To overcome its lumped character, a modified version called ModClark method was developed for HMS (Daniel and Arlen 1998). ModClark's method requires that watershed be further divided into sub-areas by intersecting it with a grid. Each of these sub-areas is assigned individual lag time, instead of one value for the whole watershed, as in the case of Clark's UH. ModClark's technique though tries to overcome the lumped character of Clark's UH, has certain limitations. The limitations that have been recognized are:

1) It is not a physically based model.
2) Dispersion effects that occur along the flow path are not captured, because the model assumes one single linear reservoir for the whole watershed.

SWAT (Soil and Water Assessment Tool)

SWAT was developed by USDA-ARS (Agriculture Research Service). Prediction of impacts of land management practices on water, sediment and agricultural chemical yields was the aim for the development of this physically based model. SWAT simulates

complete hydrologic cycle of a watershed system. "The hydrologic cycle is simulated in two phases: land phase and routing phase. The land phase hydrology controls the amount of water, sediment, nutrient and pesticide loadings. The routing phase consists of defining the movement of water, sediments, etc through the channel network of the watershed" (Neitsch et al. 2000). To capture heterogeneity in physical properties the basin is divided into subbasins, each one of them corresponding to a stream and then the sub-basins are discretized into sub-areas called HRUs, which are unique in terms of soils and land use. Physical processes modeled in SWAT can be classified based on the scale (i.e. sub-basin or HRU) assumed for lumping. For example, the precipitation input in SWAT can be provided only at the sub-basin level, whereas, runoff computations can be done at HRU level. The Green-Ampt infiltration method is one of the options that this model offers to compute excess precipitation at the HRU level, the other one being NCRS curve number method. Though the excess precipitation values are computed at the HRU level, an average of excesses over the sub-basin is assumed for overland flow computations. The overland flow routing model assumes a linear reservoir scheme. The runoff model incorporated in SWAT is lumped at the sub-basin level, because it computes an average value for spatial varied surface runoff. This is one of the limitations of the SWAT model. Presently SWAT model works only at daily time step.

MIKE SHE coupled with MIKE 11

MIKE SHE is distributed and physically based hydrologic modeling program produced by the Danish Hydraulic Institute (DHI). Its goal is to allow the user to simulate water, solutes and sediments in the entire land phase of the hydrological cycle. It has a modular design that can be used to create an integrated model. Its individual components can be used together or independently depending on data availability and project goals (Vanbrunt, 2002). Coupled with MIKE 11, DHI's one-dimensional model used for channel networks, MIKE SHE has the power to create an integrated surface water / ground water or drainage system / ground water model. MIKE SHE's basic modular components are pre and post processing (PP), and water movement (WM). The WM module is the core of MIKE SHE containing several process simulation modules that when put together describes the entire land phase of the hydrologic cycle. The WM module components are: evapotranspiration (ET), unsaturated zone flow (UZ), saturated zone flow (SZ), overland and channel flow (OC), and irrigation (IR). MIKE SHE is a watershed scale model and its applicability is limited in terms of studying climate and landcover change impact on basins at regional and global scales.

2.3 The Variable Infiltration Capacity model:

The Variable Infiltration Capacity Model (VIC) is a macro scale hydrologic model for water and energy balance, developed over the last 10 years at the University of

Washington and Princeton University. The first version of the VIC model is described in detail by Liang *et al*. (1994) and Liang *et al*. (1996a). Macro-scale Hydrological Models attempt to represent physical hydrological processes over large spatial scales. Most of MHMs are a hybrid of conceptual and physically based components, which makes the parameter estimation even more difficult. VIC model possesses a physically based component to represent the exchanges of sensible and latent heat with the atmosphere but uses empirical approximations to simulate precipitation-runoff processes and infiltration.

As compared to other land surface models, VIC's distinguishing hydrologic features are a) its representation of subgrid variability in soil moisture storage capacity as a spatial probability distribution, to which surface runoff is related (Zhao *et al*., 1980), and b) its parameterization of base flow, which occurs from a lower soil moisture zone as a nonlinear recession (Dumenil and Todini, 1992). As discussed by Lohmann *et al.* (1998a, b) the representation of soil hydrology (soil water storage, surface runoff generation and sub-surface drainage) has a critical influence on the predicted long-term water and energy balances.

Lettenmair (2001) has described the development of Variable Infiltration Capacity (VIC) model, as well as its application, through two examples. These are 1) effects of climate change on the hydrology of major continental rivers; 2) effects of vegetation change on the hydrology of the Columbia Rivers system (U.S. and Canada).

(1) Global river sensitivity to climate change:

Changes in land surface hydrology due to changing climate have potentially far reaching implications both for human populations and for regional-scale physical and ecological processes. Nijssen *et al.* (2001c) targeted nine large river basins to analyze the regional hydrological consequences of climate predictions in a global context using VIC land surface model. Climate scenarios from eight GCMs were obtained from the Intergovernmental Panel on Climate Change Data Distribution Center (IPCC-DDC). The daily data were used to drive the VIC model to calculate a set of derived components (evapotranspiration, runoff, snow water equivalent, and soil moisture) and to study the water balance of each of the continents. For each 2° × 2° model grid cell land surface characteristics such as elevation, soil, and vegetation were specified. Vegetation types were extracted from the 1 km, global land classification of Hansen *et al*. (2000). Vegetation parameters such as height and minimum stomatal resistance were assigned to each individual vegetation class. Soil textural information and soil bulk densities were derived from the 5 minute FAO-UNESCO digital soil map of the world (FAO, 1995). The remaining soil characteristics, such as porosity, saturated hydraulic conductivity, and the exponent for the unsaturated hydraulic conductivity equation were based on Cosby *et al*. (1984).

(2) Vegetation change effects on hydrology:

Matheussen et. al. (2000) analyzed the hydrological effects of vegetation changes in the Columbia River basin over the last century using two landcover scenarios, the historical and the current. Simulations were performed using the VIC hydrological model, applied at one-quarter degree spatial resolution (approximately 500 km^2 grid area) for the period of 1979 to 1990. The mean monthly flows using the current vegetation were in good agreement with the corresponding observed discharge (Matheussen et al., 2000). An annual average increase in runoff in the sub-basins ranged from 4.2 to 10.7 % and decreases in evapotranspiration ranged from 3.1% to 12.1%. Removal of forest cover was known to increase streamflow as a result of reduced evapotranspiration and to increase peak flows due to higher water tables. In regions where snow processes are important, peak flows increase due to increased snow accumulation in clearings as compared to forested areas, and more rapid snow melt due to enhanced turbulent energy transfer in harvested areas (Storck, 2000). This study provided a broad scale frame work for assessing the vulnerability of watersheds to altered streamflow regimes attributable to changes in landcover that occur over large geographical areas and long time frames.

Detailed diagnosis of VIC model results has been carried out over the central U.S. by Maurer et al. (2001a) as part of the Land Data Assimilation System (LDAS) project, which includes retrospective simulations (eventually for 50 years) for long-term validation against basin discharge and to test model parameterizations. Maurer *et al*. (2001b) in a study showed good agreement between the spatially averaged station soil moisture and simulations from the VIC model. He found an excellent model agreement with the observed moisture flux (change in soil moisture) over an annual cycle and concluded that VIC land surface model can provide fields of surface hydrologic states (soil moisture, surface temperature and snow extent and water equivalent) of sufficient accuracy to allow simulations of synthetic satellite observations.

Liang et al. (2004) used VIC - 3L land surface model at the blue river watershed (1233 km^2 area) in Oklahoma to investigate the impacts of spatially distributed precipitation and soil heterogeneity on modeling water fluxes at different spatial resolutions (1/32, 1/16, 1/18, 1/4, 1/2, and 1 degree). Their study revealed that model parameters calibrated at a coarse resolution can be applied to finer resolutions to obtain generally comparable results. However model parameters calibrated at finer resolution cannot result in comparable results when applied to resolution coarser than the identified critical resolution. In addition, while soil moisture of the total zone is more sensitive to the spatial distributions of soil properties, runoff and evaporation are more sensitive to the spatial distribution of daily precipitation of the watershed being studied. Since model calibration requires a lot of data and is time consuming in distributed modeling, their results suggest that coarser resolutions may be used as an effective alternative for

conducting preliminary analysis. Zhou et. al. (2004) found that the model-simulated streamflows often underestimate the observed peak flows significantly.

VIC model has been tested and applied at a range of spatial scales over the years, from large river basins to continental and global scales. Within North America, it has been applied at 1^o spatial resolution to the Missouri (Wood et al., 1997), Arkansas-Red river (Abdulla et al., 1996) and Columbia river basins (Nijssen et al., 1997), and at 0.5^0 resolution to the Weser river basin in Germany (Lohmann et al., 1998a, b). The grid network version of the VIC-2L model together with a linear routing scheme was able to predict fairly accurately daily, monthly and annual streamflow in the Weser river and its tributaries (Lohmann et al., 1998). A simple sensitivity analysis showed that the runoff volume produced by the VIC-2L model is strongly dependent on the soil thickness, the baseflow recession curve and the infiltration parameter.

Abdulla et al., (1995) have developed and tested a regional parameter estimation scheme for the VIC-2L model using a set of 40 catchments in the Arkansas-Red river basin. They have developed regression equation to relate the estimated VIC model parameters for the gauged catchment to catchment characteristics which can be derived from digital elevation data, land use, soil and climate data. Result has shown the model is not performing well for the arid and semi-arid catchments but performed quite well with the regional parameters for more humid area. Also simulated evaporation data has shown quite closeness to estimated values using atmospheric water budget especially in spring and summer which have higher evaporation.

Nijssen et al. (1997) have used two layer Variable Infiltration Capacity (VIC-2L) model to predict stream flow for continental river basins having drainage area of 567,000km^2 (Columbia) and 33,000km^2 (Delaware). 1^o spatial resolution was applied to the Columbia where as 0.5^0 resolution was used for the Delaware River. According to the result both annual runoff volumes as well as hydrograph shape were simulated with a considerable degree of accuracy with mean shown annual runoff volumes during the test. In addition to that it has shown model has failed in the arid region apparently owing to the absence of an infiltration excess mechanism in the model as well as strong ground surface water interaction in the particular region.

Yuan et. al. (2004) applied hydrologically based three-layer variable infiltration capacity (VIC-3L) land surface model with a new surface runoff model to simulate streamflow for the Hanjiang River basin in China. VIC-3L simulated daily runoff is routed to the outlets of six streamflow stations and compared with the daily and monthly observed streamflow at the stations. The results show that the model can simulate the observations well with reasonable accuracy.

2.4 Role of remote sensing/GIS in hydrology and hydrological modelling:

Zhou et. al. (2004) categorized applications of remote sensing in hydrological studies and water resources management as follows: (*i*) using original remote sensing imagery directly to identify hydrologically important spatial phenomena; (*ii*) using processed remote sensing data, such as precipitation, as forcings of hydrological models; (*iii*) using multispectral data, such as vegetation (land cover) types and density, to quantify surface parameters; (*iv*) direct calculation of evapotranspiration distribution in terms of spectral data of satellite remote sensing based on surface energy balance (e.g., Bastiaanssen et al., 1998); (*v*) using remote sensing derived fields, such as soil moisture, to improve model simulations through data assimilations; and (*vi*) validating model simulations using remote sensing data.

Accurate model simulations depend on a number of factors, such as good parameterizations of physical processes, a balanced representation of model complexity, good model input forcings, and good model parameters. Remotely sensed data can, at least, improve model simulations by (*i*) providing more accurate spatially distributed model parameters such as vegetation information over a study region, and (*ii*) helping to identify potential model structure weaknesses through validation, data assimilation, etc.

Accurate estimation of the spatial distribution of actual evapotranspiration over a large region is very challenging, but critically important for land surface models to obtain reasonable partitions of water and energy fluxes in water and energy budgets (Zhou et. al, 2004). Therefore, a promising approach to obtaining reasonable estimation of the spatial distribution of evapotranspiration at present is to estimate the evapotranspiration by land surface models with an effective use of remote sensing information. For instance, vegetation parameters, such as land cover and leaf area index (LAI), are important factors for obtaining accurate evapotranspiration estimation. Among remotely sensed information, hydrologically significant variables that are underutilized are vegetation parameters derived from optical remote sensing. In particular, vegetation structural parameters, such as LAI and canopy closure, are important in precipitation, interception and evapotranspiration and thus play a crucial role in land surface models.

Sandholt (2003) investigated the use of remotely sensed data in distributed hydrological modelling. He used the results of daily rainfall estimates from METEOSAT data and vegetation dynamics from NOAA AVHRR data as an input to the model and reported the potential of using a remotely sensed dryness index for validation of the model. He found that the performance of simulated discharge was improved using remotely sensed vegetation dynamics, and marginal improvement in model performance was obtained using remotely sensed precipitation.

Geographic Information System (GIS) focuses on proper integration of user and machine for providing spatial information to support operations, management, analysis and decision making (Seth, 2001). The possibility of rapidly combining data of different types in a GIS has led to significant increase in its use in hydrological applications. It also provides the opportunities to combine a data from different sources and different types. One of the typical applications is use of a digital terrain model (DTM) for extraction of hydrologic catchment properties such as elevation matrix, flow direction matrix, ranked elevation matrix, and flow accumulation matrix. It also provides the ability to analyse spatial and non-spatial data simultaneously.

2.5 Changing Landcover scenario and its impact on basin hydrology:

Dunne and Leopold (1998) discussed the effects of landuse changes on the watershed and channel hydrology. They suggested that alteration of the ground surface of a basin may change both the infiltration rate (and thence the volume of runoff from a given storm) and the lag time of the basin. Usually these operate in the same direction—increase of runoff volume and shortening of lag time. Both tend to increase peak flow from a given storm. Due to an increase in the area of low or zero infiltration capacity there is increase in the efficiency or speed of water transmission in channels or conduits. Such increase may be expected to result from a variety of landuse alterations, such as urbanization, grazing, agriculture, forest clearcutting and others. There has been a growing need to study, understand and quantify the impact of major landuse changes on hydrologic regime, both water quantity and quality. This is necessary to anticipate and minimize potential environmental hazards and to satisfy water resources requirements.

Land use and land cover change may cause important changes to the hydrology of the basin through their impacts on the land surface energy and water balance. In particular, land cover change (e.g., from a natural landscape to an agricultural system) can alter evapotranspiration, soil moisture, water yield, and river discharge (Bruijnzeel, 1990; Sahin and Hall, 1996; Wang and Eltahir, 2000; Costa et al., submitted, 2004). Foley et.al. (2004) explained that land cover and land use changes may affect the seasonal variability and magnitude of runoff and discharge through a number of interconnected processes. Changes in vegetation cover directly alter total evapotranspiration and hence runoff through differences in the water requirements of different plant communities. Additionally, changes in land cover and use alter the rate at which water runs off the land surface and infiltrates the soil column (e.g., through soil compaction, creation of impervious surfaces, straightening and lining of stream channels, etc.) and how rapidly water is removed from the soil column (e.g., through tiling and ditching of fields).

Observational studies of small watersheds (10s of km^2) in tropical, temperate, and boreal regions (as summarized in Bosch and Hewlett, 1982; Bruijnzeel, 1990; Sahin and Hall,

1996) have shown that, in general, a decrease in vegetation density (e.g., from forest to grassland or crops) can be expected to increase annual mean water yield and discharge, while an increase in vegetation density tends to reduce water yield and discharge, consistent with alterations to the total evapotranspiration and soil infiltration rates. Costa et al. confirmed this process in a very large tropical river basin (the 176,000 km^2 Tocantins River in Brazil), finding that an increase from 30% to 50% of the land used for crops between 1960 and 1995 is coincident with a 25% increase in annual mean discharge, despite no change in the mean precipitation.

Twine et. al. (2004) analysed the effects of land cover change on the energy and water balance of the Mississippi River basin using the Integrated Biosphere Simulator (IBIS) model. Results of a simulated conversion from complete forest cover to crop cover over a single model grid cell show that annual average net radiation and evapotranspiration decrease, while total runoff increases. The opposite effects are found when complete grass cover is replaced with crop cover. The simulated energy and water balance changes resulting from land cover change depend on season, crop type (winter, spring, or summer plantings) and management, and the type of natural vegetation that is removed.

Shrestha (2005) developed a spatially distributed model with SCS curve number to assess the runoff changes due to land-use changes in the Kathmandu Valley basin, Nepal. He found that the average daily monsoon flow increased by 12% for 9% deforestation and 17% urbanization. This study clearly demonstrated that interactive integration of spatial data and application of distributed hydrologic model in GIS environment provides a powerful tool for assessment of effects due to land-use changes.

Gosain et.al. (2006) studied Climate change impact assessment on hydrology of Indian river basins. A distributed hydrological model namely SWAT (Soil and Water Assessment Tool) has been used. Simulation over 12 river basins of the country has been made using 40 years (20 years belonging to control or present and 20 years for GHG (Green House Gas) or future climate scenario) of simulated weather data. The initial analysis has revealed that under the GHG scenario, severity of droughts and intensity of floods in various parts of the country may get deteriorated. Thus, climate change impacts are going to be most severe in the developing world, because of their poor capacity to adapt to climate variability. India also comes under this category. The NATCOM study was the first attempt to quantify the impact of the climate change on the water resources of the country. The Mahanadi river has been selected as the one which has been predicted to have maximum impact on account of the flood conditions. The study reveals that this river basin is expected to receive comparatively higher level of precipitation in future and a corresponding increase in evapotranspiration and water yield is also predicted.

CHAPTER 3 - MODEL OVERVIEW

3.1 Introduction to VIC model:

Variable infiltration capacity model is a macroscale hydrological model designed to represent surface energy and hydrological fluxes and states at scales from large river basins to the entire globe. It is grid based semi distributed hydrological model which quantifies the dominant hydro-meteorological process taking place at the land surface atmospheric interface. Typically grid resolution ranges from 1/8 to 2 degree (http://www.hydro.washington.edu). VIC computes the vertical energy and moisture flux in grid cell based on specification at each grid cell considering soil properties and vegetation coverage. Also it includes the representation of sub grid variability in soil infiltration capacity and all mosaic of vegetation classes in any grid cell.

The resulted runoff and base flow is routed via a separate channel routing module to produce stream flow at selected point within the domain. Figure 3.1 illustrates the Schema of Variable Infiltration Capacity model. VIC- 2L model was modified to VIC-3L by adding one thin surface layer along with a canopy layer to achieve better representation of bare soil evaporation processes after small summer rain fall event.

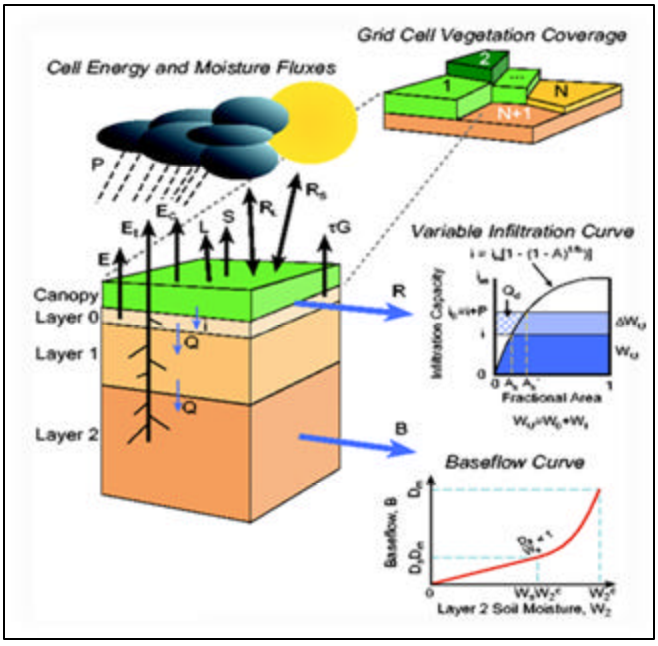

Fig 3.1 Schema of Variable Infiltration Capacity

.2 Major components of VIC model

3.2.1 **Vegetation cover**

As shown in Figure 3.2, VIC model surface is described by N+1 land cover types where n=1,…N represents N different vegetation and n=N+1 represents bare soil. All information related to vegetation is represented by vegetation library and vegetation parameter file. The land cover (vegetation) classes are specified by the fraction of the grid cell which they occupy, with their leaf area index (LAI), canopy resistance, surface albedo and relative fraction of roots in each of the soil layers.. According to the vegetation cover type within a grid cell infiltration, moisture flux between the soil layers and runoff are computed. Surface runoff and base flow are computed separately considering each vegetation type and then summed over the composition vegetation within each grid cell.

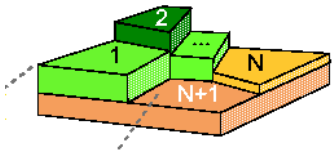

Fig 3.2 Grid cell vegetation coverage

3.2.2 **Soil layers**

Soil characteristics can be represented for a user defined number of vertical layers usually two or three as seen in Figure 3.3 dividing into thin upper layer and secondary set of layers. Soil parameters for each grid and soil layer is specified in user defined soil parameter file.

3.2.3 **Rainfall**

VIC model considers the sub-grid variability of precipitation which is distributed throughout all or a portion of grid cell as a function of rainfall intensity. Precipitation distribution can be expressed as follows,

$$\mu = (1-e^{-aI})$$

Where,

I = Precipitation intensity

a = coefficient which describes the effect of grid cell size and geography

Change in precipitation intensity of a storm changes the fractional coverage accordingly. When intensity increases, the fractional coverage over a grid cell increases and when decreased fractional coverage decreases. Before the occurrence of a storm the soil water content throughout the grid cell is set to average. However, forcing data plays an important role and accordingly simulation can be done hourly, 3 hourly, daily or monthly.

3.2.4 **Snow cover**

VIC model is also capable of doing reliable simulation of snow pack process across a wide range of grid resolution in high altitude areas. Effect of vegetation cover on snow accumulation and melt is described internally within the VIC model through a coupled snow model.

3.2.5 **Evapotranspiration**

Three types of evaporation which are evaporation from canopy layer of each vegetation class, transpiration from each vegetation class and evaporation from the bare soil are considered to calculate total evapotranspiration over a grid cell. Penman-Monteith formula given below is used to calculate the evapotranspiration for each class. Figure 3.3 represents the different energy components of VIC model.

$$\lambda ET = \frac{\Delta(R_n - G) + \rho_a c_p \frac{(e_s - e_a)}{r_a}}{\Delta + \gamma\left(1 + \frac{r_s}{r_a}\right)}$$

Where R_n = net radiation,

G = soil heat flux,

$(e_s - e_a)$ = vapor pressure deficit of the air

$?_a$ = mean air density at constant pressure

c_p = specific heat of the air

? = slope of the saturation vapor pressure temperature relationship

γ = psychometric constant

r_s and r_a are the (bulk) surface and aerodynamic resistances

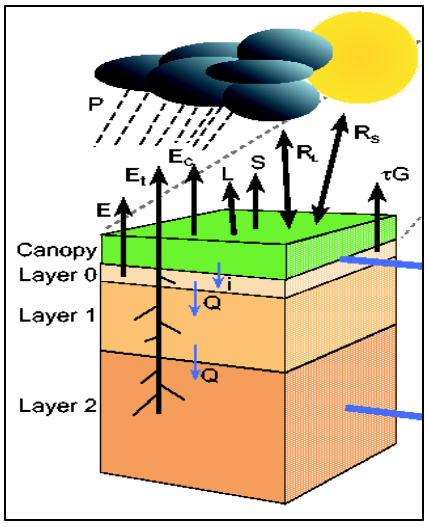

Fig 3.3: Cell energy components and soil layers

E - Evaporation from soil layer

E_t - Evapotranspiration

E_c- Canopy interception evaporation

R_L - Long wave radiation,

R_S - Shortwave radiation

G - Ground heat flux

L - Latent heat flux

S - Sensible heat flux

Q - Percolation

3.2.6 **Infiltration**

This model assumes that infiltration capacity of the soil is not uniform. Hence runoff generation and evaporation vary within an area owing to variations in topography, soil and vegetation. It also considers that infiltration capacity is storage and not a rate. Sub-grid variability scheme in infiltration is used to account Variable Infiltration capacity. This uses a spatial probability distribution to represent variable infiltration capacity as a function of relative saturated area of the grid cell. VIC uses infiltration formula used in Xinanjang model which assumes that precipitation in excess of the available infiltration capacity forms surface runoff. Figure 3.4 shows the variable infiltration capacity curve. Spatial variation of infiltration capacity is expressed as,

$$i = i_m [1-(1-A)^{1/b_i}]$$

i = Infiltration capacity upto which the soil is filled

i_m = Maximum infiltration capacity

A = represents the saturated fraction of the grid cell (0 = A = 1)

b_i = shape parameter

Maximum soil moisture of soil layer W_{c1} is related to i_m and b_i as,

$$W_{C1} = \frac{i_m}{1+b_i}$$

Also VIC model assumes that runoff is generated by areas where precipitation added to soil moisture storage at the end of the previous time step exceeds the storage capacity of the soil. Also there is no rate limitation mechanism in the model instead the formulation is a surrogate for the saturation excess mechanism, as it leads to a fraction of saturated areas. The direct runoff Q_d from the fraction of saturated area is given by,

$Q_d = P - W_{c1} + W_1^-$ $\qquad i_0 + P = i_m$

$Q_d = P - W_{c1} + W_1^- + W_{c1}\left(1 - \frac{i_0 \; p}{i_m}\right)$ $\qquad i_0 + P = i_m$

W_1^- = soil moisture content in layer 1 at beginning of the time step

i_0 = infiltration capacity of the saturated area.

For bare soil, water balance layer is described by,

$W_1^+ = W_1^- + P - Q_d - Q_{12} - E$

W_1^+ = Soil moisture content in layers at the end of each time step

Q_{12} = drainage from layer 1 to layer 2

$$Q_{12} = K_s \left(\frac{W_1^- - W_{cr}}{W_{c1} - W_{cr}} \right)^{\frac{2}{B_p}+3}$$

K_s = Saturated hydraulic conductivity

B_p = Pore size distribution index

Normally $W_{cr} = 0.3\ W_{c1}$

$W_{cr} = Ø_r D_1$

Where W_{cr} = residual moisture content in the upper layer of depth D in terms of the residual moisture fraction $Ø_r$

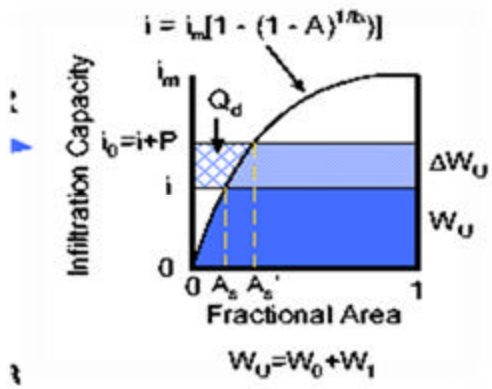

Fig 3.4 Infiltration Capacity Curve

3.2.7 **Base flow**

Drainage between soil layers is gravity derived as well as unsaturated hydraulic conductivity is a function of the degree of saturation of the soil. Base flow is derived as the function of soil moisture in the lowest soil layer using Arno-non linear formula.

$$Q_b = \frac{D_s D_m}{W_s W_{c2}} W_2^- \quad 0 \le W_2^- W_s W_{c2}$$

$$Q_b = \frac{D_s D_m}{W_s W_{c2}} W_2^- + \left(1 - \frac{D_s}{W_s}\right) D_m \left(\frac{W_2^- - W_s W_{c2}}{W_{c2} - W_s W_{c2}} \right)^2 \quad \text{for} \quad W_2^- \ge W_s W_{c2}$$

Where, Dm= Maximum base flow parameter

D_s = Fraction of Maximum base flow

W_s = Fraction of maximum soil moisture

W_{c2} = Maximum soil moisture in layer 2

W_2^- = soil moisture content at the beginning of time step in layer 2

As seen in Figure 3.5 the relationship becomes nonlinear at high soil moisture content resulting in rapid base flow response in wet condition. Below user defined value of soil moisture it behaves linearly reducing the responsiveness of base flow in dry condition.

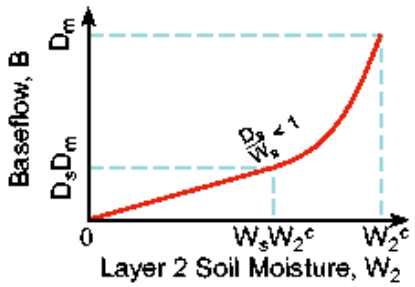

Fig 3.5 Base flow curve

3.3 **Routing**

Routing is used to predict the outflow hydrograph of watersheds subjected to a known amount of precipitation. Routing model associated with VIC mainly consists of within grid cell routing and routing between cells. Within grid routing component considers the time required for produced runoff within a grid cell to reach an arbitrary outlet. The runoff generated by VIC model for each grid cell is convolved with a discrete unit hydrograph,

$$R_1 = \sum_{j=1}^{i<j} \cdot Q_j \quad H_{i-j-1}$$

R_1 = internally routed runoff at the grid cell outlet

Qj = Run off outflow at Vic

I = Time step of unit hydrograph

j = Time step of runoff time series

i = Total number of time steps in runoff time series.

H = Unit hydrograph ordinates

While routing between cells, the internally routed runoff R_1 is transported downstream through the flow network after lagging with an effective velocity of 1 ms^{-1}. The effective velocity is near the lower end of the range suggested by Susen. The inclusion of the river routing model (Fig 3.6), developed by Lohmann et al. (1998a, b) permits comparisons between the model-derived discharge and observations at gauging stations.

3.4 Various modes of VIC model

3.4.1. **Water Balance**

Water balance mode assumes that land surface temperature equals air temperature. Although it does not solve the full surface energy balance, exception is the snow algorithm that still solves the surface energy balance to determine the fluxes needed to

drive accumulation and ablation processes. It requires comparatively less time for computation than other modes due to removal of the ground heat flux solution and iterative procedure needed to close the surface energy balance. The time step ranges from hourly to daily.

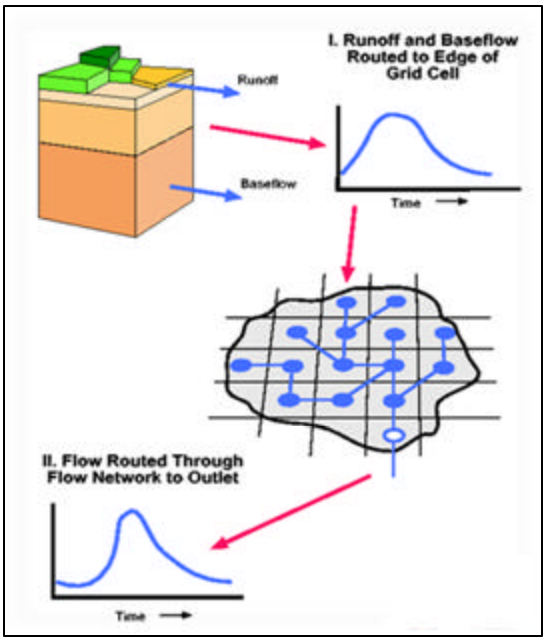

Fig 3.6 River Network Routing Model

The daily water balance mode is significantly faster than sub-daily simulations. Parameters required for daily solutions are different from those used for sub-daily solutions. Although the daily water balance model can be used to simulate discharge from a basin, calibration parameters for the daily water balance model are unlikely to be transferable to any model run with a sub-daily time step. Usually daily water balance model experiences higher evaporation, resulting in lower soil moistures and base flows.

3.4.2 **Energy Balance**

Full energy balance mode calculates all water and energy fluxes near the land surface, and run time step may be one or three hours. The surface energy balance is closed by an iterative process which tries to find a surface temperature which adjusts surface energy fluxes (sensible heat, ground heat, ground heat storage, outgoing long wave and indirect latent heat). Hence this mode requires more computational time than water balance as well as require sub-daily simulation time step. Finally this mode simulates the surface energy fluxes, which are important to understand the hydrologic cycle as well as land surface-atmosphere interactions in a basin. It has been proved that moisture fluxes generated from both energy balance and water balance modes are similar.

3.4.3 **Frozen Soil**

Frozen soil affects on both moisture and energy fluxes. It solves thermal fluxes at nodes through the soil column using the finite difference method as well as it computes the maximum unfrozen water content at each soil node based on the nodal temperature. Also ice content for each soil moisture layer is computed from the nodal values and is used to restrict infiltration and soil moisture drainage. In addition to that the nodal ice contents are also used to derive the soil thermal conductivity and volumetric heat capacity for the next model time step. It has been observed that frozen soil algorithm increases peak flows in the spring and decreases base flow in the winters.

3.4.4 **Special Cases**

Optimization of output, model state and debug code modes are special cases which can be applied to both energy balance and water balance to get output as desired by the user. They modify output in the described fashion and can be controlled by pre-processor commands in user_def.h which needs to be set before the source code is compiled.

3.5 **Specific features of VIC**

As compared to other land surface models, VIC's distinguishing hydrologic features are

a) VIC explicitly represents effects of multiple vegetation covers on water and energy budgets and simultaneously solves full surface energy and water balances giving multiple outputs.

b) It represents of subgrid variability in soil moisture storage capacity as a spatial probability distribution, to which surface runoff is related (Zhao et al., 1980).

c) It incorporates the representation of subgrid spatial variability of precipitation with the representation of spatial variability of infiltration to simulate energy and water budgets (e.g., energy fluxes, runoff, and soil moisture).

d) It includes both the saturation and infiltration excess runoff processes in a model grid cell with a consideration of the subgrid-scale soil heterogeneity (Liang and Xie, 2001) and the frozen soil processes for cold climate conditions (Cherkauer and Lettenmaier, 1999).

e) It belongs to the category of surface vegetation atmospheric transfer scheme (SVATS) and has an ability to couple with Global Circulation Models (GCM) and other Climate models.

CHAPTER 4 - STUDY AREA (The Mahanadi River Basin)

This chapter gives a brief overview of geographic setting of the Mahanadi river basin describing location and extent, river system, hydro-meteorological hazards faced by the population. A brief description of climate, physiography, soils, agriculture and landuse is also presented.

4.1 Location and Extent of the Basin:

The Mahanadi basin lies encompassed within geographical co-ordinates of 80°30' to 86°50' East longitudes and 19°20' to 23°35' North latitudes. The total catchment area of the basin is 1,41,600 sq.km. Basin is bounded in the North by Central India hills, in the South and East by the Eastern Ghats and in the West by Maikala hill range. The Chiroli Hills form the watershed dividing the Wainganga valley from the Mahanadi Basin, the upper portion of which is called as the Chattisgarh plain. It is a typical basin considered from geographical and geological point of view covering major parts of Orissa, Chattisgarh, small portions of Madhya Pradesh, Maharashtra and Jharkhand (Table 4.1). The average elevation of the drainage basin is 426 m with a maximum of 877 m and a minimum of 193 m. In the upper drainage basin of the Mahanadi, which is centered on the Chhattisgarh Plain, periodic droughts contrast with the situation in the delta region where floods may damage the crops in what is known as the rice bowl of Orissa.

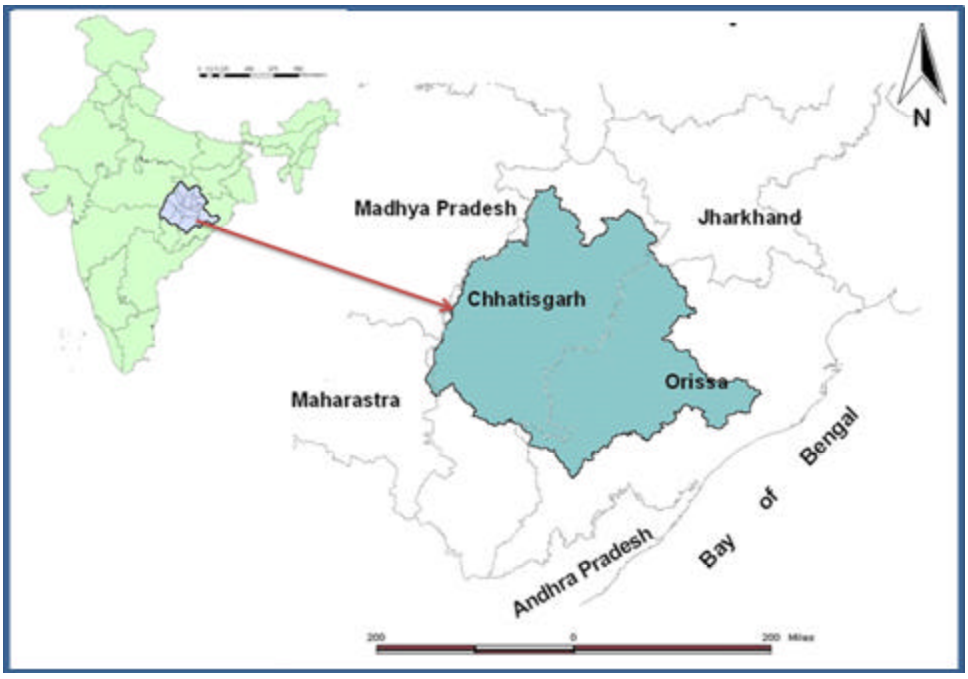

Fig. 4.1 Location of Study Area (Mahanadi river basin)

Catchment Area in Sq. km					
Jharkhand	M. P.	Chattisgarh	Maharashtra	Orissa	Total
126	107	75229	238	65889	141589

Table 4.1 Spread of the Basin in different States
(Source: CWC Handbook, 2006)

4.2 The Mahanadi river system:

The river Mahanadi is one of the major inter-state east flowing rivers in peninsular India. It originates at an elevation of about 442 m. above Mean Sea Level near Pharsiya village in Raipur district of Chattisgarh. During the course of its traverse, it drains fairly large areas of Chhatisgarh and Orissa and comparatively small area in the state of Jharkhand and Maharashtra. The total length of the river from its origin to confluence of the Bay of Bengal is about 851 km., of which, 357 km. is in Chattisgarh and the balance 494 km. in Orissa. During its traverse, a number of tributaries join the river on both the flanks. There are 14 major tributaries of which 12 nos. are joining upstream of Hirakud reservoir and 2 nos. downstream of it. On the Left Bank six tributaries namely the Seonath, the Hasdeo, the Mand, the Ib, the Kelo and Borai drain into main channel upstream of Hirakud reservoir. Figure 4.2 shows the extent of the river basin with Mundali near Cuttack (Orissa) as an outlet. The figure also shows the drainage network of major tributaries of the Mahanadi river.

The drainage system upstream of Hirakud reservoir is more extensive on the left bank of Mahanadi as compared to that on the Right Bank. On the Right Bank six tributaries namely the Pairi, the Jonk, the Sukha, Kanji, the Lilar and the Lath join upstream of Hirakud reservoir and two tributaries namely Tel and Ong join downstream of it. The three major tributaries namely the Seonath and the Ib on the Left Bank and the Tel on the Right Bank together constitute nearly 46.63% of the total catchment area of the river Mahanadi. The Seonath, which is the largest tributary of Mahanadi, drains three districts of Chhatisgarh namely Durg, Rajnandgaon and Bilaspur. The Tel, which is the second largest tributary of Mahanadi river drains four districts of Orissa namely Koraput, Kalahandi, Balangir and Phulbhani. The Ib, which is the third largest tributary of Mahanadi, drains Raigarh district of Chhatisgarh and two districts of Orissa, namely Sundergarh and Sambalpur. Below the dam the Mahanadi turns south along a tortuous course, piercing the Eastern Ghats through a forest-clad gorge. Bending east, it enters the Orissa plains near Cuttack and enters the Bay of Bengal at False Point by several channels.

Numerous dams, irrigation projects, and barrages (barriers in the river to divert flow or increase depth) are present in the Mahanadi River basin, the most prominent of which is

Hirakud Dam. At the time of its completion in 1957, Hirakud Dam was the longest earthen dam in the world; it remains the largest reservoir in Asia with a surface area of 746 km^2, and a live storage capacity of 5.37 x 109 m3 (cubic meters). Approximately 65 percent of the basin is upstream from the dam. The average annual discharge is 1,895 m^3/sec, with a maximum of 6,352 m^3/sec during the summer monsoon. Minimum discharge is 759 m^3/s and occurs during the months October through June.

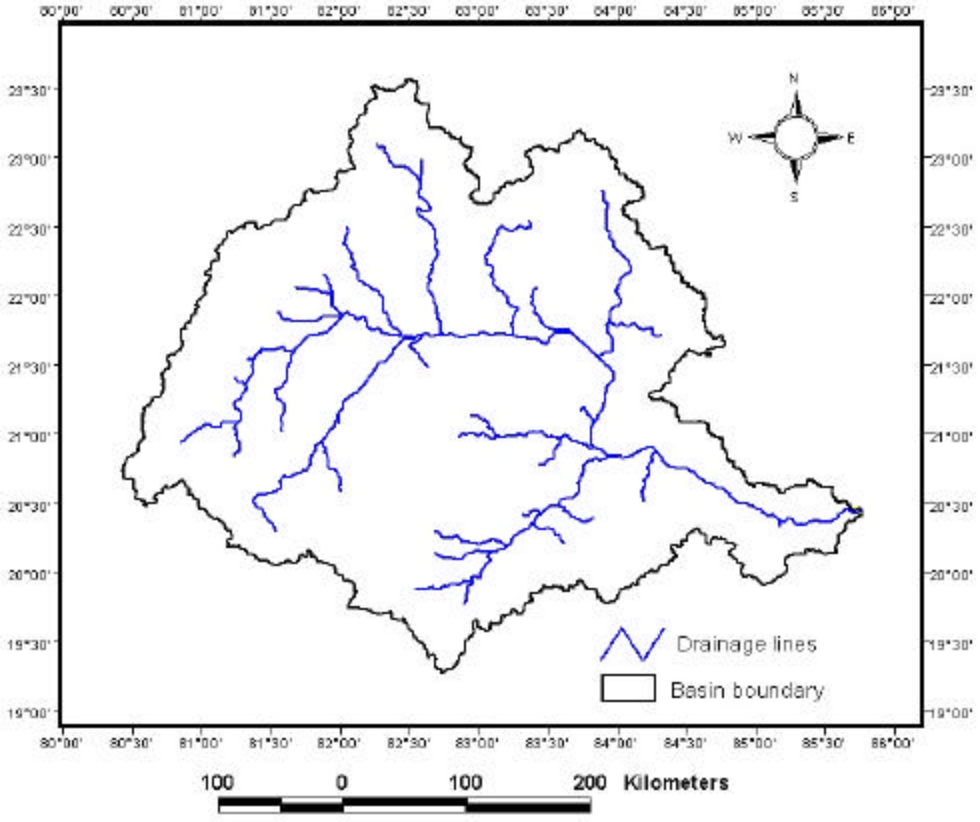

Fig.4.2Basin boundary with drainage network

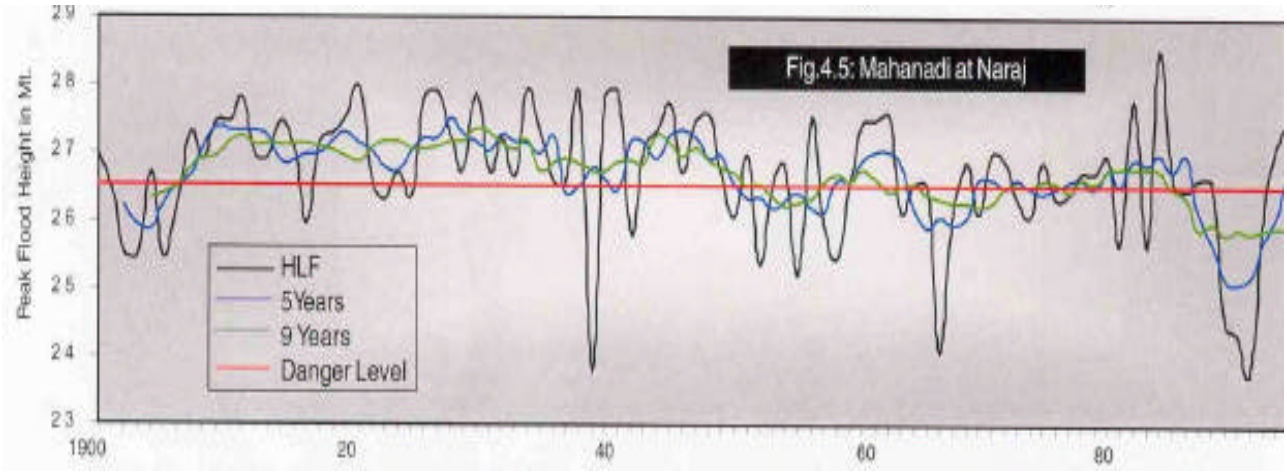

Fig.4.3 The HFL of Mahanadi at Naraj for various Recurrence Intervals (Source: Mishra, 2001)

4.3 Challenges faced by the Basin (Problem of Floods and Droughts):

Mahanadi is the largest river in Orissa with an extensive delta responsible for most of the devastating flood hazards in the coastal zone. Because of a large number of distributaries, the flood discharge at Naraj implies flood in most of the distributaries remaining downstream. Over a period of 146 years between 1855 to 2000, there were 28 high flood years, 57 medium flood years and 48 low flood years (Orissa State Disaster Management Authority). The recurrence interval of a high flood in the Mahanadi is 5 years and that of a medium and low flood is 3 years. It is needless to stress here that the Mahanadi experiences flood every year be it a high, medium or low. The Hirakud dam (1957) was made to alleviate the problem of flood and since then it is serving the purpose to a large extent but possibly will not in the coming future owing to the serious problem of siltation which accounts for the reduction in its volumetric storage capacity. It is evident from the figure 4.3 that after the construction of Hirakud dam in 1957, the flood level was reduced considerably. The inhabited inner basin Chhattisgarh plain and KBK (Koraput, Bolangir, Kalahandi districts) in western Orissa at the boundary of Chattisgarh & Orissa suffers frequent droughts whereas the fertile deltaic area has been wrecked by repeated floods.

4.4 Climate:

Mahanadi basin enjoys a tropical monsoon type of climate like most other parts of the country. The south-west monsoon normally arrives in 1st week of June in the coastal plain, and by 1st July the whole of the basin is under the full sway of the south-west monsoon. The maximum precipitation is usually observed in the month of July, August and first half of September. Normal annual rainfall of the basin is 1360 mm (16% CV) of which about 86% i.e. 1170 mm occurs during the monsoon season (15% CV) from June

to September (Rao, 1993). The river passes through tropical zone and is subjected to cyclonic storms and seasonal rainfall. The cyclonic storm usually originates in the Bay of Bengal and travels generally in North-Westerly direction opposite to the flow of the river Mahanadi. Heavy rainfall first occurs in delta and then spreads in-land covering in about two days. Owing to the topographical characteristics the climate is variable. In the winter the mean daily minimum temperature varies from 4°C to 12°C. The month of May is the hottest month, in which the mean daily maximum temperature varies from 42°C to 45.5°C.

4.5 Physiography and Soils:

Physiographically, the basin can be divided into following regions, namely Northern Plateau, the Eastern Ghats, Chattisgarh plains, the Coastal Plain and the erosional Plains of Central Table Land. The first two are hilly regions. The coastal plain is the central interior region of the basin, traversed by the river and its distributaries. The main soil types found in the basin are red and yellow soils, mixed red and black soils (laterite soils). Clay predominates in the middle and lower reaches of the drainage channels and in the upstream channel somewhere rocks are also found. The Central Table Land comprising the Mahanadi – Tel basin as well as the whole of the northern portion of the region from Sundargarh to Mayurbhanj contains red soil which is somewhat poor for plant life. The river basin contains some of the fertile parts of the state, mostly in Bolangir, Sambalpur, and Dhenkanal districts. The Mahanadi-Tel basin in the northwestern part of the region is the most populous and agriculturally prosperous part of the area with compact settlements. As per the rain factor, the northern plateau, the central tableland, the Eastern Ghat and the coastal regions may be included in the semi-humid type.

4.6 Agriculture and Landuse:

Agriculture is the mainstay of basin's economy and sustenance of the life of the people. The Mahanadi irrigates a fertile valley whose chief crops are rice, oilseed, and sugarcane. Development of Agriculture in the basin has lagged behind due to several constraints, such as traditional method of cultivation, inadequate capital formation and low investment, inadequate irrigation facilities and uneconomic size of holdings. Among the crops, paddy is is a staple cereal and is raised by the tribal people as a cash crop also. Rice is most widely cultivated in the river valley; millets are cultivated in drier interior parts. Gram, mung, black gram, pea, mustard, linseed, groundnut, jute, sugarcane are other miscellaneous crops. In general, region has highly diversified cropping pattern, which minimize risk arising out of moisture stress. Forests are largely controlled by rainfall and temperature conditions of the region. Most of the areas in lower Mahanadi basin are dominated by forest. The forest types include the tropical moist deciduous, the

tropical dry deciduous and the coastal forests. Most of the reserve forests are concentrated in the north and north-east of the Mahanadi.

4.7 Socio-economic Aspects:

The basin is heavily populated, with a population density of 3.6 people per sq km, with some areas exceeding 36 people per sq km. The indigenous tribal population constitutes a good portion of Chattisgarh as well as Orissa's population. Whatever developmental activities have taken place have more or less bypassed them and they remain marginalised and outside the mainstream. This is a major developmental challenge both in terms of economic growth and, more importantly, socio-cultural perspective. Three important urban centres in the basin are Raipur, Durg & Cuttack. Mahanadi, because of its rich mineral reserve and adequate power resource has a favourable industrial climate. The important industries presently existing in the basin are iron & steel plant at Bhilai, aluminum factories at Hirakund and Korba, paper mill near Cuttack and cement industries at Sundargarh. Other industries based primarily on agricultural produce are sugar, textile and oil mills. Mining of coal, iron and manganese are other industrial activities.

Field photographs collected during field work has been shown in fig. 4.4. Various landcover type predominant in the basin are illustrated. The basin outlet (Barrage) at Mundali station is shown in the last photograph.




Paddy fields in Orissa and Chattisgarh




Waste land

Industrial area




Forested land near Cuttack, Orissa

Basin outlet: Mundali

Fig 4.4 Field photographs showing landcover types and basin outlet

CHAPTER 5 - MATERIALS AND METHODOLOGY

This chapter deals with the description of various datasets used in the study and elaborates the step by step methodology of the work carried out. Procedures for generating various input parameters and thematic layers to model hydrology and map historical and current landcover of the Mahanadi basin has been described. Method of simulation, calibration and validation of the model has also been mentioned.

5.1 **Materials used in the study**

5.1.1 **Remote Sensing data:**

IRS-P6 AWiFs data: Cloud free satellite data of AWiFs (Advanced Wide Field Sensor) dated 25 Jan 2006 (path 103 row 58) covering whole of the Mahanadi river basin was acquired from National Remote Sensing Agency (NRSA) Hyderabad. IRS-P6 AWiFs data has been widely used to monitor croplands, crop acreage estimation and crop yield forecasting. With its high repetivity, radiometric and spatial resolution and wide coverage, it is particularly suitable for studying landcover dynamics on regional scales. The specifications of AWiFs sensor are listed in Table 5.1 and a false colour composite has been shown in Fig. 5.1. This data was used to prepare landcover map for the period 2003-06.

IGFOV (Spatial resolution)	56 m (nadir) 70 m (at field edge)
Spectral Bands	B1 (VIS): 0.52-0.59
	B2 (VIS): 0.62-0.68
	B3 (NIR): 0.77-0.86
	B4 (SWIR): 1.55-1.7
Satellite	IRS-P6 (Resourcesat-1)
Swath	740 km (combined)
Quantization	10 bits

Table 5.1 Specifications of AWiFs Sensor onboard IRS-P6 (Resourcesat-1) satellite

NOAA AVHRR data: AVHRR (Advanced Very High Resolution Radiometer) multidate geo-referenced images of the study area were acquired from the website http://www.class.ngdc.noaa.gov/saa/products. The multidate images were of 1st Nov 1985 and 11th April 1985 and were used to map landcover for the year 1985. AVHRR data provide opportunities for studying and monitoring vegetation conditions in ecosystems including forests, tundra and grasslands. Applications include agricultural assessment,

land cover mapping, producing image maps of large areas such as countries or continents, and tracking regional and continental snow cover. AVHRR data are also used to retrieve various geophysical parameters such as sea-surface temperatures and energy budget data. The specification of AVHRR data use here is listed in Table 5.2. A colour composite made out of AVHRR imagery is shown in Fig. 5.2.

Data type:	Full Resolution Area coverage (FRAC) Level 1B
Spatial resolution	1.1 km
Spectral bands	5
Scanning frequency	twice per day
Satellite	NOAA series

Table 5.2 Specifications of AVHRR

LANDSAT MSS data: LANDSAT was the first earth observing satellite series (started in 1970's) providing high resolution low cost satellite images of almost all areas of the world. It therefore, became the first choice to derive historical landcover information of the 1970's. Landsat MSS (Multi Spectral Scanner) data of Mahanadi basin was downloaded from Earth Science Data interface of GLCF (Global Land Cover Facility) website (http://glcfapp.umiacs.umd.edu:8080/esdi). Various scenes of multiple dates were downloaded since a single scene does not cover whole basin. Images were acquired for the month of Jan-Feb, Nov-Dec 1972-73 to map the historical landcover over the basin. Table 5.3 shows specifications of MSS sensor and Fig. 5.3 shows a standard false colour composite (mosaic image and haze reduction) of the area.

Spatial Resolution:	80-meter
Swath Width:	185 km
Revisit Time:	16 -18 days
Operational Dates:	since 1972
Wavelength Regions	0.50 to 0.60 um [green] 0.60 to 0.70 um [red] 0.70 to 0.80 um [NIR] 0.80 to 1.10 um [IR]

Table 5.3 LANDSAT MSS Specifications

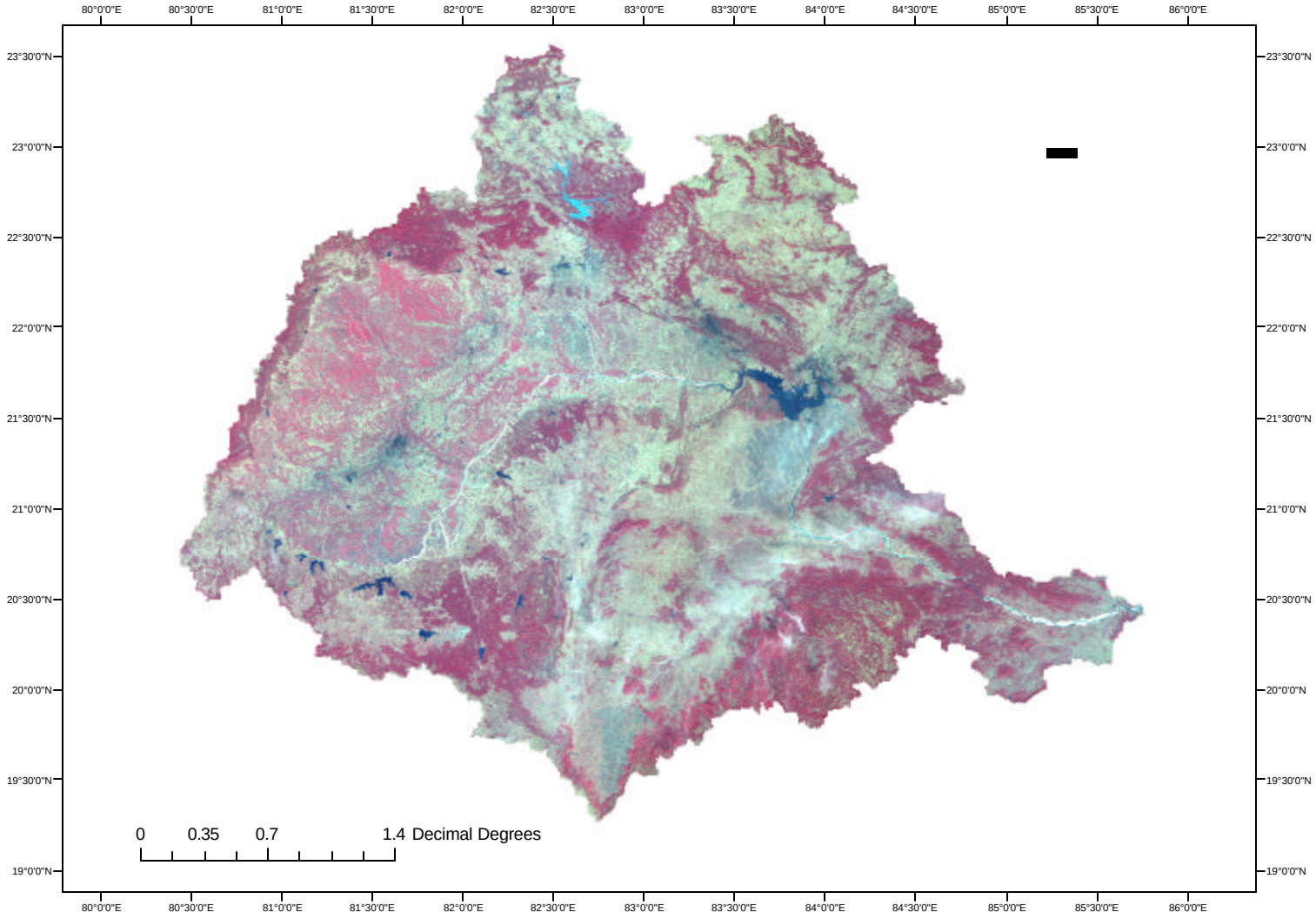

Fig. 5.1 AWiFs FCC of Mahanadi basin dated 25th Jan'06

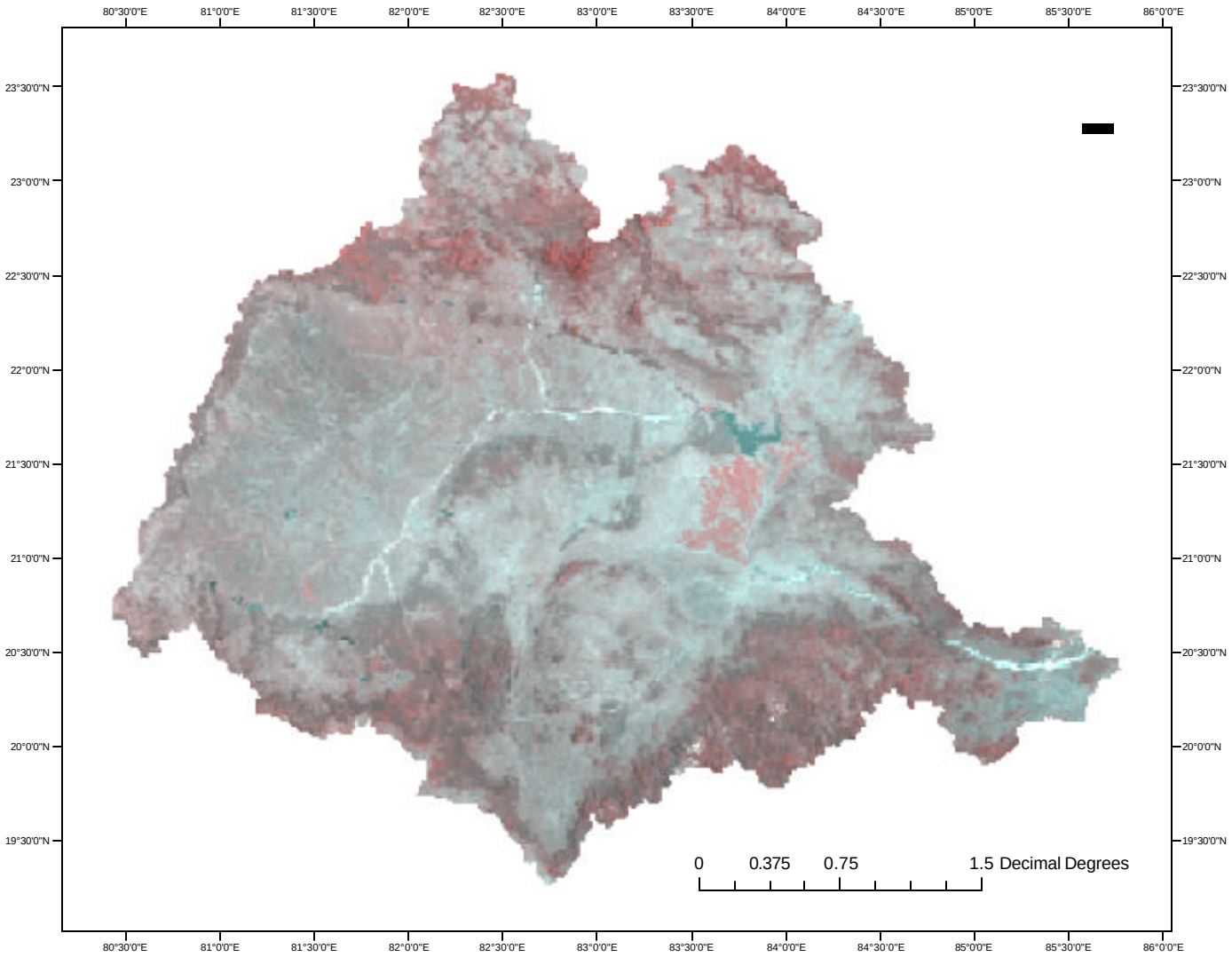

Fig. 5.2 AVHRR FCC of Mahanadi basin dated 1st Nov'85

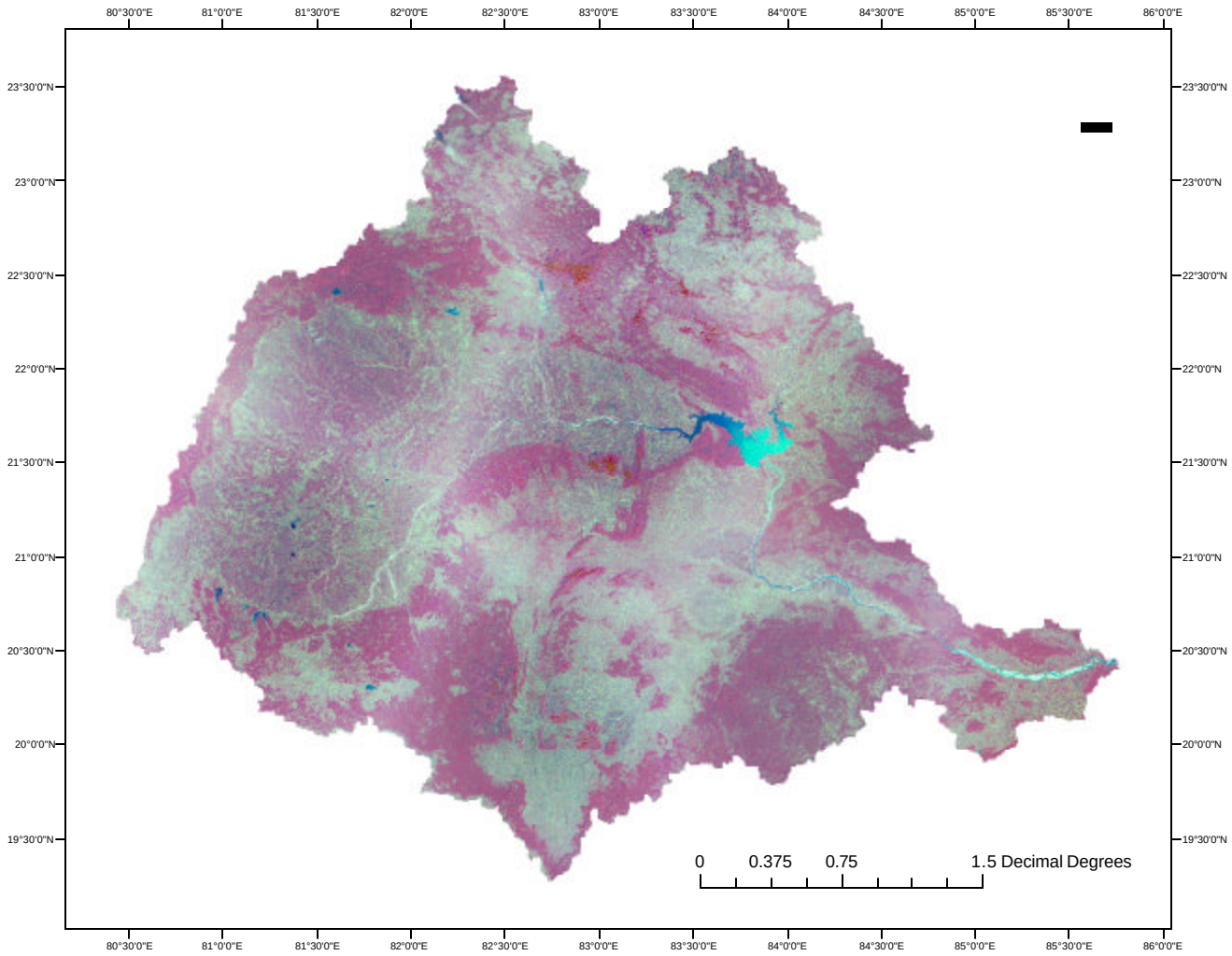

Fig. 5.3 FCC of Landsat MSS (1972) of Mahanadi basin (Mosaic)

MODIS Leaf Area Index (MODIS 15A02)**:**

The LAI variable defines the number of equivalent layers of leaves relative to a unit of ground area, whereas FPAR measures the proportion of available radiation in the photosynthetically active wavelengths that are absorbed by a canopy. Both variables are used as satellite-derived parameters for calculating surface photosynthesis, evapotranspiration and net primary production, which in turn are used to calculate terrestrial energy, carbon, water cycle processes, and biogeochemistry of vegetation. Leaf Area Index/ FPar (8-Day L4 Global 1 km ISIN Grid V004) data product derived from MODIS reflectance onboard MODIS/TERRA satellite platform was used for derivation of Leaf area indices for the study area. The data product has 1 km spatial resolution and was downloaded from NASA's Goddard Space Flight Centre website (http://modis-land.gsfc.nasa.gov) for the 2nd and 3rd week of each month of year 2003. The processed LAI stacked image is shown in fig. 5.4. Water bodies have been masked.

MODIS Albedo Product (MOD43B3)**:**

Albedo is defined as the ratio of upwelling to downwelling radiative flux at the surface. Downwelling flux may be written as the sum of a direct component and a diffuse component. Black-sky Albedo (Directional hemispherical reflectance, albedo in the absence of a diffuse component) and white-sky Albedo (bi-hemispherical reflectance, albedo in the absence of direct component mark the extreme cases of completely direct and completely diffuse illumination. Actual Albedo is a value which is interpolated between these two as a function of the fraction of diffuse skylight which itself is a function of aerosol optical depth.

The MOD43B3 Albedo Product provides both the white-sky albedos and the black-sky albedos (at local solar noon) for MODIS bands 1-7 as well as for three broad bands (0.3-0.7µm, 0.7-5.0µm, and 0.3-5.0µm). While the total energy reflected by the earth's surface in the shortwave domain is characterized by the shortwave (0.3-5.0µm) broadband albedo, the visible (0.3-0.7µm) and near-infrared (0.7-5.0µm) broadband albedos are often also of interest due to the marked difference of the reflectance of vegetation in these two spectral regions. MODIS/ TERRA Albedo (16-Day L3 Global 1 km SIN Grid V004) data product of 1 km spatial resolution was downloaded from NASA's GSFC website one for each month of the year 2003. The processed shortwave broadband Albedo image for study region is shown in fig. 5.5.

GTOPO 30 Digital Elevation Model:

GTOPO30 is a global digital elevation model (DEM) with a horizontal grid spacing of 30 arc seconds (approximately 1 kilometer). GTOPO30 was derived from several raster and vector sources of topographic information. GTOPO30, completed in late 1996, was developed over a three year period through a collaborative effort led by staff at the U.S. Geological Survey's Center for Earth Resources Observation and Science (EROS). The data was acquired from the URL: (http://edc.usgs.gov/products/elevation/gtopo30/gtopo30.html) for basin delineation and drainage network extraction.

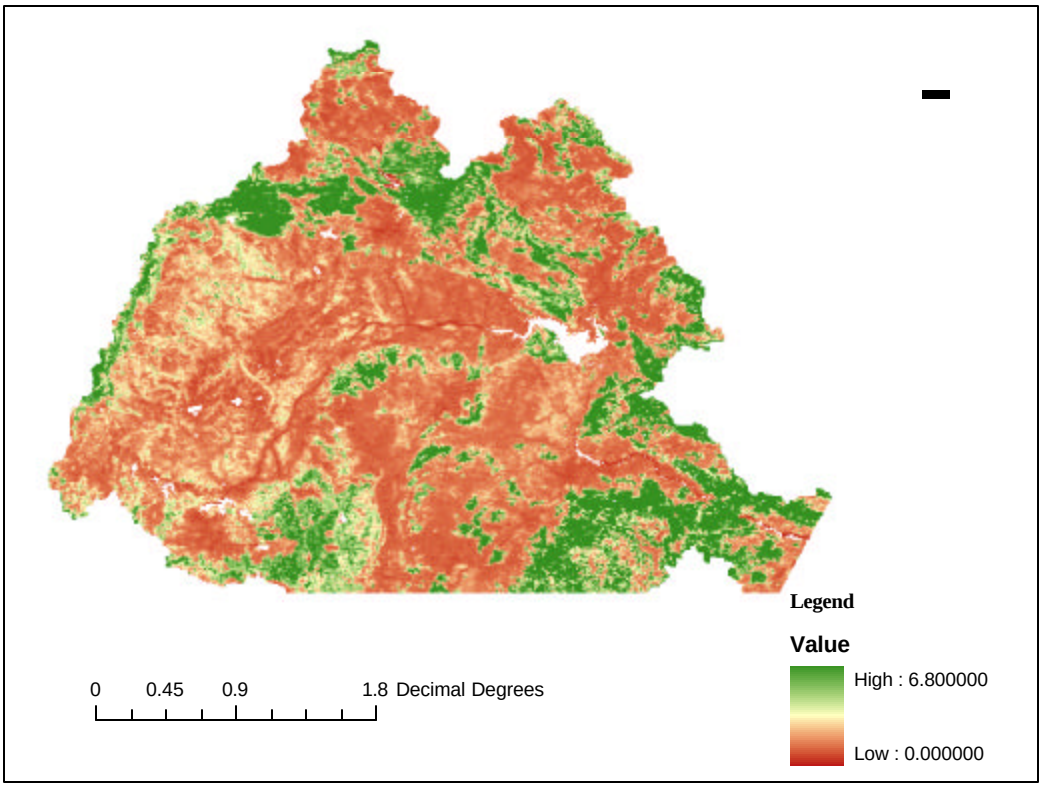

Fig. 5.4 Leaf Area Index map

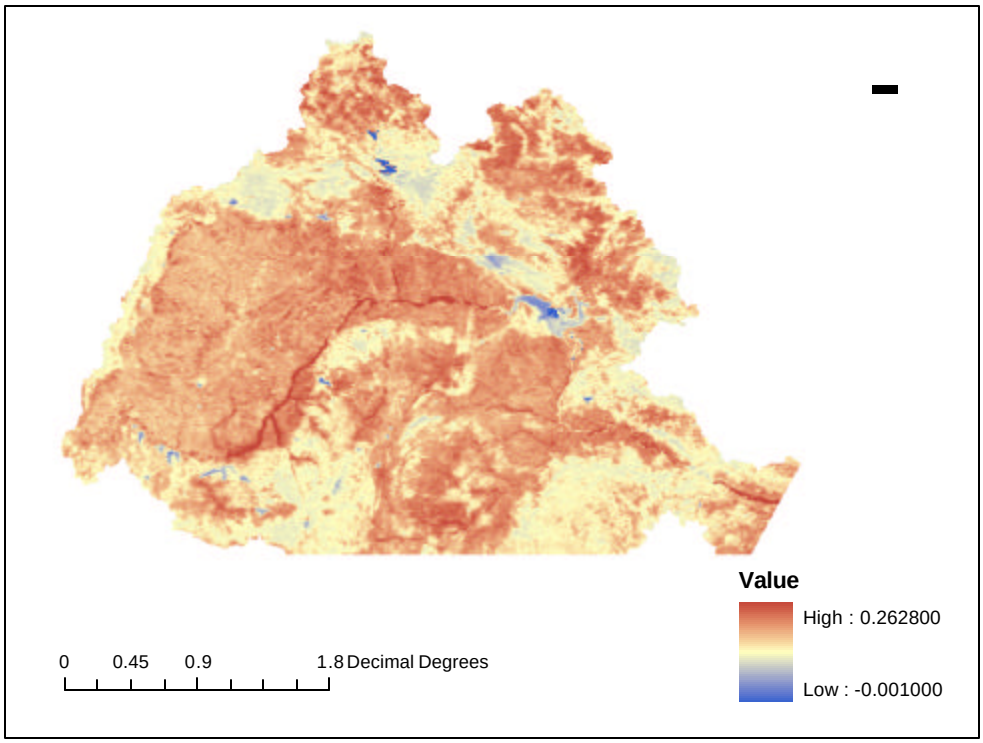

Fig. 5.5 MODIS Albedo map

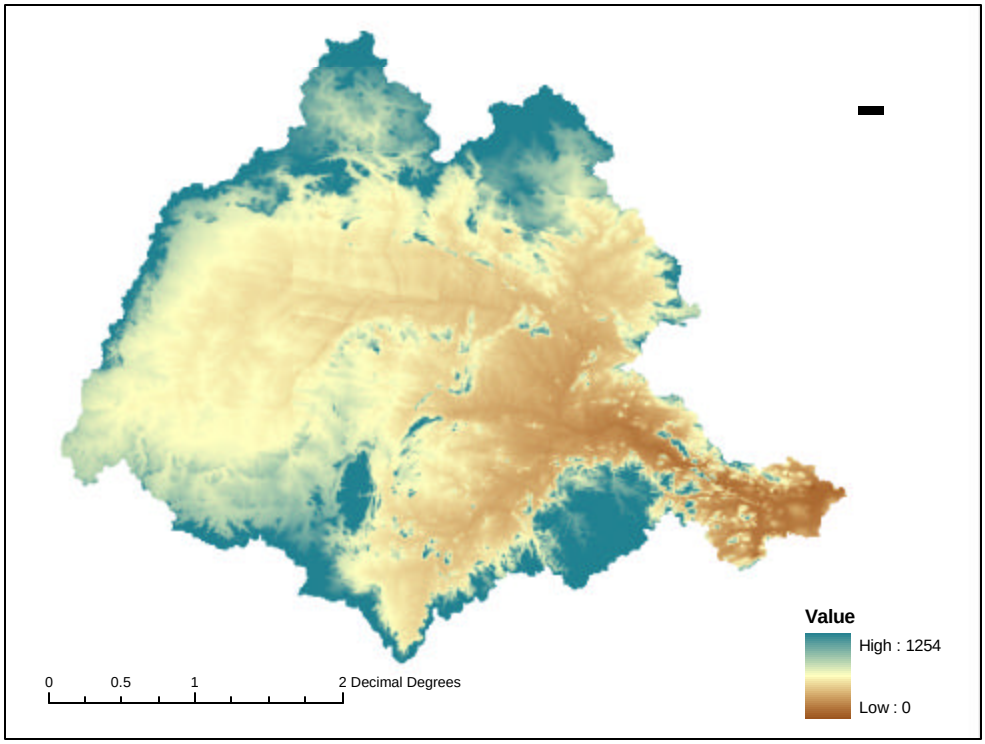

Fig 5.6 GTOPO 30 Digital Elevation Model of Mahanadi basin

5.1.2 Hydro-meteorological data:

Rainfall:

An interpolated $1^{o}x1^{o}$ gridded daily rainfall dataset (Rajeevan et al., 2006) developed by India Meteorological Department (IMD) Pune was used to derive daily rainfall in mm over the study watershed. The IMD product uses gauge data from 1803 stations from period 1951 to 2003 to estimate accumulated rainfall in the 24 hours ending 0830 IST (0300 Z). Comparison with similar global gridded rainfall data sets revealed that the present rainfall analysis is better in accurate representation of spatial rainfall variation (Rajeevan et. al.2006). The Global data sets underestimate the heavy rainfall along the west-coast and over Northeast India. The inter-annual variability of southwest monsoon seasonal (June-September) rainfall was found to be similar in all the data sets.

Temperature:

Daily maximum and minimum temperature data was obtained from NCDC (national Climatic Data Centre) of NOAA. This point dataset is available for selected station worldwide. In the present study data was available for 6 stations for year 2003 namely Balasore, Bhubaneshwar, Raipur, Jabalpur, Jagdalpur and Jharsuguda falling within the basin. Data was downloaded from the web link (http://www.ncdc.noaa.gov/oa/mpp).

Discharge data (Observed):

Observed hydrological and meteorological data were collected for model calibration and validation of the results. These includes the discharge data from Central Water Commission (CWC), Bhubaneswar and Hirakud Dam Project (HDP), Burla in Orissa. Station wise availability of data is presented in table 5.4.

Sl. No.	Station Name	Gauge Incharge	Discharge Data	Stage Discharge	Rain fall Data
1	Kantamal	CWC	A	N.A	N.A
2	Sundergarh	CWC	A	N.A	N.A
3	Simga	CWC	A	N.A	N.A
4	Seorinarayan	CWC	A	N.A	N.A
5	Andhiarkore	CWC	A	N.A	N.A
6	Baminidihi	CWC	A	N.A	N.A
7	Mundali	HDP	A	A	A

Table 5.4 Availability of data at different gauging sites

(CWC: Central Water Commission, **A**: Available, **N.A**: Not Available)

5.1.3 Ancillary data:

NBSSLUP soil map:

Digitized soil maps of Madhya Pradesh and Chattisgarh were obtained at 1:50,000 scale. Soil mapping for Indian region has been done by NBSSLUP (National Bureau of soil survey and Landuse planning), Nagpur. Some of the associated soil properties were also derived from it.

Reference Landcover maps:

Global Land Cover (GLC 2000) for South-Asian region developed by Indian Institute of Remote sensing, Dehradun was used as a reference for mapping landcover in the region. This global landcover dataset can be obtained from link (http://www-gvm.jrc.it/glc2000/Products). Biodiversity maps of Chattisgarh and Orissa from the project entitled 'Biodiversity characterization at Landscape level' were also referred to derive vegetation cover type in the area.

Others:

LDAS 8th database and MM5 Terrain dataset for extraction of physical parameters of the vegetation was used.
(http://ldas.gsfc.nasa.gov/LDAS8th/MAPPED.VEG/web.veg.monthly.table.htnl)

5.1.4 Software's used:

ERDAS Imagine 8.7, ArcGIS 9.1, ENVI, Hec-GeoHMS.

5.2 METHODOLOGY

5.2.1 Basin delineation and stream network extraction:

Basin boundary and drainage characteristics of the watershed were derived in HEC - GeoHMS module in ArcView 3.2a software using GTopo30 USGS Digital elevation model (1 km resolution) as major input. Following operations were performed step by step:

- Fill Sinks
- Flow Direction
- Flow Accumulation
- Stream Definition
- Stream Segmentation
- Watershed Delineation
- Watershed Polygon Processing
- Stream Segment Processing
- Watershed Aggregation

In the first step, a fill grid map is generated after correcting the Digital elevation model for sinks. Flow direction map is derived from this fill sink map and subsequently a flow accumulation map is derived from it. Stream definition is derived from this flow accumulation by specifying the maximum threshold area for delineating drainages. A sub-watershed for each delineated stream is then extracted. To extract the basin boundary, an outlet at Mundali station in the Mahanadi river basin was defined. Finally, a basin for the defined outlet is delineated along with the river network. It can further subdivide basin into desired number of sub-watersheds by specifying various outlets where the gauging station exists along the extracted drainage. The flowchart of derivation is illustrated in Fig 5.7, 5.8, 5.9 and 5.10.

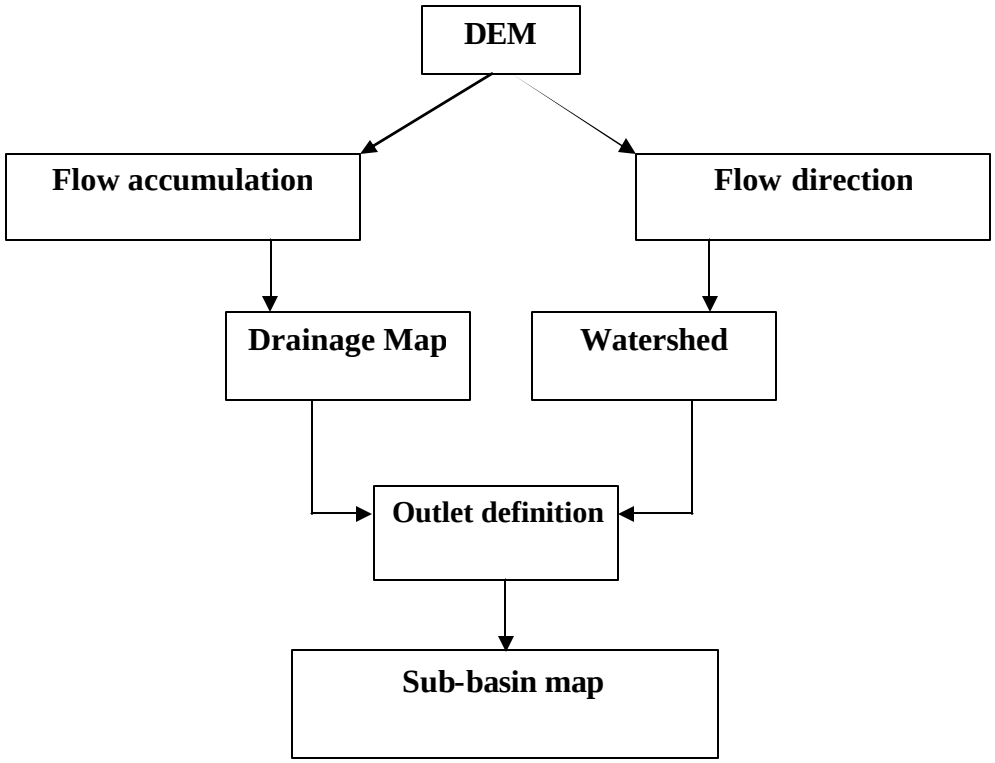

Fig 5.7 Flow chart showing Sub-Basin delineation

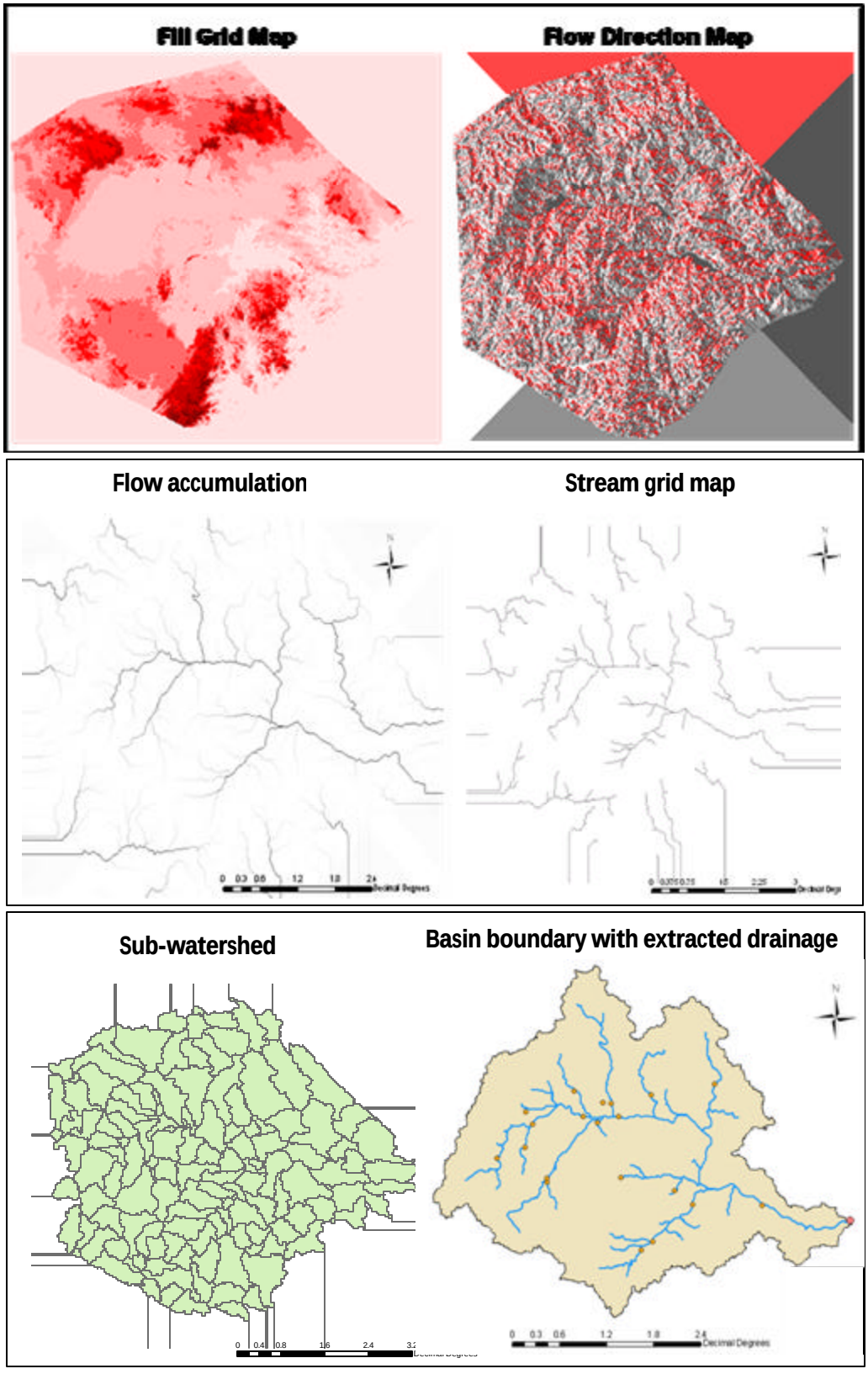

Fig.5.8 Basin delineation and drainage extraction from Digital elevation model

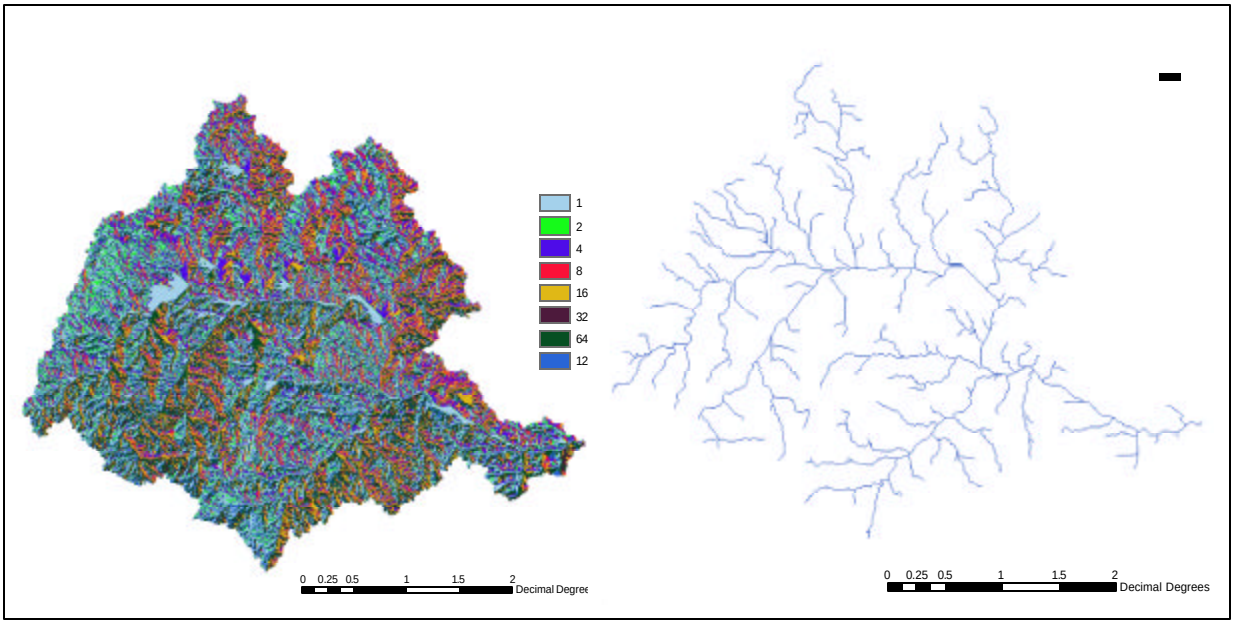

Fig 5.9 Extracted flow direction (L) and dense stream network (R) of the Mahanadi basin

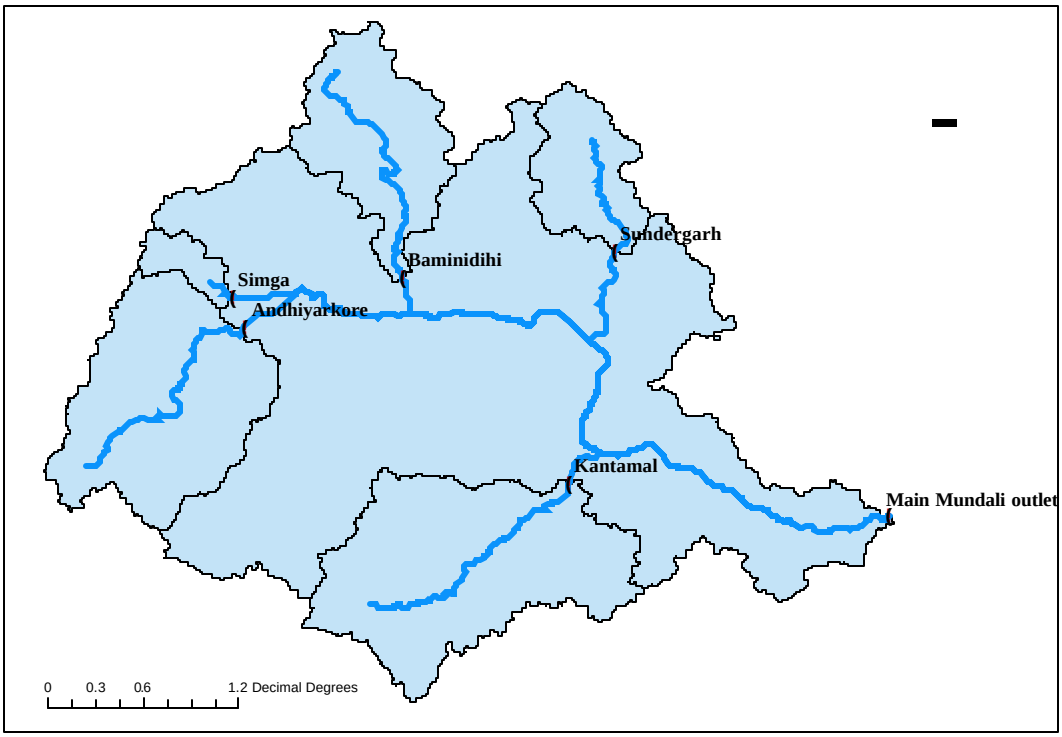

Fig 5.10 Mahanadi basin with 6 sub-basins and river network

5.2.2 Grid generation over the Basin:

A square grid of area 25 X 25 square km (Fig 5.11) was generated over the study region. There were in all 267 such grids falling in the basin. This extracted grid network for the basin was used to overlay with the other thematic layers and hence define the distribution of various parameters and properties in the basin. VIC model requires the definition of input parameters for each grid distributed uniformly over the area.

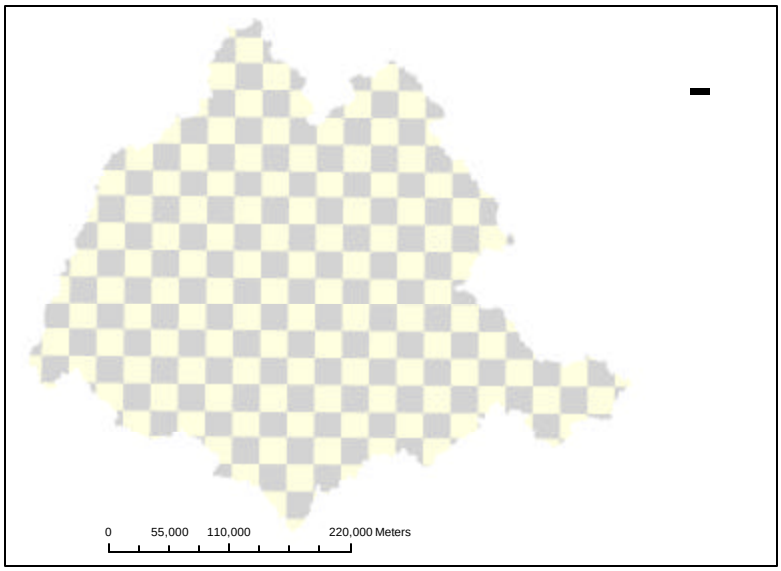

Fig 5.11 Grid map over basin (25x25 sq. km)

5.2.3 Landuse landcover mapping of the basin:

Historical and current landcover mapping of the Mahanadi river basin was done to see the changes that have taken place over time. Remote sensing based satellite images being most reliable and offering synoptic views of large areas were the viable option to study landcover dynamics on a regional scale.

LANDSAT MSS images of 1972-73 were downloaded, preprocessed and mosaicked to create a seemless image of the whole basin. Since the individual images were of different dates, classifying the mosaic into landcover types was not feasible. So, the individual images were classified using unsupervised classification (Isodata clustering) technique into several classes (200) and they were merged based on their spectral signatures into 7 landcover types (Table 5.5). The preliminary classified layer was then improved using visual interpretation approach. Thus, an integrated digital and visual classification was attempted to map landcover since a single technique would not have been feasible for regional mapping. The individual classified images were then mosaicked and clipped by the basin boundary (Fig 6.1). Landcover mapping for 1985 was done using NOAA AVHRR images (1 km resolution) whereas AWiFs (56 m resolution) was used to prepare

for the year 2003. The same approach of unsupervised classification and visual interpretation technique was followed to perform the task. The landuse/ landcover maps of Mahanadi basin for 1985 and 2003 are shown in fig. 6.2 and 6.3. GCP's (ground control points) were used to improve and validate classification scheme. Classification accuracy of more than 70% was achieved using this approach.

1	Water body
2	DF/moist deciduous forest
3	SF/dry deciduous forest
4	Agriculture
5	Built up/settlement
6	Barren land
7	River bed (dry)

Table 5.5 Identified landcover classes

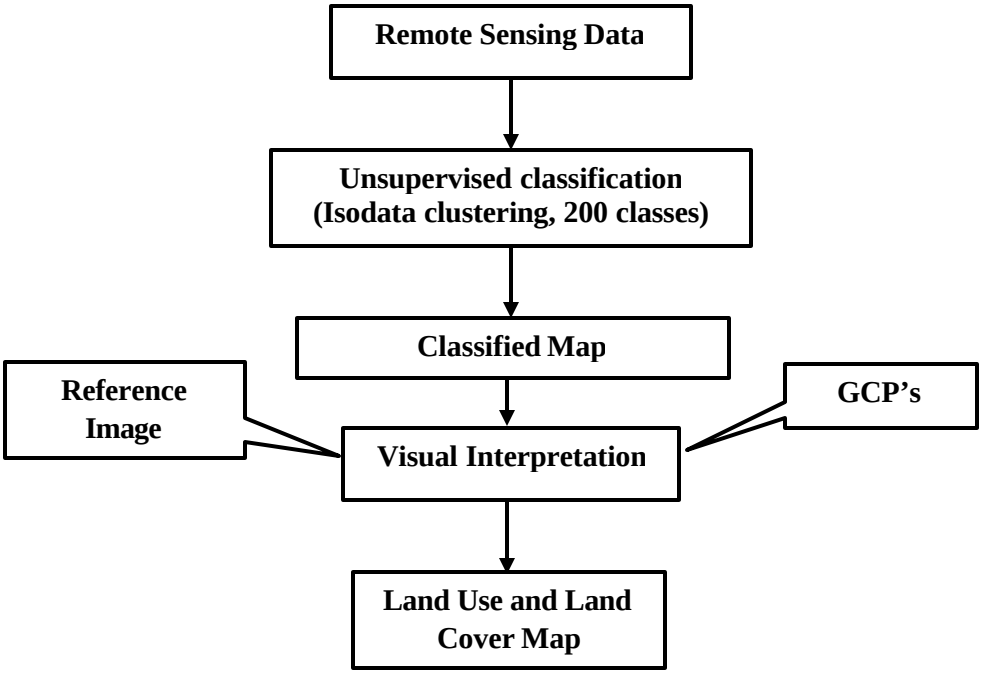

Fig 5.12 Flow diagram of landuse/ landcover map preparation

5.3 Preparation of Input database for modelling:

Four major input files are required to make the VIC model input database. They are Vegetation parameter file, Vegetation Library file, Soil parameter file and Forcing files. The data in these files is stored in the ASCII format.

5.3.1 S**oil parameter file:**

A soil parameter file describes the characteristics of each soil layer for each grid cell. This is also where other basic grid cell information is defined like grid cell no., lat-long of the grids (which serves as a link to other parameter files), mean elevation etc (Table 5.6). The parameters needed to be specified in Soil parameter file are listed in the following table:

Sl no	**Variable Name**	**Units**	**Values**	**Description**
1	RUN	N/A	1	1 = Run Grid Cell, 0 = Do Not Run
2	gridcel	N/A	1	Grid cell number
3	lat	degrees	1	Latitude of grid cell
4	lon	degrees	1	Longitude of grid cell
5	infilt	N/A	1	Variable infiltration curve parameter (b_{infilt})
6	Ds	fraction	1	Fraction of Dsmax where non-linear baseflow begins
7	Dsmax	mm/day	1	Maximum velocity of baseflow
8	Ws	fraction	1	Fraction of maximum soil moisture where non-linear baseflow occurs
9	c	N/A	1	Exponent used in infiltration curve, normally set to 2
10	expt	N/A	Nlayer	Parameter describing the variation of Ksat with soil moisture
11	Ksat	mm/day	Nlayer	Saturated hydrologic conductivity

12	Phi_s	mm/mm	Nlayer	Soil moisture diffusion parameter
13	Int_moist	mm	Nlayer	Initial layer moisture content
14	elev	m	1	Average elevation of grid cell
15	depth	m	Nlayer	Thickness of each soil moisture layer
16	bulk_density	kg/m^3	Nlayer	Bulk density of soil layer
17	soil_density	kg/m^3	Nlayer	Soil particle density, normally 2685 kg/m^3
18	off_gmt	hours	1	Time zone offset from GMT
19	Wrc_fract	fraction	Nlayer	Fractional soil moisture content at the critical point (~70% of field capacity) (fraction of maximum moisture)
20	wpwp_fract	fraction	Nlayer	Fractional soil moisture content at the wilting point (fraction of maximum moisture)
21	rough	m	1	Surface roughness of bare soil
22	annual_prec	mm	1	Average annual precipitation.
23	resid_moist	fraction	Nlayer	Soil moisture layer residual moisture.
24	fs_active	1 or 0	1	Set to 1, frozen soil algorithm is activated for the grid cell. 0 indicates that frozen soils are not computed even if soil temperatures fall below 0°C.

Table 5.6: Soil and thermal Parameter file (Source: http://www.hydro.washington.edu)

Mean elevation values for each grid were derived from Digital elevation model. The primary data source to prepare this input was digital soil texture map prepared from NBSS & LUP (National Bureau of Soil Survey and Landuse Planning, Nagpur) soil maps (scale-1:50,000) shown in Fig 5.13. Soil texture map was rasterised and overlaid with the

grid map to extract dominant soil type in each grid. The second soil layer was taken as FAO global soil map of the world. All other parameters except c, elev, depth, off_gmt, rough, and annual prec are a function of soil texture and were derived using soil hydraulic properties index defined in VIC model documentation (http://www.hydro.washington.edu).

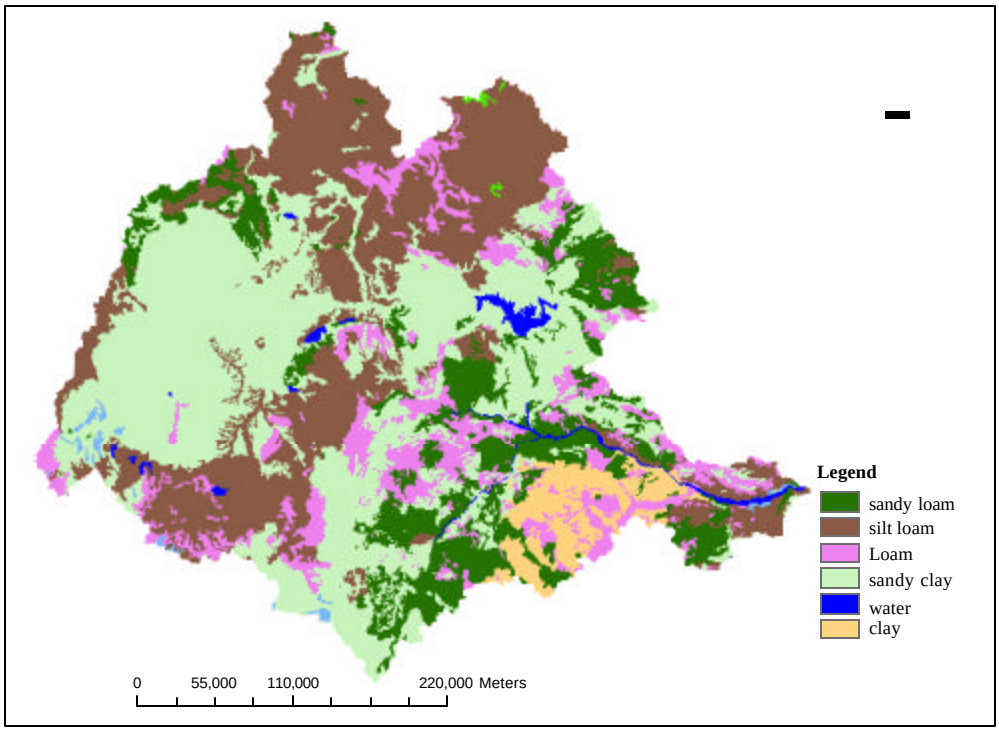

Fig 5.13 NBSS & LUP soil map of Mahanadi river basin

5.3.2 **Vegetation parameter file**:

The vegetation parameter file describes the vegetative composition of each grid cell, and uses the same grid cell numbering as the soil file (latitudes and longitudes are not included in the file). This file cross-indexes each vegetation class (from any land-cover classification scheme) to the classes listed in the vegetation library. To prepare this file, landuse map was overlaid on the grid map and the no. of vegetation classes as well as fraction of grid covered by those classes was extracted. A small code in C language was used to read this information from crossed map and arrange it in the format specified by the model. Root depths for landcover types were accepted as recommended by Canadell et. al. (1996). Description of the variables required to be specified in the Vegetation parameter file are given in Table 5.7:

Sl. no	Variable Name	Units	Description
1	Gridcel	N/A	Grid cell number
2	Vegetation_type_no	N/A	Number of vegetation types in a grid cell
3	Veg_class	N/A	Vegetation class identification number
4	Cv	fraction	Fraction of grid cell covered by vegetation type
5	Root_depth	m	Root zone thickness (sum of depths is total depth of root penetration)
6	Root_fraction	fraction	Fraction of root in the current root zone

(Source: http://www.hydro.washington.edu)

Table 5.7 Vegetation parameter file

It was assumed that the specified root zone contains all of the roots of a landcover type.

5.3.3 **Vegetation library file:**

For the selected land cover classification of the study area, a vegetation library file was set up. This describes the static (varying by month, but the same values year-to-year) parameters associated with each land cover class. Table 5.8 below lists various parameters required to be specified in the vegetation library file.

Sl. no	Variable Name	Units	Number of Values	Description
1	veg_class	N/A	1	Vegetation class identification number (reference index for library table)
2	overstory	N/A	1	Flag to indicate whether or not the current vegetation type has an overstory (TRUE for overstory present, FALSE for overstory not)
3	rarc	s/m	1	Architectural resistance of vegetation type (~2 s/m)
4	rmin	s/m	1	Minimum stomatal resistance of vegetation type (~100 s/m)
5	LAI		12	Leaf-area index of vegetation type
6	albedo	fraction	12	Shortwave albedo for vegetation type
7	rough	m	12	Vegetation roughness length (typically 0.123 * vegetation height)
8	displacement	m	12	Vegetation displacement height (typically 0.67 * vegetation height)
9	wind_h	m	1	Height at which wind speed is measured.
10	RGL	W/m^2	1	Minimum incoming shortwave radiation at which there will be transpiration. For trees this is about 30 W/m^2, for crops about 100 W/m^2.

11	rad_atten	fraction	1	Radiation attenuation factor. Normally set to 0.5, though may need to be adjusted for high latitudes.
12	wind_atten	fraction	1	Wind speed attenuation through the overstory. The default value has been 0.5.
13	trunk_ratio	fraction	1	Ratio of total tree height that is trunk (no branches). The default value has been 0.2.
14	comment	N/A	1	Comment block for vegetation type. Model skips end of line so spaces are valid entries.

Table 5.8: Vegetation library file
(Source: http://www.hydro.washington.edu)

LAI defines an important structural property of a plant canopy as the one sided leaf area per unit ground area. For derivation of LAI, MODIS LAI maps (MOD 15A02 product) were downloaded from NASA's gsfc website (www.modis-land.gsfc.nasa.gov). For each month of the year 2003 two images of the middle weeks were downloaded, imported to .img format in ERDAS Imagine, reprojected to Albers conical equal area projection (Table 5.9), averaged and multiplied by a scale factor 0.1 and subsetted using the boundary of the basin. The 12 images so obtained were stacked into one having 12 layers. For each landuse class, sufficient no. of cloud free points were chosen and their LAI profile on the stacked image was drawn. An average monthly value of those points was taken as the LAI value in each month for that landuse class. Fig 5.14 below shows the trend in LAI values for each landuse type. Albedo was also derived from MODIS BRDF/ Albedo product in the same way (Fig 5.15). Other variables like roughness length, displacement height, overstory, architectural resistance, minimum stomatal resistance were derived from LDAS 8th database (http://ldas.gsfc.nasa.gov/LDAS8th/MAPPED.VEG/web.veg.monthly.table.html) and MM5 terrain dataset.

Projection	Albers Conical Equal Area Projection
Spheroid	WGS-84
Datum	WGS-84
Latitude of 1st standard parallel	12:00:00:00 N
Latitude of 2nd standard parallel	28:00:00:00 N
Longitude of Central meridian	78:00:00:00 E
Latitude of Origin of projection	20:00:00:00 N
False easting at central meridian	2000000 m
false northing at origin	2000000 m

Table 5.9 Parameters of Albers conical equal area projection

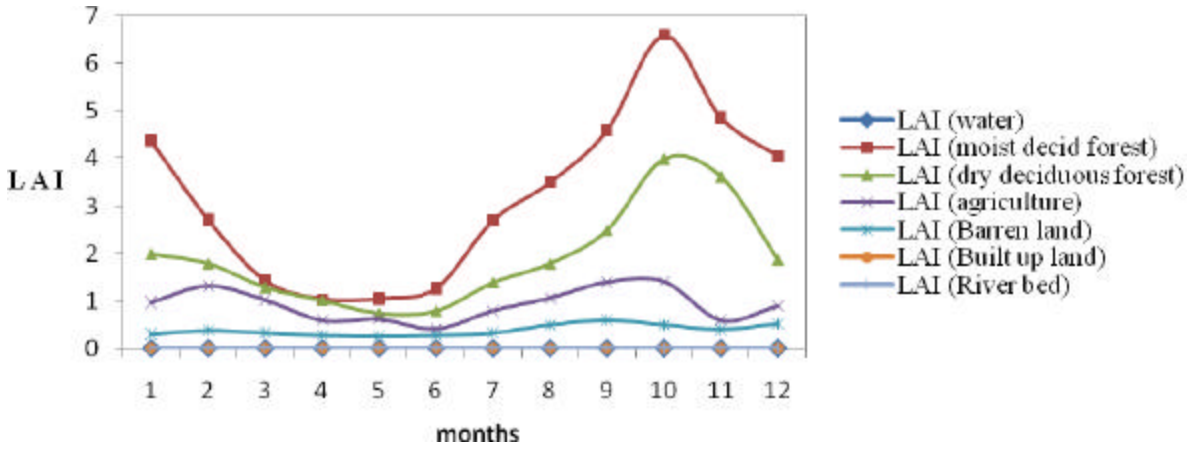

Fig 5.14 Variation of monthly LAI derived from MODIS LAI/FPAR product

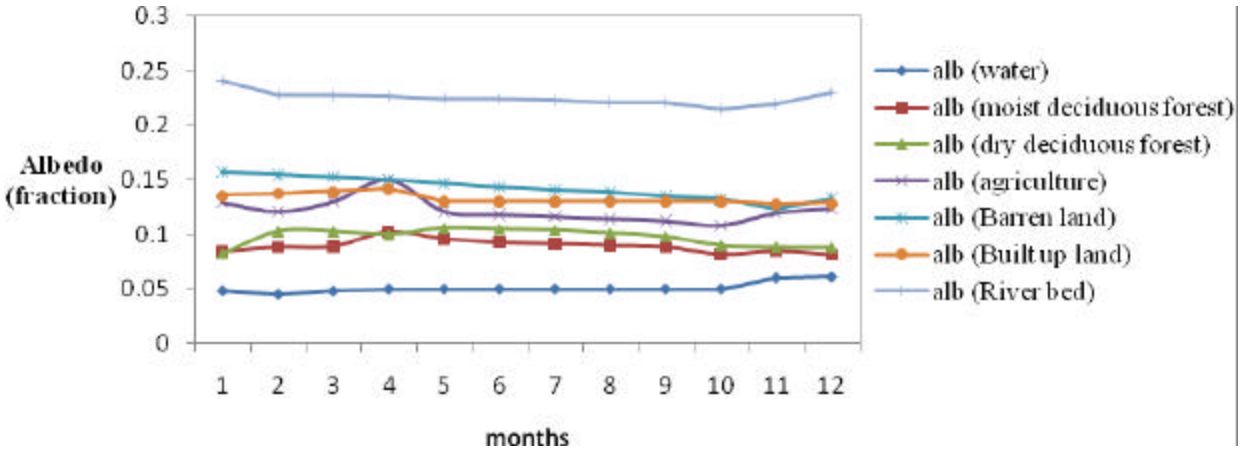

Fig 5.15 Variation of monthly Albedo derived from MODIS BRDF/Albedo product

5.3.4 **Meteorological forcing file:**

This file contains meteorological variables required to force the VIC model like daily precipitation, daily maximum and minimum air temperature (Table 5.10). Forcing data files play big role in the model input to produce all the outputs in both water balance and full energy balance modes of the model. Accurate streamflow simulation requires forcing input of high accuracy as it is the most influential variable generating runoff and driving hydrological cycle.

Sl. no	Variable name	Unit	Description
1	precp	mm	Daily precipitation
2	Tmax	°C	Daily maximum temperature
3	Tmin	°C	Daily minimum temperature

Table 5.10 Forcing parameter file (Source: http://www.hydro.washington.edu)

Precipitation input was prepared using IMD's $1^{o}X1^{o}$ gridded rainfall dataset. Daily rainfall values for each 1 degree grid falling in the basin were extracted for 365 days in the year 2003. Rainfall grids were then overlaid with the basin grids to extract precipitation in each basin grid. VIC model requires one forcing file for each grid having 365 rows and 3 columns in ASCII format. Temperature data from NCDC (National Climatic Data Centre, NOAA) is available for some selected stations in the study area. This point temperature data was used to derive maximum and minimum temperature of each basin grid using nearest neigbour and lapse rate method since it is assumed that temperature varies with the altitude. The following relation was applied in MS Excel spreadsheet:

$$T_{grid} = T_{nearest\ point} + 5.5/1000*(elevation_{nearest\ point} - grid\ elevation)$$

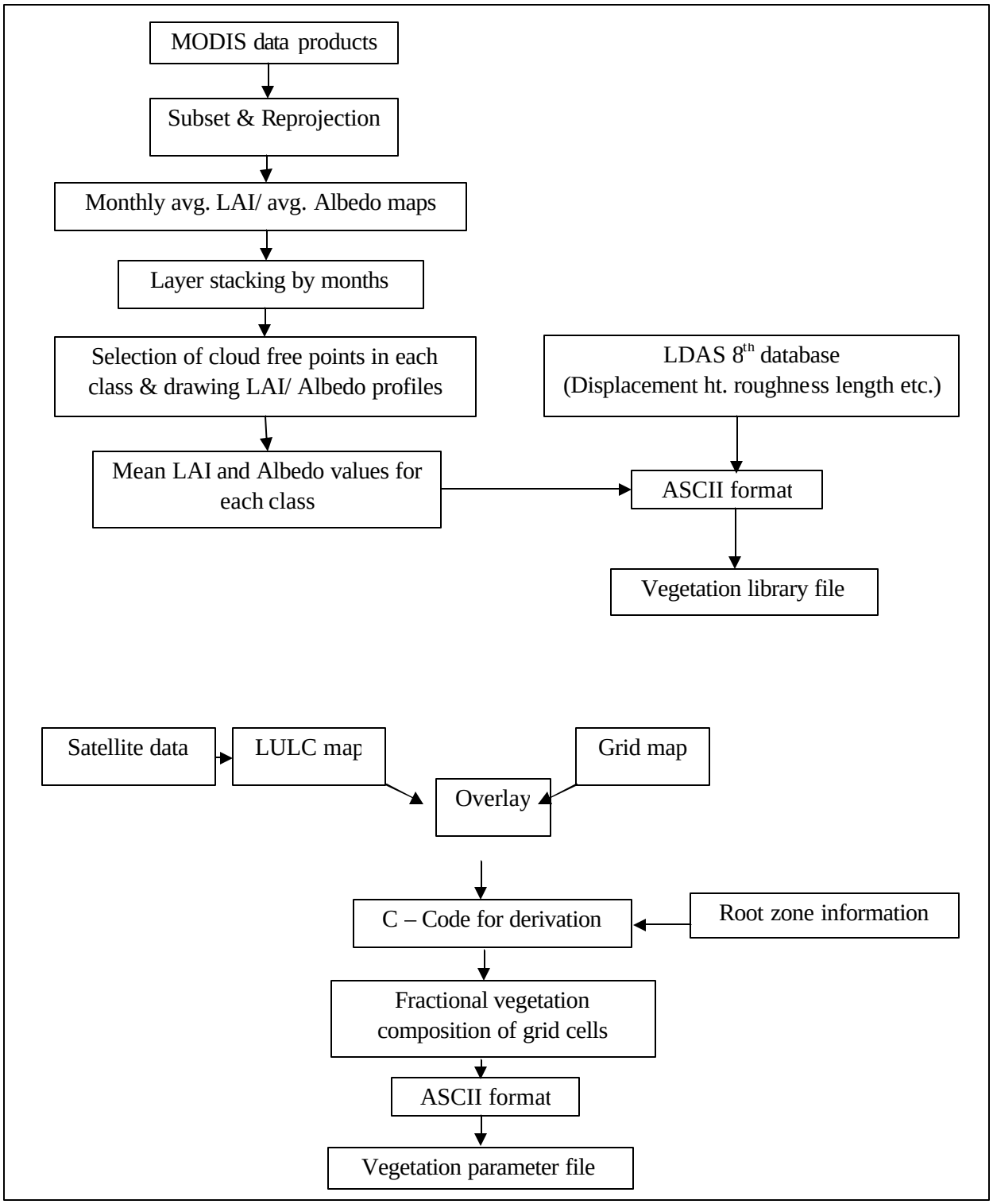

Fig 5.16 Flowchart to derive vegetation library and vegetation parameter file

5.3.5 **Preparation of global control file and VIC model simulation:**

A Global control file where the necessary information to specify various user preferences and parameters are was prepared. It contains information like N-layers, Time step, start time, end time, Wind_H, snow temp, rain temp., Location of the input output files, modes which are to be activated etc. VIC 4.0.5 source code was downloaded from the site and the code were unzipped and untared into local source code directory. Then VIC was compiled using gcc complier on Linux operating system. The code was compiled using the make file included in the archive, by typing 'make'. The compiled code creates an executable entitled 'vicNl'. To begin running the model, '**vicNl -g (global control file name)**' was written at the command prompt. Global control parameters were modified according to the input characteristics and to activate the ware balance. In addition to that input and output path were specified.

5.4 VIC model run and routing the surface flow:

VIC source code was executed in the LINUX environment to generate the flux files for each basin grid. These flux files contain fluxes of surface runoff, evapotranspiration, baseflow, soil moisture etc. produced at that location. In order to simulate streamflow at an outlet, routing of runoff component was done using a routing model developed by Lohmann et. al (1998a, b). Primary input files required by the routing model are:

- Flow direction file (compulsory)
- Fraction file
- Diffusion file
- Flow velocity file
- Station location file (compulsory)
- Grid cell impulse response function (compulsory)
- Unit hydrograph file (compulsory)

Above stated input files were prepared using DEM as the primary input. A control file defining user preferences and location of input files was used to call the routing code in LINUX environment. Routing was done for 6 sub-basins namely Mundali (main outlet), Kantamal, Andhiyarkore, Simga, Baminidihi and Sundergarh. Daily and monthly streamflows in Cusec and mm for each outlet location was obtained as the output.

5.5 Model Calibration and Validation of the results:

Calibration of a hydrological model is an iterative process which involves changing the values of sensitive model parameters to obtain best possible match between the observed and simulated values. In general, before conducting numerical simulations, six model parameters of the VIC-2L model need to be calibrated because they cannot be determined

well based on the available soil information (Yuan, 2004). These six model parameters are the depths of the upper and lower soil layers (*di*, *i* = 2, 3); the exponent (*B*) of the VIC-2L soil moisture capacity curve, which describes the spatial variability of the soil moisture capacity; and the three subsurface flow parameters (i.e., *D*m, *D*s, and *W*s, where *D*m is the maximum velocity of base flow, *D*s is the fraction of *D*m, and *W*s is the fraction of maximum soil moisture).

The following three criteria were selected for model calibration:

(i) **Relative error (Er in percent)** between the simulated and observed mean annual runoff, defined as

$$E_r = (\overline{Q}_c - \overline{Q}_o) / \overline{Q}_o,$$

where $\overline{Q}_c$ and $\overline{Q}_o$ are the simulated and observed mean annual runoff (mm), respectively; and

(ii) **The Nash–Sutcliffe coefficient** (Ce) (Nash and Sutcliffe, 1970), defined as

$$C_e = \frac{\sum (Q_{i,o} - \overline{Q}_o)^2 - \sum (Q_{i,c} - Q_{i,o})^2}{\sum (Q_{i,o} - \overline{Q}_o)^2},$$

where $Q_{i,o}$ is the observed streamflow (in m3/s), $Q_{i,c}$ is the model-simulated streamflow (in m^3/s), and Q_o is the mean observed streamflow (in m^3/s).

The Nash-Sutcliffe model efficiency coefficient is used to assess the predictive power of hydrological models. Nash-Sutcliffe efficiencies can range from -8 to 1. An efficiency of 1 (*E*=1) corresponds to a perfect match of modeled disharge to the observed data. An efficiency of 0 (*E*=0) indicates that the model predictions are as accurate as the mean of the observed data, whereas an efficiency less than zero (-8 <*E*<0) occurs when the observed mean is a better predictor than the model. Essentially, the closer the model efficiency is to 1, the more accurate the model is. It should be noted that Nash-Sutcliffe efficiencies can also be used to quantitatively describe the accuracy of model outputs other than discharge. This method can be used to describe the predicative accuracy of other models as long as there is observed data to compare the model results to. For example, Nash-Sutcliffe efficiencies have been reported in scientific literature for model simulations of discharge, and water quality constituents such as sediment, nitrogen, and phosphorus loadings.

(iii) **Coefficient of Determination, R^2**

The Coefficient of Determination is the square of the Pearson's Product Moment Correlation Coefficient (i.e., R2 = r2) and describes the proportion of the total variance in the observed data that can be explained by the model. It ranges from 0.0 (poor model) to 1.0 (perfect model) and is given by

$$R^2 = \left\{ \frac{\sum_{i=1}^{N} (O_i - \bar{O})(P_i - \bar{P})}{\left[\sum_{i=1}^{N} (O_i - \bar{O})^2\right]^{0.5} \left[\sum_{i=1}^{N} (P_i - \bar{P})^2\right]^{0.5}} \right\}$$

where O and P denotes the observed and predicted discharges, the over-bar denotes the mean for the entire time period of the evaluation.

5.6 Historical and current streamflow simulation:

After calibration and validation of the model, streamflow was simulated using VIC and routing model. The vegetation parameter for 1972 and 1985 were derived from respective landuse/ landcover maps. Only the vegetation cover and related parameters were changed in the simulations; the model meteorological forcings and soil parameters were kept same for both the current and historical scenarios. In this way, the effects of vegetation change on basin hydrology were isolated from the effects of climate variability. Finally, the analysis to look for the change that has occurred in streamflows in various sub-basins over 3 decades was performed.

CHAPTER 6 - RESULTS AND DISCUSSION

This study attempts to model the hydrology of Mahanadi river basin and assess landcover change impacts on streamflows at various locations along the river in the basin. For this purpose, mapping of landuse/ landcover was carried out in detail to represent the present and historical landcover conditions and changes that have taken place over whole of the basin in a span of three decades. Analysis of the changes in landcover between 1972 and 2003 has been presented in this chapter. The simulation results obtained while calibrating and validating the Variable Infiltration Capacity land surface hydrologic model were analysed and simulated streamflows were compared with the observed discharge at 6 stations to look for the model efficiency in representing hydrological conditions accurately. The trend of changes in hydrological processes due to landcover changes has been analysed at the end of this chapter.

6.1 Landuse/ landcover changes in the Mahanadi river basin

6.1.1 Landcover mapping:

Mapping of present and historical landuse/ landcover conditions in the Mahanadi river basin was attempted to assess the changes that have taken place in the area possibly due to human induced activities. Satellite images being reliable and unbiased were the prime source for mapping landcover dynamics. Landsat MSS (80 m resolution), NOAA AVHRR (1 km resolution) and IRS-P6 AWiFs (56 m resolution) data was used to prepare landcover maps for year 1972, 1985, and 2003 respectively. Digital classification was performed to identify categories of land use based on spectral characteristics using unsupervised classification technique and visual interpretation. GCP's (ground control points) were used to improve and validate classification scheme. The landuse/landcover maps are shown in Fig.6.1, 6.2 and 6.3. Seven landcover types were identified and mapped in the basin depending on the spatial resolution of the data and availability of the vegetation related parameters required by the model.

The accuracy assessment of the landuse/ landcover classification was done for all the 3 years (Table 6.1, 6.2 and 6.3). An overall accuracy of 80.95% was achieved for year 2003 whereas for year 1972 and 1985 it was 75.71% and 73.21%. The accuracy was found better for higher spatial resolution (56 m, AWiFs) image as compared to lower spatial resolution (1 km AVHRR and 80 m MSS) image for the same number of landcover types.

Class Name	Reference Totals	Classified Totals	Number Correct	Producers Accuracy	Users Accuracy
Water Body	5	6	5	100.00%	83.33%
Dense forest	7	6	6	85.71%	100.00%
Sparse forest	6	6	5	83.33%	83.33%
Agriculture	5	6	5	100.00%	83.33%
Built up land	4	6	4	100.00%	66.67%
Barren/scrub	8	6	5	62.50%	83.33%
River bed	7	6	4	57.14%	66.67%
Totals	42	42	34		

Overall Classification Accuracy = 80.95%
Overall Kappa Statistics = 0.7778

Table 6.1 Classification accuracy report of year 2003 (AWiFs, 56 m resolution)

Class Name	Reference Totals	Classified Totals	Number Correct	Producers Accuracy	Users Accuracy
Water Body	7	8	7	100.00%	87.50%
Dense forest	9	8	7	77.78%	87.50%
Sparse forest	8	8	6	75.00%	75.00%
Agriculture	7	8	6	85.71%	75.00%
Built up land	7	8	4	57.14%	50.00%
Barrren/scrub	10	8	6	60.00%	75.00%
River bed	8	8	5	62.50%	62.50%
Totals	56	56	41		

Overall Classification Accuracy = 73.21%
Overall Kappa Statistics = 0.6875

Table 6.2 Classification accuracy report of year 1985 (AVHRR, 1 km resolution)

Class Name	Reference Totals	Classified Totals	Number Correct	Producers Accuracy	Users Accuracy
Water body	11	10	9	81.82%	90.00%
Dense forest	10	10	9	90.00%	90.00%
Sparse forest	9	10	7	77.78%	70.00%
Agriculture	13	10	8	61.54%	80.00%
Built up land	9	10	7	77.78%	70.00%
Barrren/scrub	9	10	7	77.78%	70.00%
River bed	9	10	6	66.67%	60.00%
Totals	70	70	53		

Overall Classification Accuracy = 75.71%
Overall Kappa Statistics = 0.7167

Table 6.3 Classification accuracy report of year 1972 (Landsat MSS, 80 m resolution)

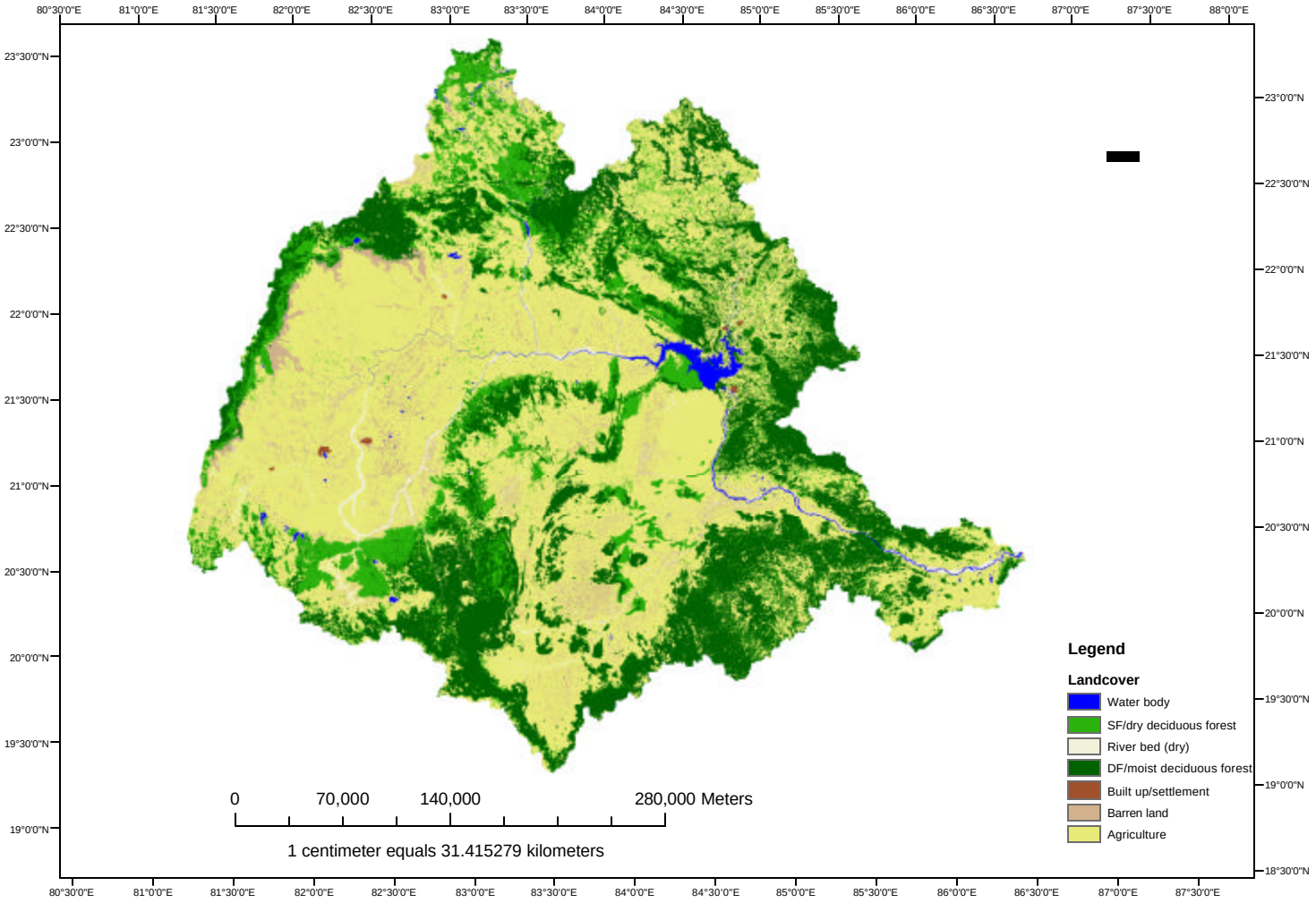

Fig.6.1 Landcover map of Mahanadi basin for year 1972-73

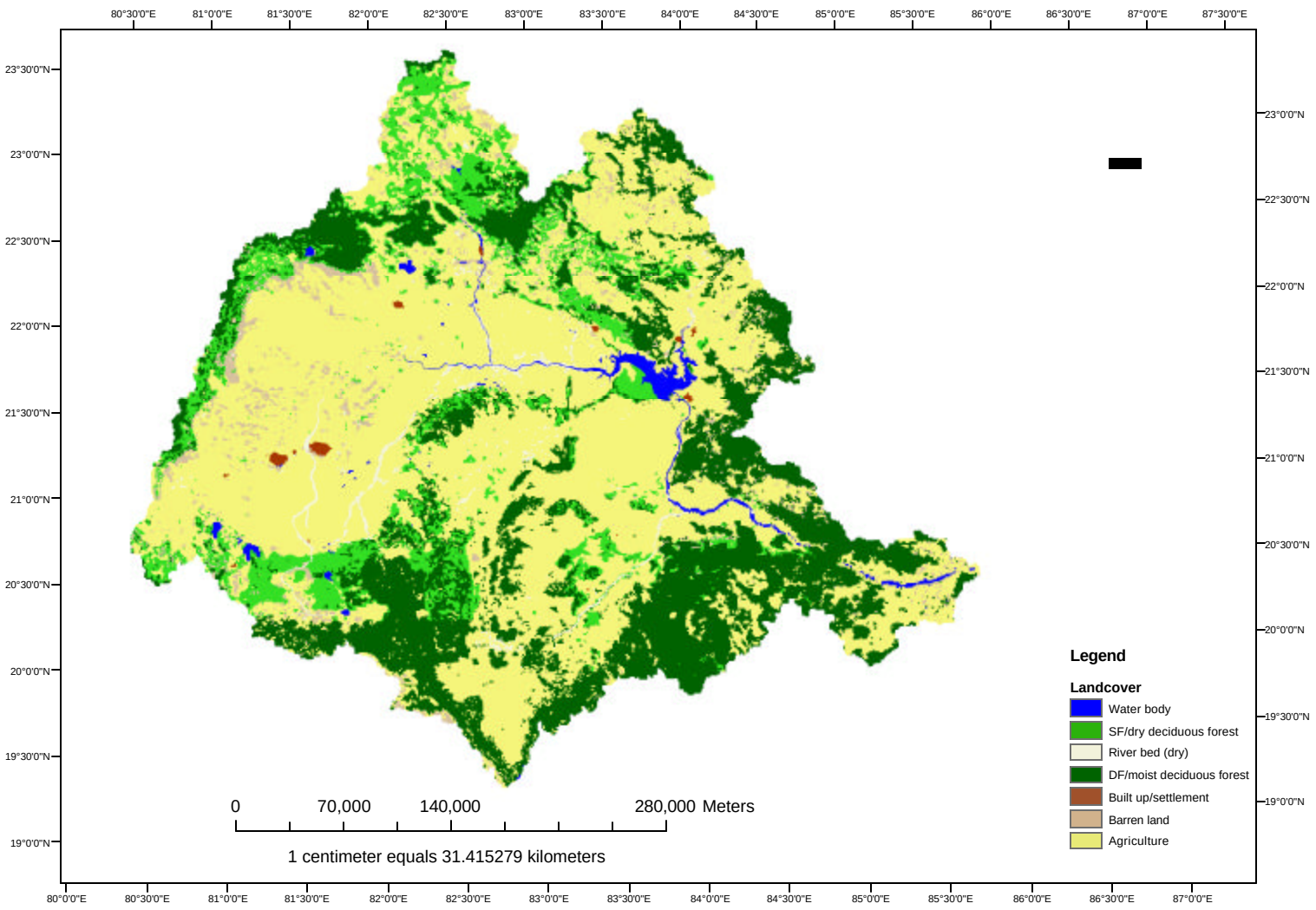

Fig.6.2 Landcover map of Mahanadi basin for year 1985-86

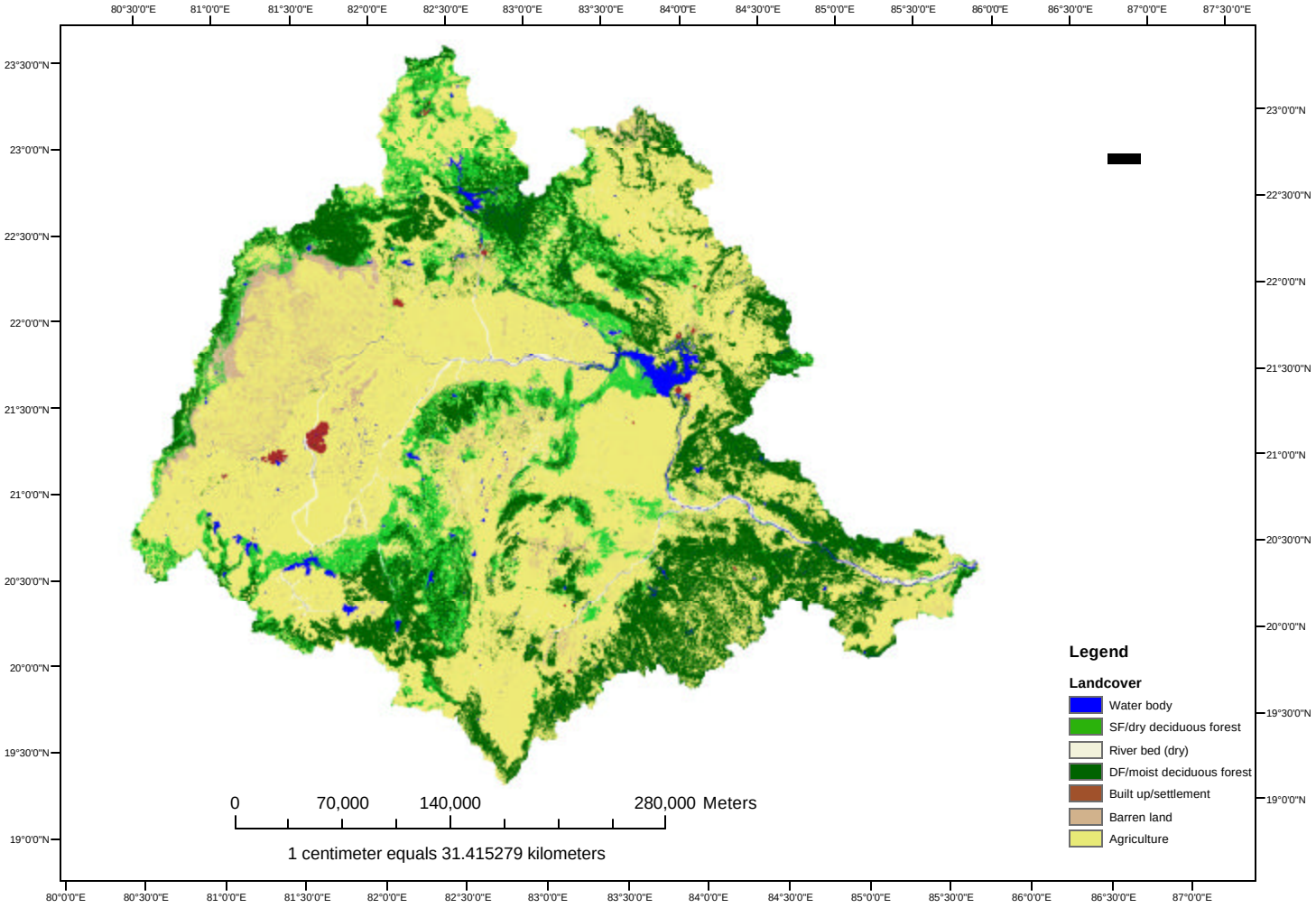

Fig.6.3 Landcover map of Mahanadi basin for year 2003-06

6.1.2 **Landuse/ landcover changes:**

Assessing landcover dynamics and change is important for assessment of its impact on various natural processes. Several methods, based on satellite remote-sensing data, are used to describe patterns and processes of land-use/ land-cover changes quantitatively. In this study, land-use change amplitude and landuse conversion matrices (Wang et al, 2007) were used to reveal the characteristics of land-use variations. The analytical method used is as follows:

Measurement index, the variation amplitude P_i of a single land type is used to form the respective mathematical expression:

$$P_i(\%) = \frac{LU_{it1} - LU_{it0}}{LU_{it0}} \times 100$$

where LU_{it0} and LU_{it1} are the areas of i^{th} land-use and land-cover type at the beginning and at t respectively in the study region.

In order to explore the internal conversion between different land-use classes, a land-use change conversion matrix was implemented. The percentage of 'conversion loss' or 'conversion gain' in relation to the total watershed area was calculated according to the following formulas.

$$P_{loss(i),j} = \frac{\left(a_{j,i} - a_{i,j}\right)}{A} \times 100$$

$$P_{gain(i),j} = \frac{\left(a_{i,j} - a_{j,i}\right)}{A} \times 100$$

where, $P_{loss(i),j}$ is the percentage of total area taken by class i contributed to class j; similarly, $P_{grain(i),j}$ is the percentage of total area taken by class j contributed to class i. $a_{i,j}$ stands for the area of class i converted to class j, and $a_{j.i}$ stands for the area of class j converted to class i A is the total study area. The change in each land-use class from 1972 to 2003 is illustrated clearly in Fig 6.4. Table **6.4 - 6.7** shows the internal conversion (matrices) of different land-use classes at different periods.

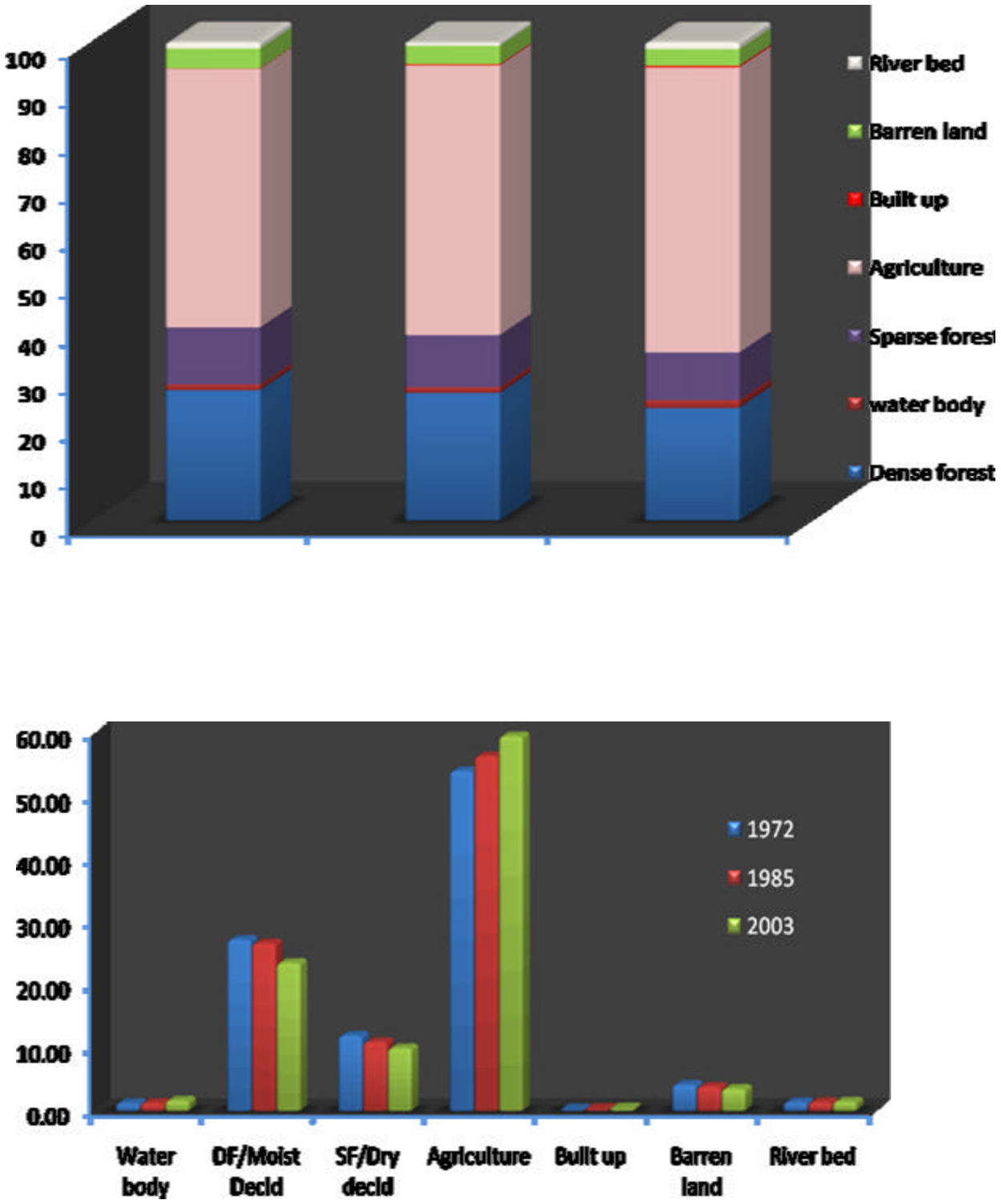

Fig 6.4 Landuse/cover change in Mahanadi basin from 1972 to 2003

	Water body (%)	DF/Moist Decid (%)	SF/Dry decid (%)	Agriculture (%)	Built up (%)	Barren land (%)	River bed (%)
1972	1.16	27.23	11.96	54.08	0.08	4.15	1.34
1985	1.19	26.64	10.92	56.41	0.22	3.83	1.35
2003	1.62	23.52	9.96	59.63	0.31	3.51	1.46
1972-85							
P_i	2.55	-2.16	-8.64	4.31	169.07	-7.63	0.79
1985-03							
P_i	36.81	-11.71	-8.86	5.71	37.54	-8.50	7.52
1972-03							
P_i	40.30	-13.63	-16.74	10.27	270.09	-15.48	8.37

Table 6.4 Characteristics of Landcover changes in Mahanadi basin (1972-2003)

		Landcover 1972						
		WB	**DF**	**SF**	**A**	**BU**	**BL**	**RB**	**Change**
	WB	0.0000	-0.0066	0.0318	-0.1187	-0.0024	0.0042	0.1186	**0.027**
	DF	0.0066	0.0000	-0.4647	0.1556	-0.0074	-0.5014	-0.0029	**-0.814**
1985	**SF**	-0.0318	0.4647	0.0000	-1.2175	-0.0041	-0.2887	-0.0169	**-1.094**
	AG	0.1187	-0.1556	1.2175	0.0000	-0.1074	1.0590	-0.0373	**2.095**
	BU	0.0024	0.0074	0.0041	0.1074	0.0000	0.0104	0.0079	**0.140**
	BL	-0.0042	0.5014	0.2887	-1.0590	-0.0104	0.0000	-0.0755	**-0.359**
	RB	-0.1186	0.0029	0.0169	0.0373	-0.0079	0.0755	0.0000	**0.006**

From 1972 to 1985:	
% increase in water body	0.03
% decrease in total forest cover	-1.908
% increase in Agricultural area	2.09
% increase in Built up area	0.14
% decrease in barren land	-0.36
% increase in River bed	0.01

WB	Water body
DF	Moist decid forest
SF	Dry decid forest
AG	Agriculture
BU	Built up
BL	Barren land
RB	River bed (dry)

Table 6.5 Landuse conversion matrix and percent change in classes (1972-85)

		andcover 1985						
		WB	**DF**	**SF**	**A**	**BU**	**BL**	**RB**	**Change**
	WB	0.0000	0.1166	0.1485	0.2700	0.0023	0.0696	-0.1677	0.439
	DF	-0.1166	0.0000	-0.0803	-3.0253	0.0059	0.2985	0.0068	-2.911
2003	**SF**	-0.1485	0.0803	0.0000	-0.8024	-0.0038	-0.0439	0.0029	-0.915
	AG	-0.2700	3.0253	0.8024	0.0000	-0.0598	-0.0448	0.0565	3.510
	BU	-0.0023	-0.0059	0.0038	0.0598	0.0000	0.0127	0.0153	0.083
	BL	-0.0696	-0.2985	0.0439	0.0448	-0.0127	0.0000	-0.0190	-0.311
	RB	0.1677	-0.0068	-0.0029	-0.0565	-0.0153	0.0190	0.0000	0.105

From 1972 to 1985:	
% increase in water body	0.439
% decrease in total forest cover	-3.826
% increase in Agricultural area	3.510
% increase in Built up area	0.083
% decrease in barren land	-0.311
% increase in River bed	0.105

Table 6.6 Landuse conversion matrix and percent change in classes (1985-03)

		Landcover 1972							
		WB	**DF**	**SF**	**A**	**BU**	**BL**	**RB**	**Change**
	WB	0.000	0.146	0.139	0.199	-0.004	0.018	-0.032	**0.466**
	DF	-0.146	0.000	-0.538	-2.857	-0.005	-0.164	-0.001	**-3.710**
	SF	-0.139	0.538	0.000	-2.134	-0.004	-0.230	-0.031	**-2.001**
2003	**AG**	-0.199	2.857	2.134	0.000	-0.177	0.829	0.108	**5.551**
	BU	0.004	0.006	0.004	0.177	0.000	0.024	0.010	**0.223**
	BL	-0.018	0.164	0.230	-0.829	-0.024	0.000	-0.166	**-0.642**
	RB	0.032	0.001	0.031	-0.108	-0.010	0.166	0.000	**0.112**

From 1972 to 2003:	
% increase in water body	0.47
% decrease in total forest cover	-5.71
% increase in Agricultural area	5.55
% increase in Built up area	0.22
% decrease in barren land	-0.64
% increase in River bed	0.11

Table 6.7 Landuse conversion matrix and percent change in classes (1972-03)

Analysing landuse changes from 1972 to 2003, it may be concluded that the total forest cover has declined by 5.71% of the total area of the basin. A reduction in barren land (0.64%) is followed by increase in areas of surface water bodies (0.47%), built up land (0.22%), river bed (0.11%) and most prominently agriculture (5.55%). This implies that the total forest cover and barren land has declined at the expense of increase in water body, river bed, agriculture and built up land in a span of 30 years.

Variation amplitude (Table 6.4) from 1972 to 2003 showed reduced forest cover accounting for 13.63% (of the area of moist deciduous forest cover in 1972) of total change, 2.16% occurring from 1972 to 1985, and 11.71% from 1985 to 2003; reduced dry deciduous cover (16.74% of total change, 8.64% occurring from 1972-1985, 8.86% from 1985-2003); increased Agriculture (10.27% of total change, 4.31% from 1972-85 and 5.71% between 1985-03); increased built up (270.09% of total change, 169.07% occurring from 1972-85, 37.54% from 1985-2003); reduced barren (15.48%); increased river bed (8.37%); increased water body (40.30%). Taking the internal conversion of various landuse classes into account from 1972-85, the major changes were from sparse forest/dry deciduous to barren and agriculture, from moist deciduous to dry deciduous forest; from 1985 to 2003 the predominant change was found from forest to agriculture. An overall trend from 1972 to 2003 saw changes from forest and some barren land to agriculture; conversion of dense forest to sparse and agriculture, forest have gone into water bodies and built-ups.

Number of large and small reservoirs/dams has been constructed in the period between 1985-2003 in regions like Dhamtari, Kanker, Raipur districts of Chattisgarh at the cost of deforestation. A sufficiently large storage reservoir was constructed on Hasdeo tributary of Mahanadi in Korba district of Chattisgarh removing large areas of dry-deciduous forest cover. Urban expansion has also taken place at the cost of natural cover. Large industrial and manufacturing complexes have come up in the vicinity of Raipur, Durg and Bhilai districts of Chattisgarh. Intensive cultivation practices gave rise to the agricultural expansion and thus a decrease in forest cover and barren land was seen. Such dynamics in landcover may cause an increased surface runoff, reduced base-flow and soil water retaining capacity which would finally lead to increased streamflows (floods) in the downstream and low soil moisture (agricultural drought) in the upstream basin. Depletion of forest cover aggravates soil erosion which would fasten the siltation process in storage structures reducing their storage capacity.

The landuse/ landcover classification for different periods was carried out using satellite data of different spatial resolutions viz. 56 m (AWiFs), 80 m (MSS) and 1 km (AVHRR). A high resolution data facilitates more detailed mapping of landuse/ landcover with higher accuracy. Whereas the poor spatial resolution of a dataset is responsible for generalization and hence over or under estimation of the areal extents of landcover classes. This limitation of the present study can be overcome by using remotely sensed data of nearly uniform spatial resolution.

6.2 Hydrological Modelling using VIC land surface model

6.2.1 **Pre-calibration simulation:**

The vegetation, soil, and forcing (meteorological) data described in chapter 5 were applied to the VIC-2L model to simulate evapotranspiration, runoff, and soil moisture at each grid over the Mahanadi River basin for year 2003. To compare the VIC-2L model simulated runoff with the observed streamflow, the simulated runoff is routed through the river network using a simple routing model (Lohmann et al, 1996). Runoff was routed to the outlets of six sub-basins namely Mundali, Kantamal, Andhiyarkore, Simga, Baminidihi and Sundergarh. These outlets were chosen based on the availability of observed discharge data. The routed daily and monthly runoff at these stations was compared with the daily and monthly observed streamflows, respectively.

The preliminary comparisons of simulated and observed daily streamflows are presented for 6 outlets location in fig 6.5. The coefficient of determination showing agreement between the trends of simulated and observed streamflow records were found to be as 0.747, 0.327, 0.309, 0.428, 0.606, 0.495 for Mundali, Andhiyarkore, Baminidihi, Kantamal, Simga and Sundergarh respectively prior calibration. No consistency in the simulation results was observed which implies the need for model calibration.

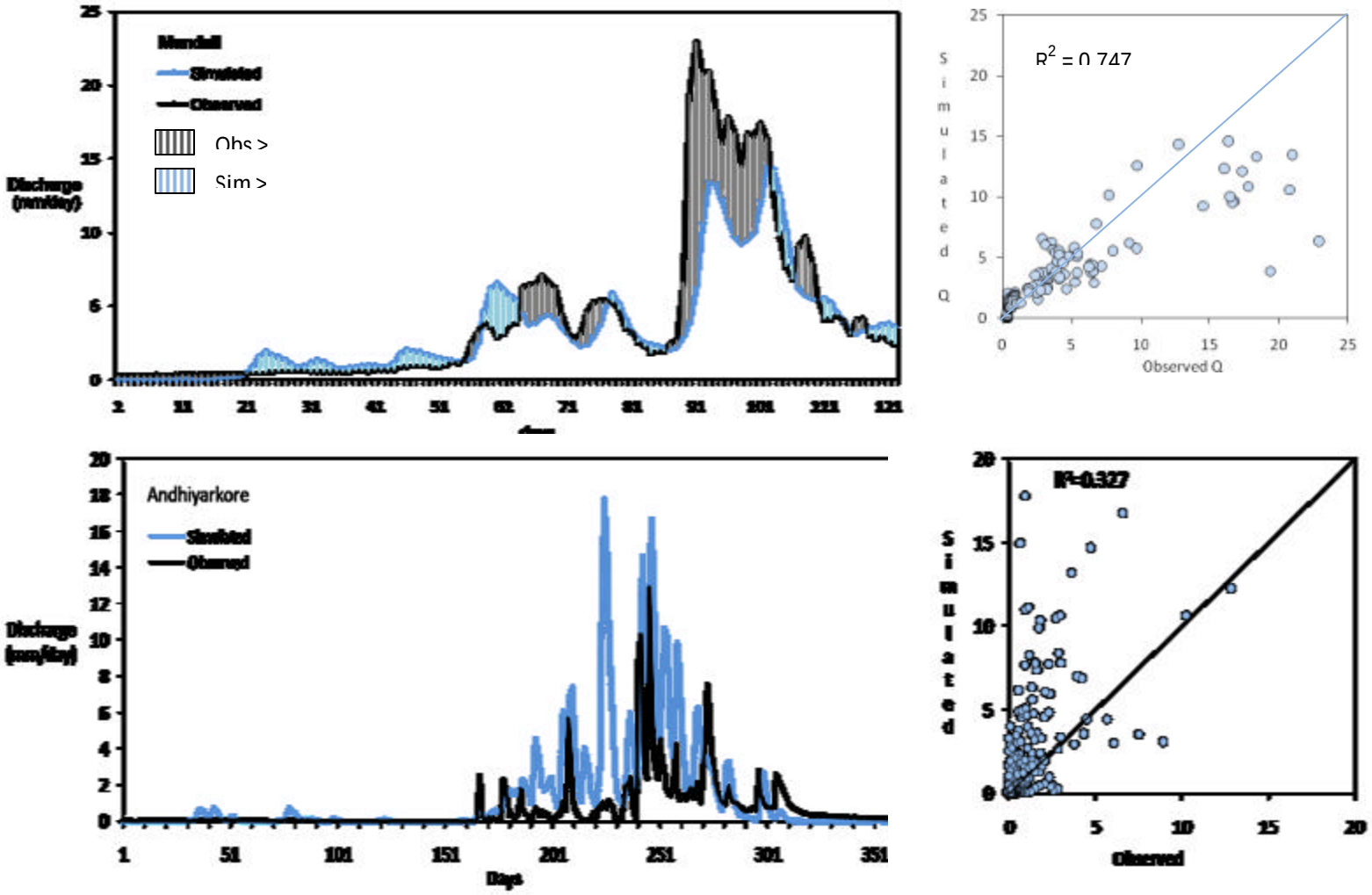

Fig 6.5 Pre-calibration Comparison b/w Observed & Simulated daily discharges (cont…)

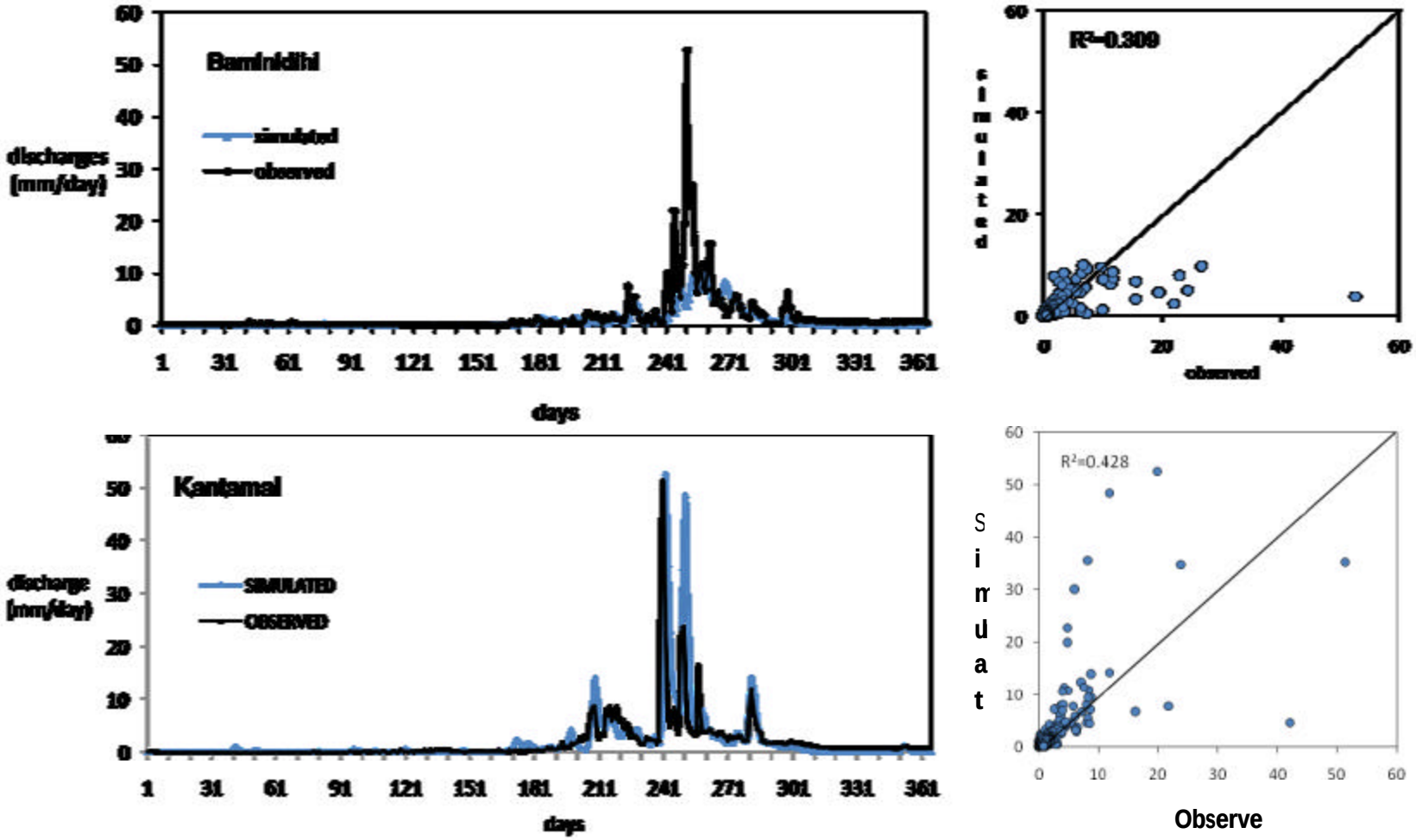

Fig 6.5 (Pre-calibration Comparison b/w Observed & Simulated daily discharges) cont…

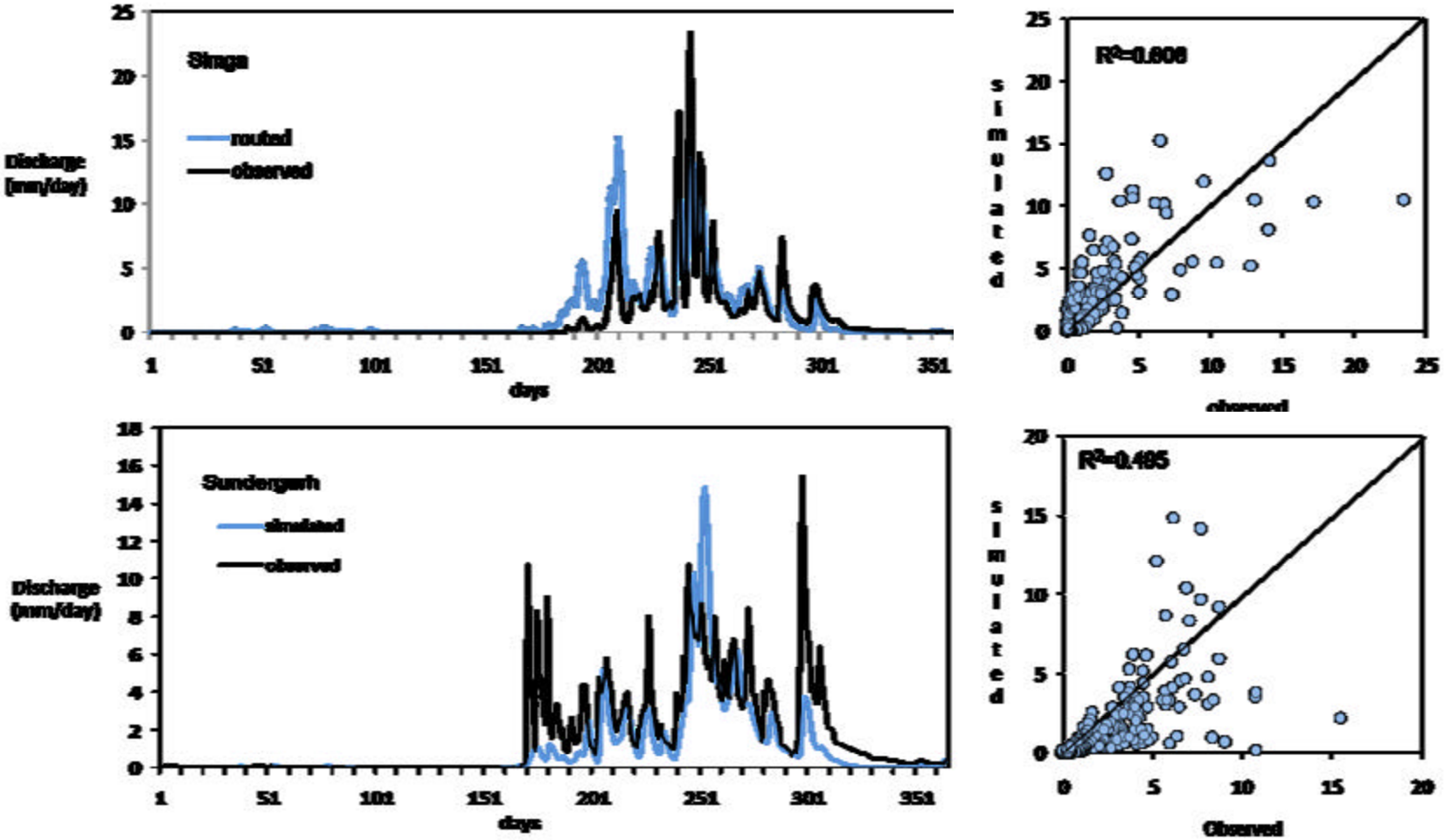

Fig 6.5 (Pre-calibration Comparison b/w Observed & Simulated daily discharges)

6.2.2 **Model Calibration and validation:**

Model calibration may be defined as the procedure of adjusting model parameters which cannot be determined exactly through available methods. Calibration of a hydrological model is an iterative method which involves changing the values of model parameters to obtain best possible match between the observed and simulated values. Since streamflow can be measured with relatively high accuracy compared with other water fluxes in the watershed it is mostly used to calibrate model parameters.

In general, before conducting numerical simulations, six model parameters of the VIC-2L model need to be calibrated because they cannot be determined well based on the available soil information (Yuan, 2004). These six model parameters are the depths of the upper and lower soil layers (di, i = 2, 3); the exponent (B) of the VIC-2L soil moisture capacity curve, which describes the spatial variability of the soil moisture capacity; and the three subsurface flow parameters (i.e., Dm, Ds, and Ws, where Dm is the maximum velocity of base flow, Ds is the fraction of Dm, and Ws is the fraction of maximum soil moisture). In this study, these six parameters are assigned values as: B = 2.0, Dm = 15.0, Ds = 0.02, Ws = 0.8 and di = 0.5 and 2.0 m for i = 2 and 3. The velocity parameter was also adjusted (increased to 2.3 m/s) since the simulated runoff was coming delayed. The stream discharge at Mundali outlet for a period of 6 months was considered as the reference for calibration.

The following two criteria were selected for model calibration: (i) relative error (E_r in percent) between the simulated and observed mean annual runoff, and (ii) the Nash-Sutcliffe coefficient (E) described in chapter 'Materials & methods' section 5.5. Post calibration comparison of observed and simulated hydrograph at Mundali is shown in fig 6.7. A good agreement between the observed and simulated values was found with an R square (Coefficient of determination) value of 0.836, Nash-Sutcliffe model efficiency coefficient of 0.821 and Relative error of -8. 49 %. It can be seen that low flow simulations were overestimated and an underestimation was found during high flows.

VIC is a model primarily designed to assess and evaluate long term climate and landcover changes on basin hydrology. It therefore essentially ignores the effect due to human induced activities. VIC simulates naturalized flows without considering any effect of reservoirs, dams or any other structural intervention. The Mahanadi basin contains several storage reservoirs and diversion structures and the observed streamflows are thus bias and are not really appropriate for the purpose of calibration. This may be a reason of disagreement between observed and simulated discharge. During low flows, reservoirs come into play and store most of the river waters whereas during high flows a reservoir

has to throw out all waters coming into it once filled. This may be the possible reason of overestimation during low flows and underestimation during high flows.

The simulations were performed at other five sub-basin outlets for year 2003 to validate the model performance. Both daily and monthly comparisons were made. For daily simulations, model performed well at Simga, Kantamal and Sundergarh. Better simulation results were obtained for monthly time-step when compared with daily and good agreement at Mundali, Simga, Kantamal and Sundergarh was found. Comparisons of observed versus simulated hydrographs during model validation (daily) are shown in fig. 6.7-6.12. Monthly comparisons were found good for Mundali, Simga, kantamal and Sundergarh sub-basins (fig. 6.13). The values for Coefficient of determination, Nash-Sutcliffe coefficient and relative error for each simulation is given in Table 6.8.

The VIC model simulated runoff compares well with the daily observed streamflow in general, but significant overestimations of the streamflows are evident. This may be because of erratic spatial distribution of precipitation. Streamflows are most sensitive to vegetation and forcing input, thus near perfect simulations require accurate estimation of these parameters. In the present simulation, precipitation information has spatial resolution of 1 degree which is coarser, high resolution is therefore expected to improve simulation.

	Daily simulation			Monthly simulation		
	R^2	N_s	R.E.	R^2	N_s	R.E.
Mundali	0.836	0.821	-0.085	0.920	0.890	-0.087
Kantamal	0.826	0.669	-0.103	0.921	0.812	-0.132
Simga	0.744	0.706	-0.268	0.920	0.815	-0.207
Andhiyarkore	0.748	0.154	-0.762	0.777	-2.840	1.152
Baminidihi	0.464	0.321	-0.428	0.916	0.680	-0.489
Sundergarh	0.534	0.409	-0.283	0.819	0.756	-0.243

Table 6.8 Performance indicators during model validation

Though the agreement between observed and simulated discharges for some outlets is good, under-estimations and over-estimations are inherent in the simulation. This is because of the fact that VIC simulates naturalized flows and the observed discharge used for validation is biased and affected by human interventions. Model performance was found to be good at Kantamal, Simga and Sundergarh during validation, the reason being the absence of structural interventions in these sub-basins. Mundali also showed good agreement inspite of a large reservoir since calibration was performed at this outlet. It may be seen from the simulation results that model has generally overestimated (S>O)

during months of June, July and under-estimated during August and September. The possible reason may be initial reservoir storage in June-July due to which observed flows are less as compared to simulated whereas observed flow exceeds once the reservoir capacity is filled (in Aug, Sept.).

It may be concluded that the agreement between and observed and simulated hydrological components is largely dependent on the hydrological and landcover conditions in the basin and model assumptions. The synoptic view and landuse/landcover conditions of various sub-basins are shown in the figure 6.6. The landcover classes are same as shown for whole of the Mahanadi basin (fig. 6.1) with Mundali as an outlet.

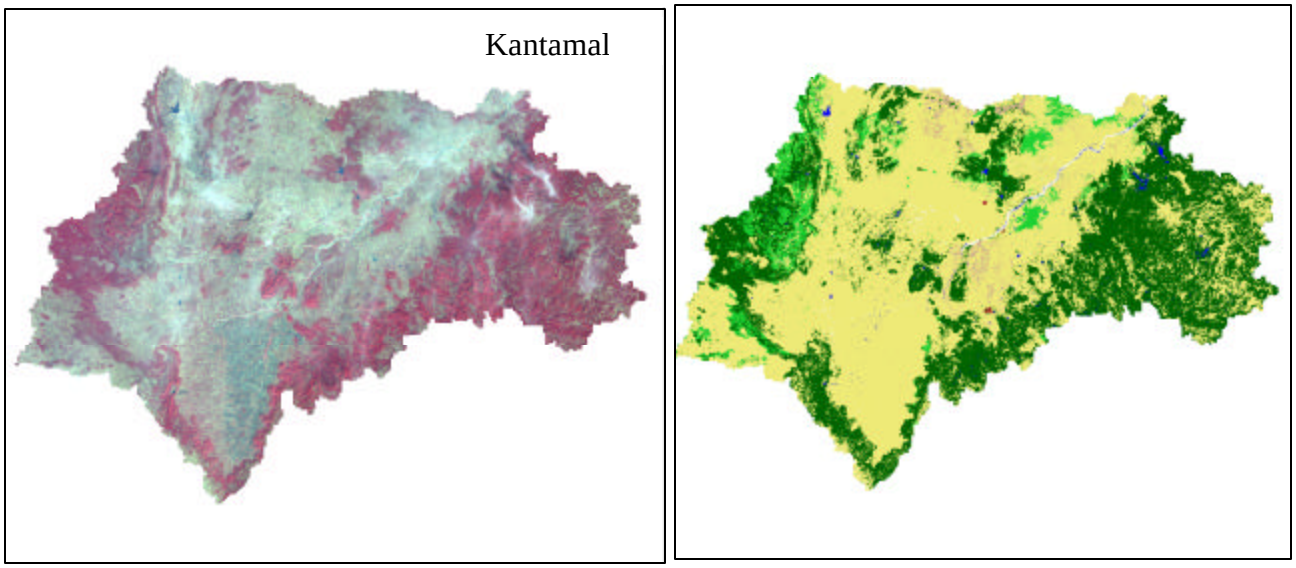

Fig 6.6 AWiFs image and landcover conditions of various sub-basins in 2003 (contd..)

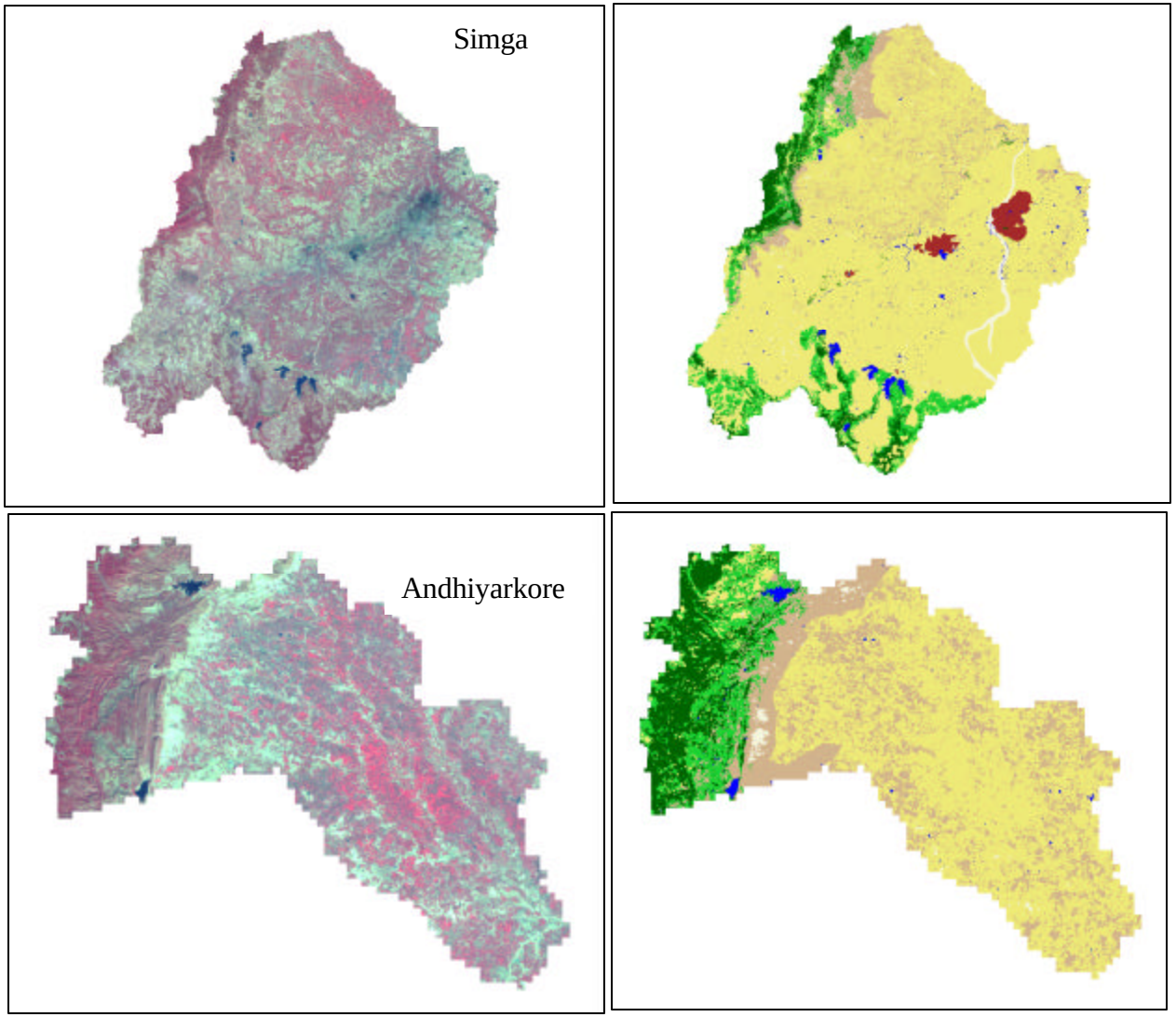

ig 6.6 AWiFs image and landcover conditions of various sub-basins in 2003 (contd..)

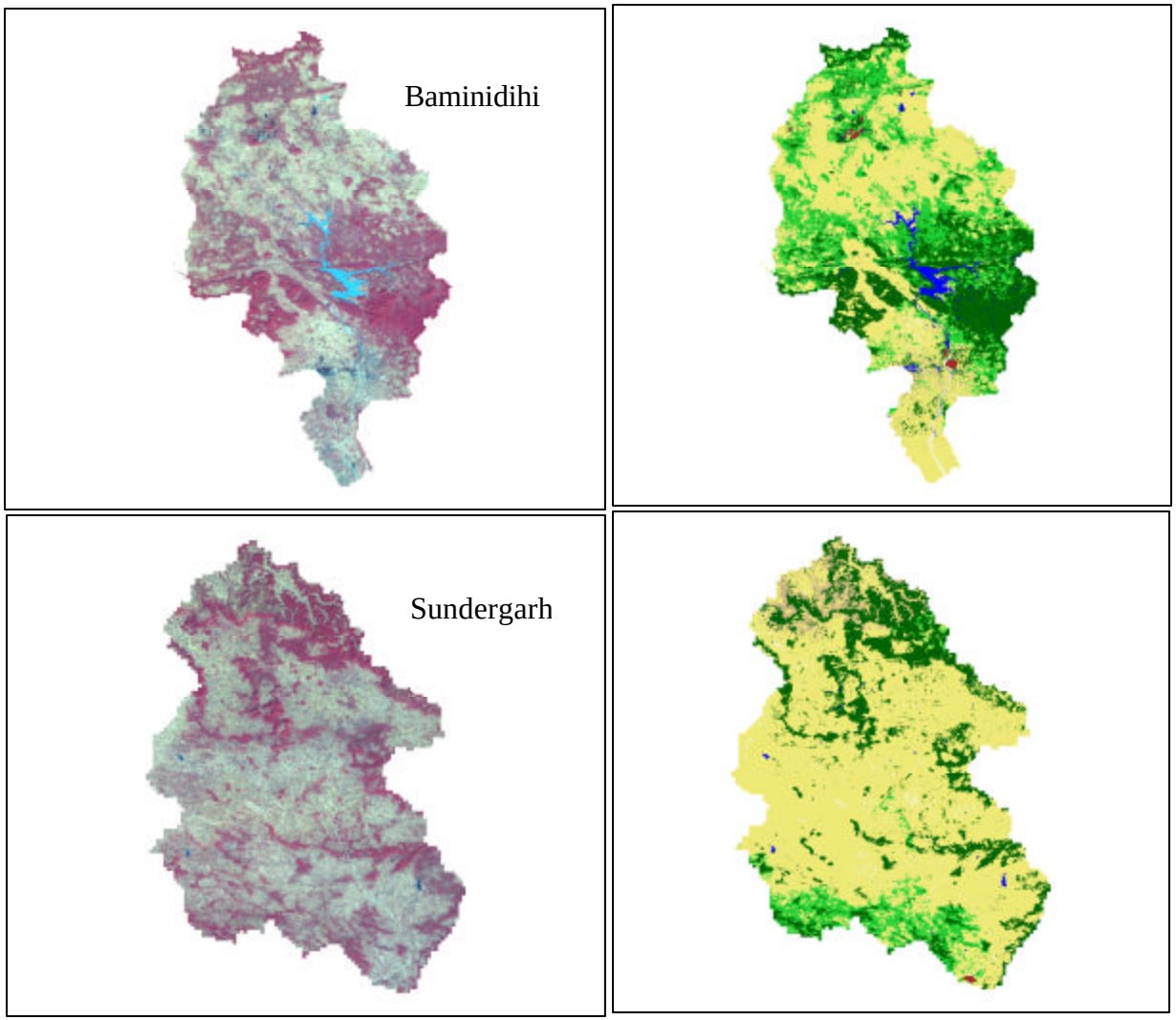

ig 6.6 AWiFs image and landcover conditions of various sub-basins in 2003 (contd..)

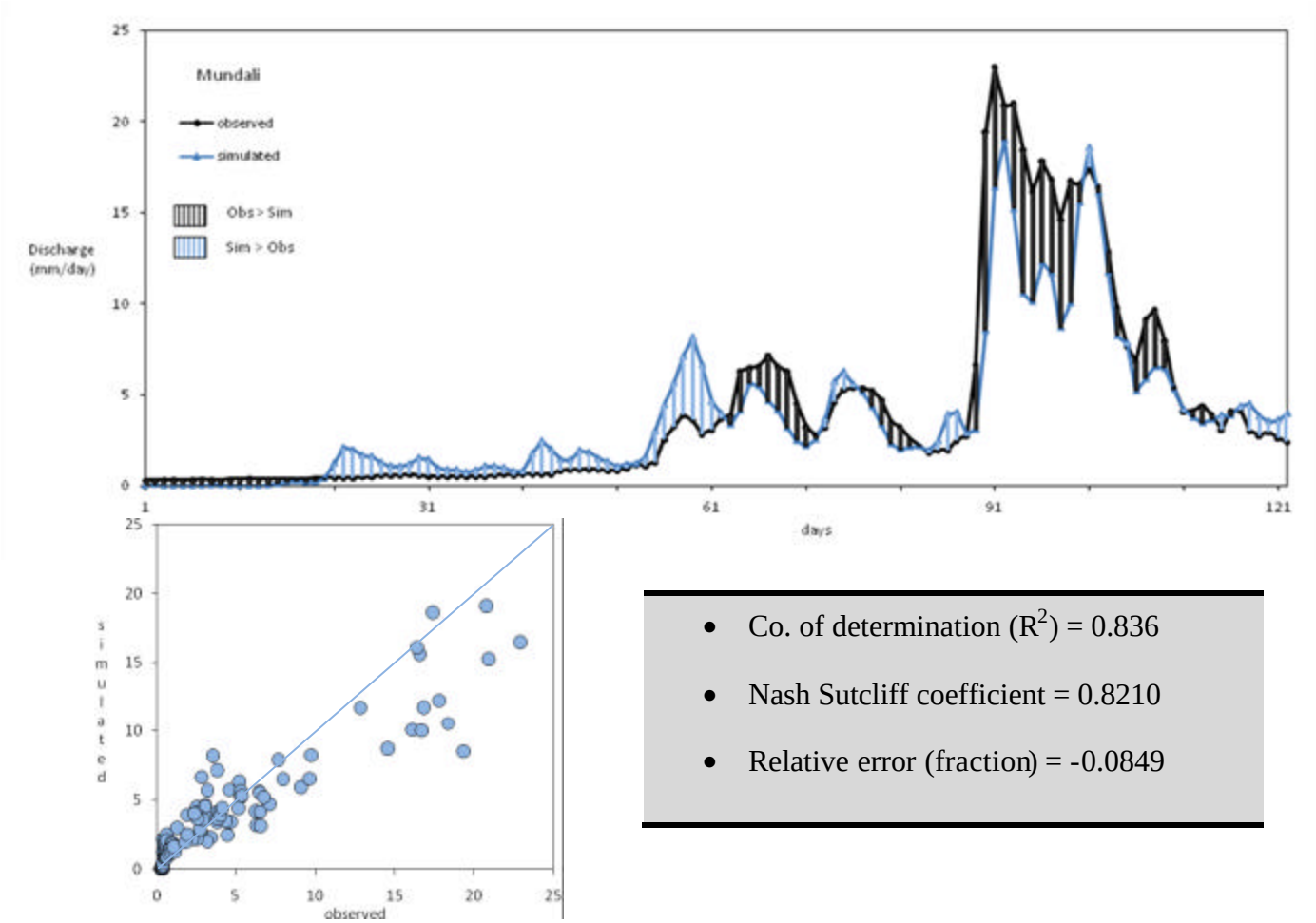

- Co. of determination (R^2) = 0.836
- Nash Sutcliff coefficient = 0.8210
- Relative error (fraction) = -0.0849

Fig.6.7 Comparison of Hydrograph at main outlet (Mundali): **Calibration period**

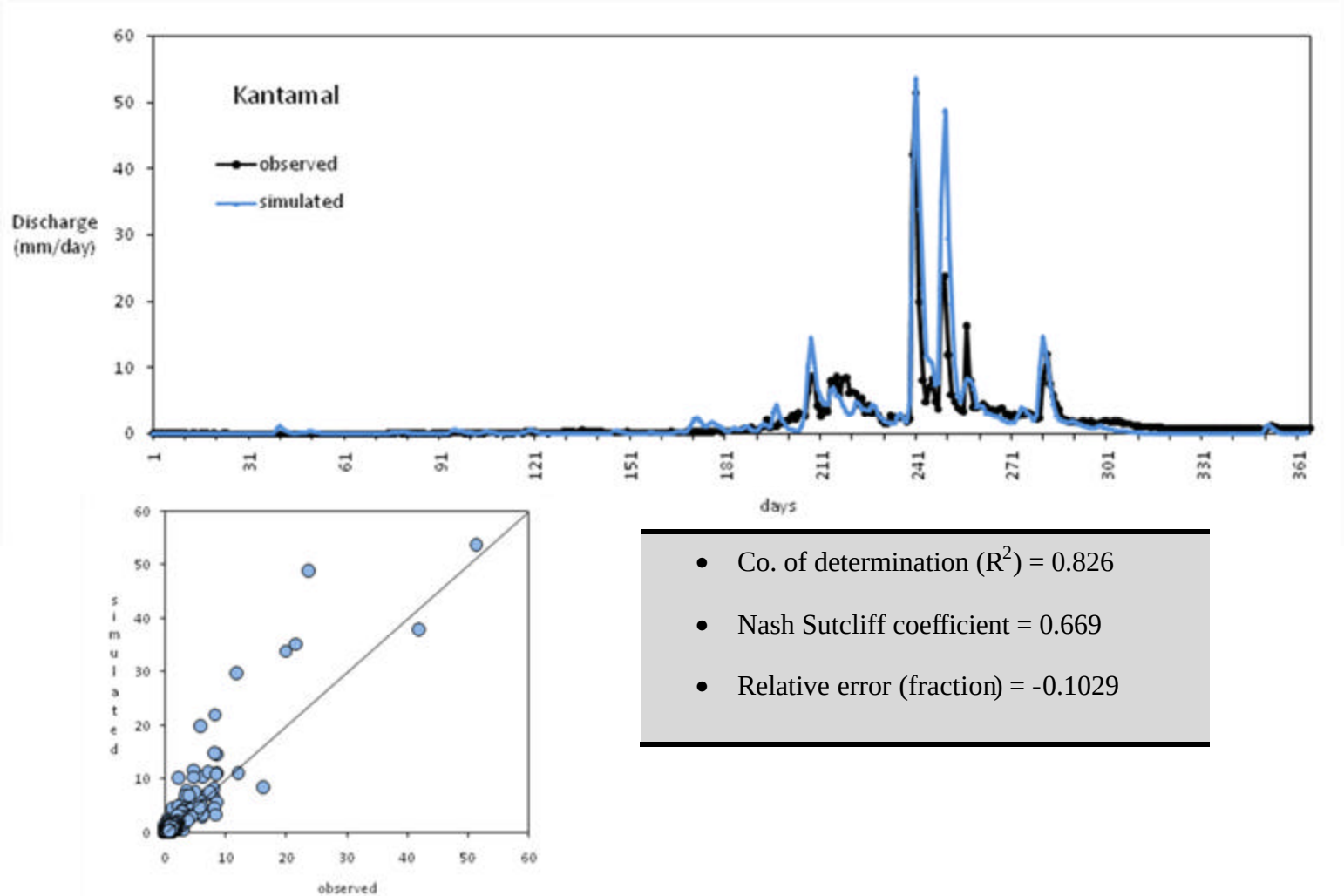

- Co. of determination (R^2) = 0.826
- Nash Sutcliff coefficient = 0.669
- Relative error (fraction) = -0.1029

Fig.6.8 Simulated and Observed hydrograph at Kantamal outlet: **Validation period** (2003)

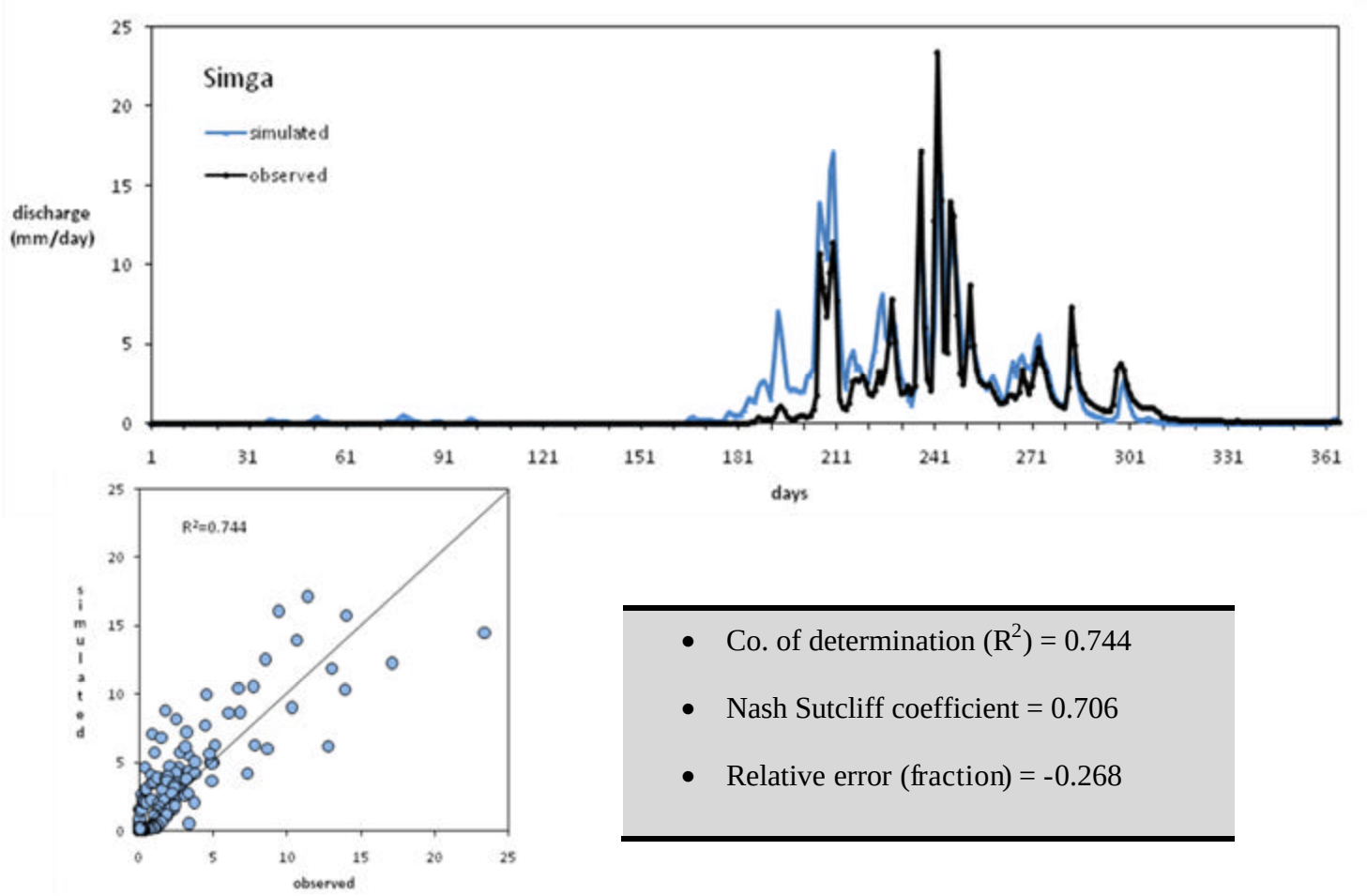

- Co. of determination (R^2) = 0.744
- Nash Sutcliff coefficient = 0.706
- Relative error (fraction) = -0.268

Fig.6.9 Simulated and Observed hydrograph at Simga outlet: **Validation period (2003)**

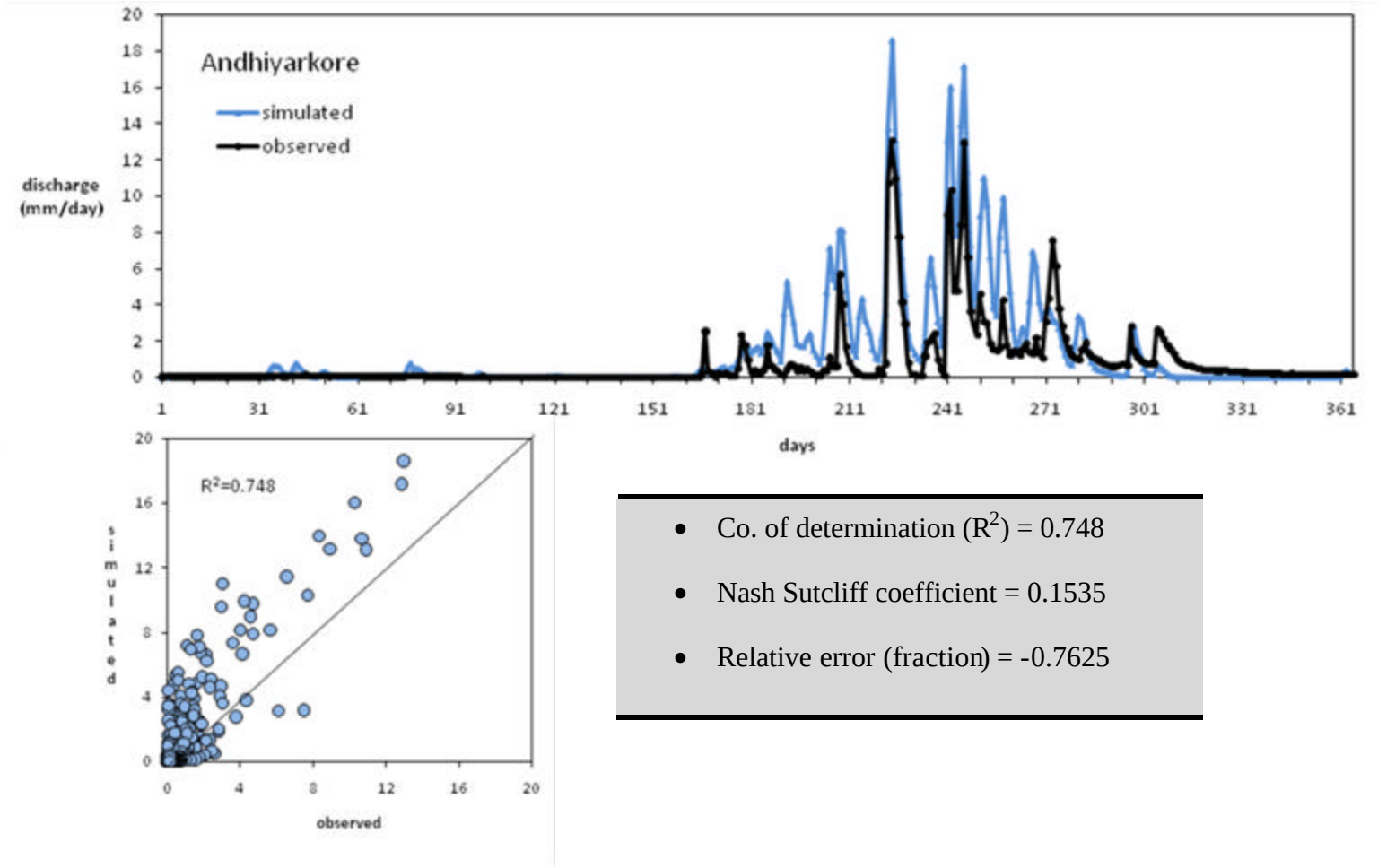

- Co. of determination (R^2) = 0.748
- Nash Sutcliff coefficient = 0.1535
- Relative error (fraction) = -0.7625

Fig.6.10 Simulated and Observed hydrograph at Andhiyarkore outlet: **Validation period (2003)**

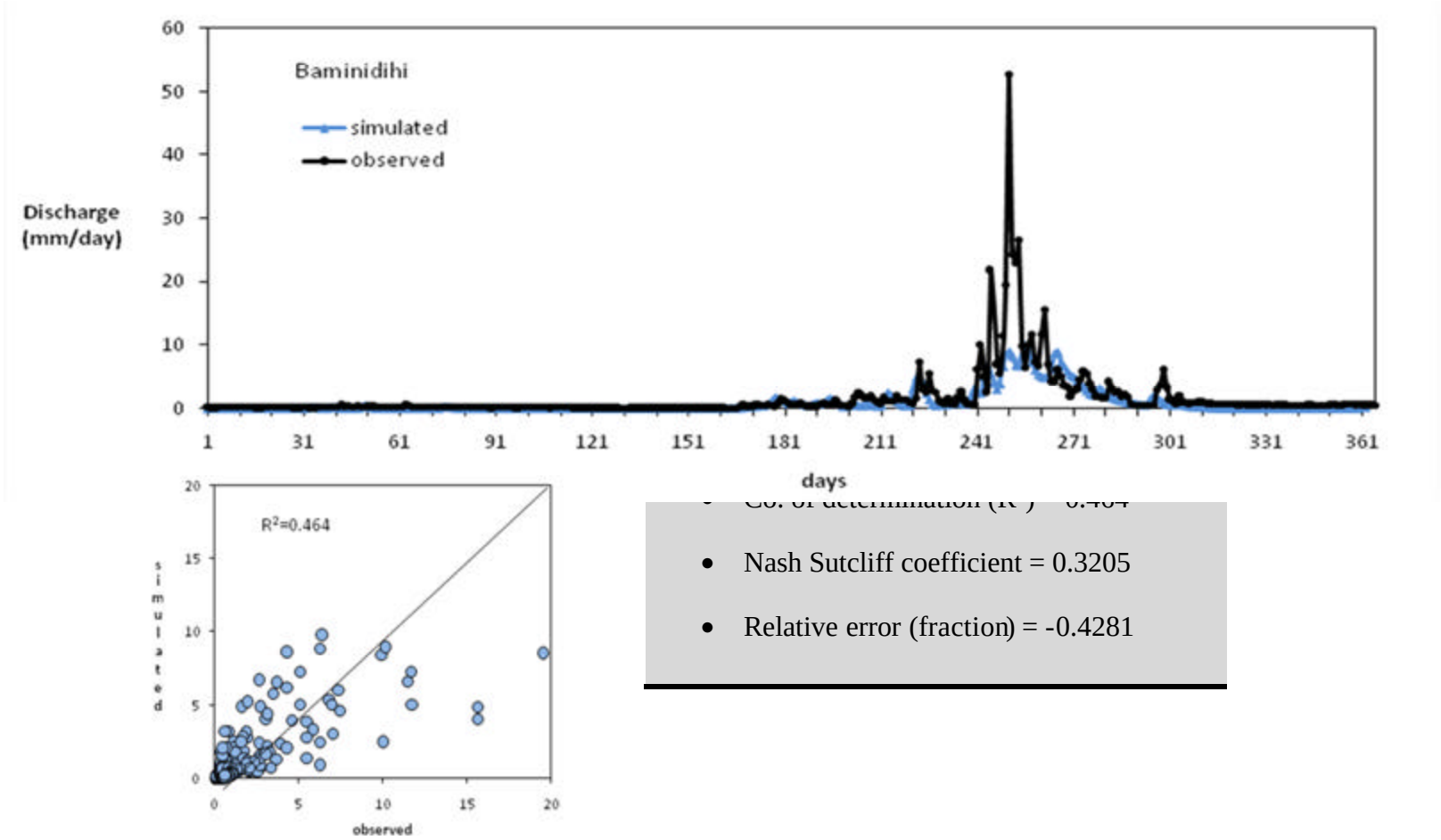

- Co. of determination (R^2) = 0.464
- Nash Sutcliff coefficient = 0.3205
- Relative error (fraction) = -0.4281

Fig.6.11 Simulated and Observed hydrograph at Baminidihi outlet: **Validation period (2003)**

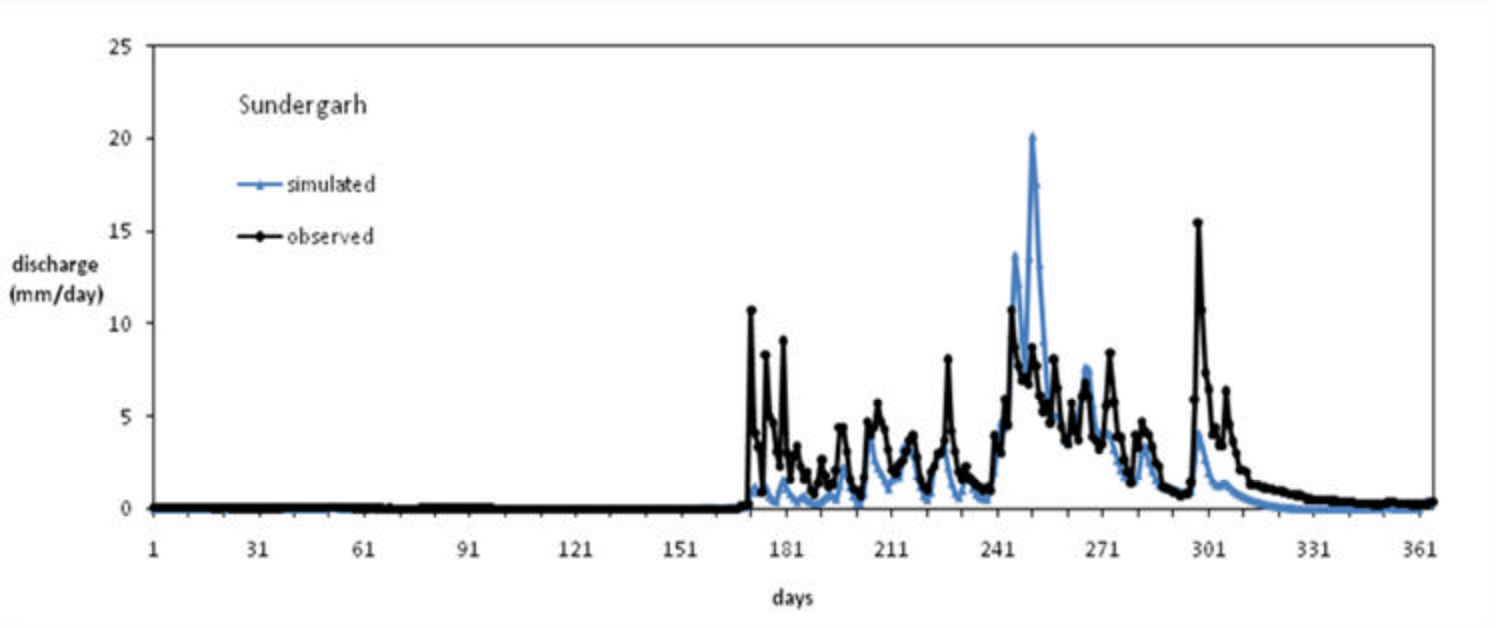

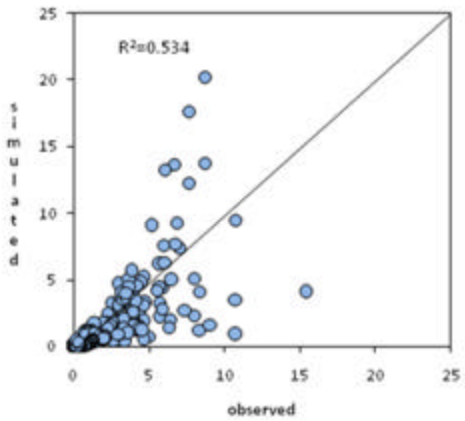

- Co. of determination (R^2) = 0.534
- Nash Sutcliff coefficient = 0.4094
- Relative error (fraction) = -0.2826

Fig.6.12 Simulated and Observed hydrograph at Sundergarh outlet: **Validation period (2003)**

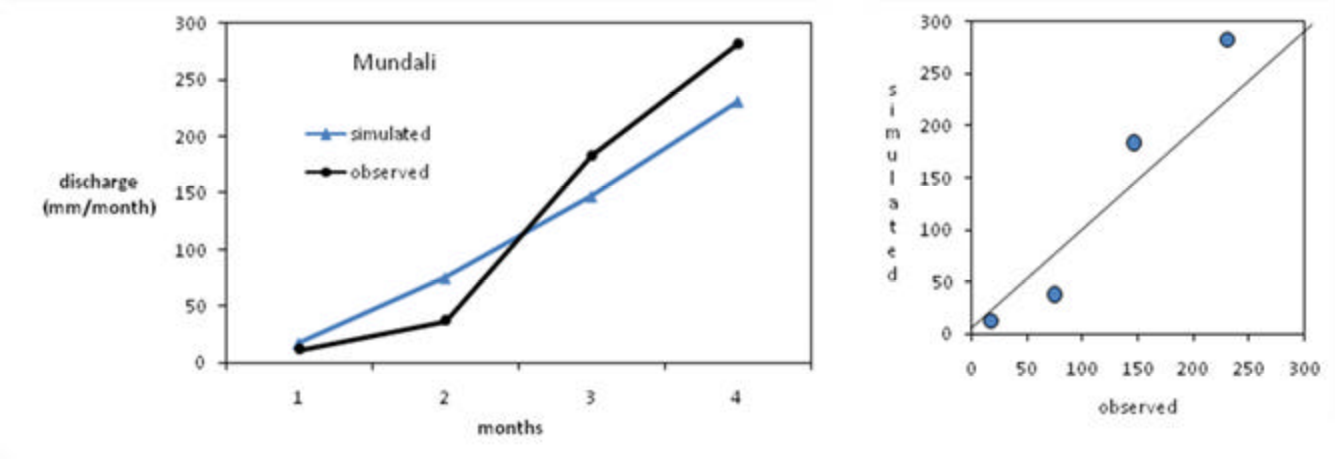

- Co. of determination (R^2) = 0.92
- Nash Sutcliff coefficient = 0.8896
- Relative error (%) = -0.0870

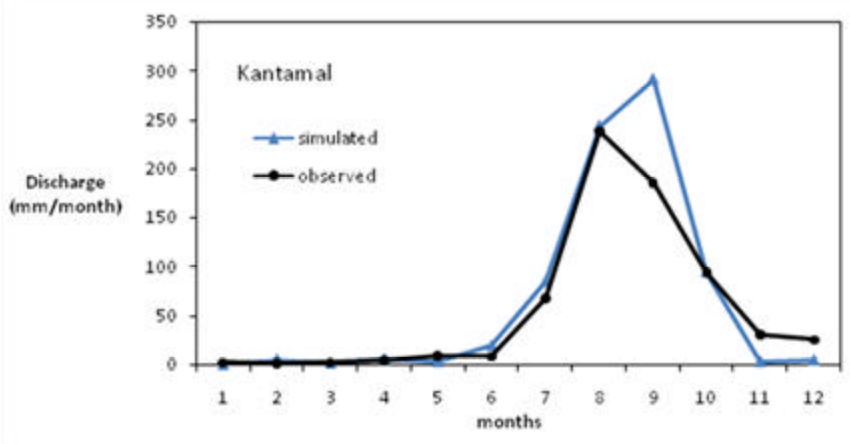

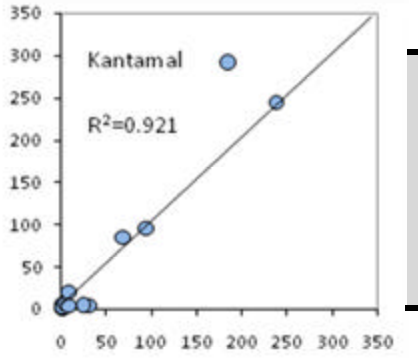

- Co. of determination (R^2) = 0.921
- Nash Sutcliff coefficient = 0.8121
- Relative error (fraction) = -0.1317

Fig.6.13 Simulated and observed monthly hydrographs at various outlets in the basin (contd..)

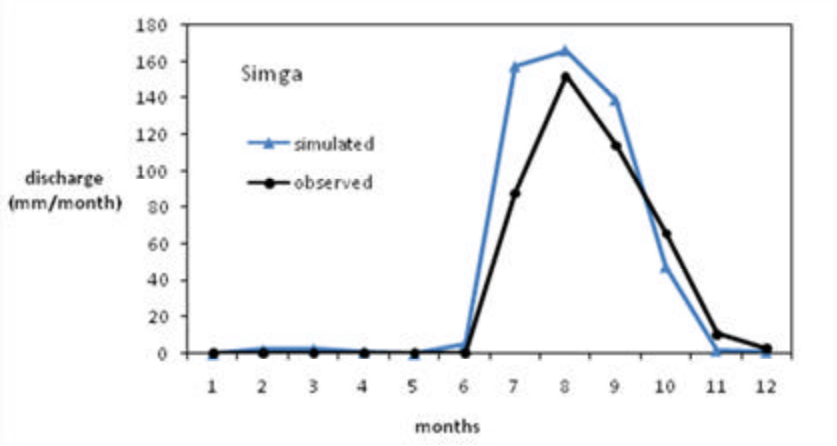

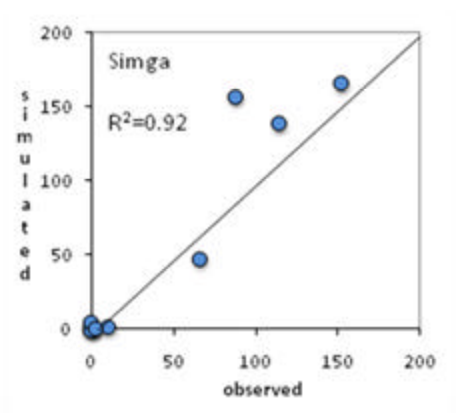

- Co. of determination (R^2) = 0.920
- Nash Sutcliff coefficient = 0.8145
- Relative error (fraction) = -0.2068

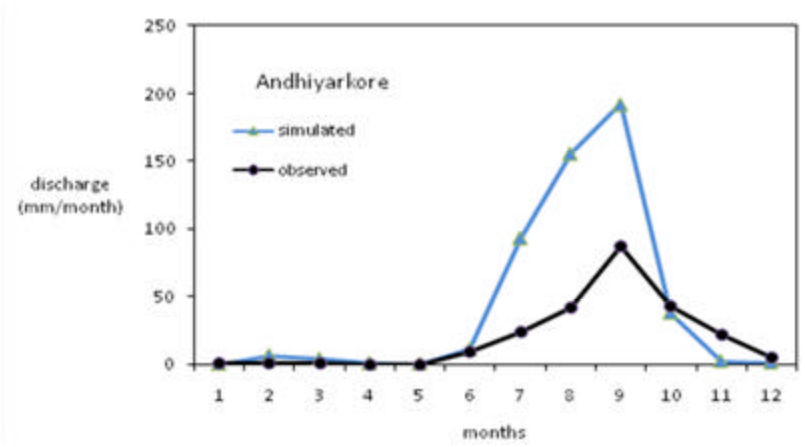

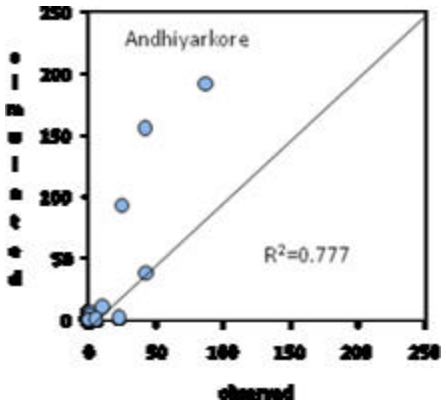

- Co. of determination (R^2) = 0.777
- Nash Sutcliff coefficient = -2.84
- Relative error (fraction) = 1.152

Fig.6.13 Simulated and observed monthly hydrographs at various outlets in the basin (contd..)

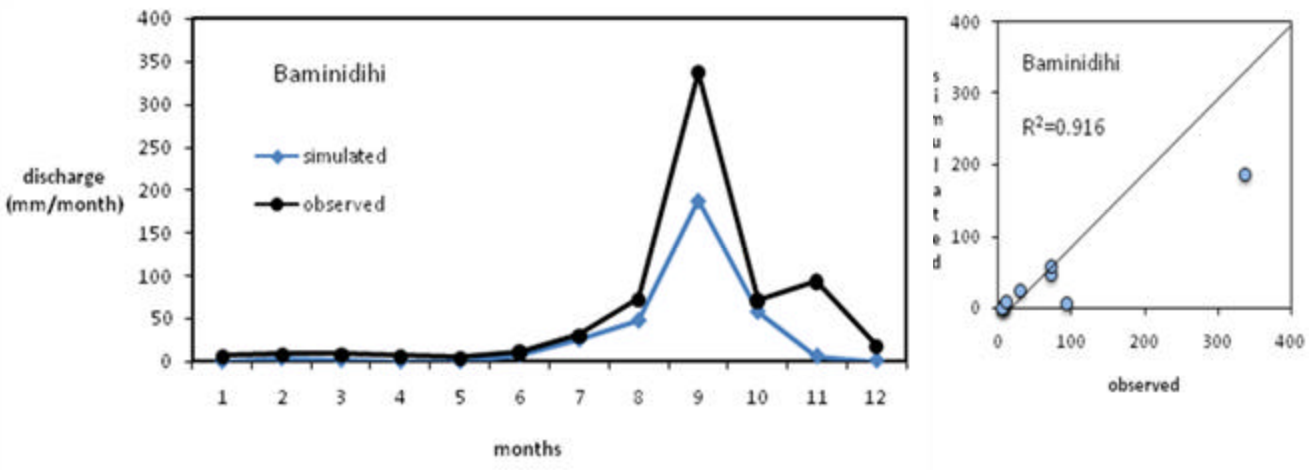

- Co. of determination (R^2) = 0.916
- Nash Sutcliff coefficient = 0.68
- Relative error (fraction) = -0.489

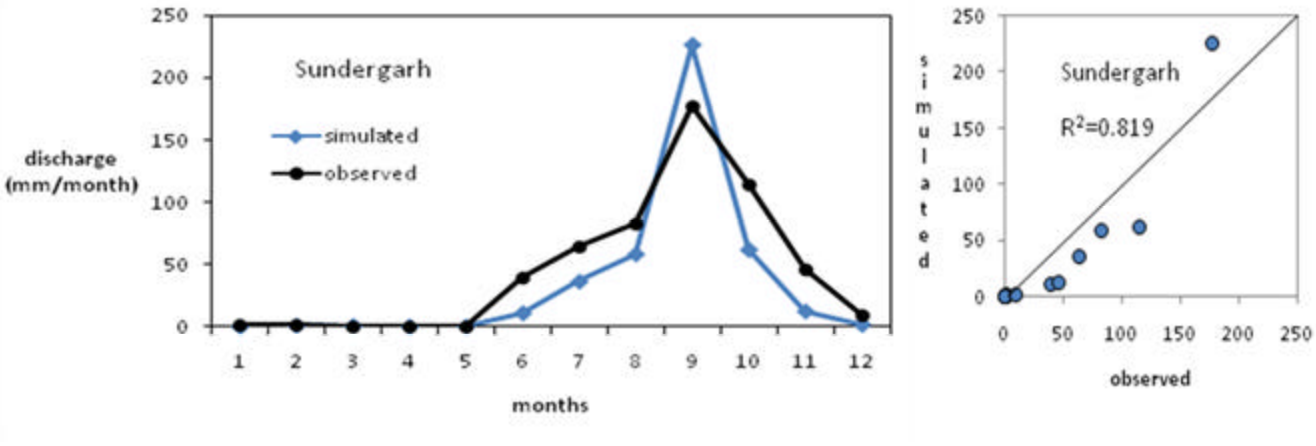

- Co. of determination (R^2) = 0.819
- Nash Sutcliff coefficient = 0.7558
- Relative error (fraction) = -0.2434

Fig.6.13 Simulated and observed monthly hydrographs at various outlets in the basin

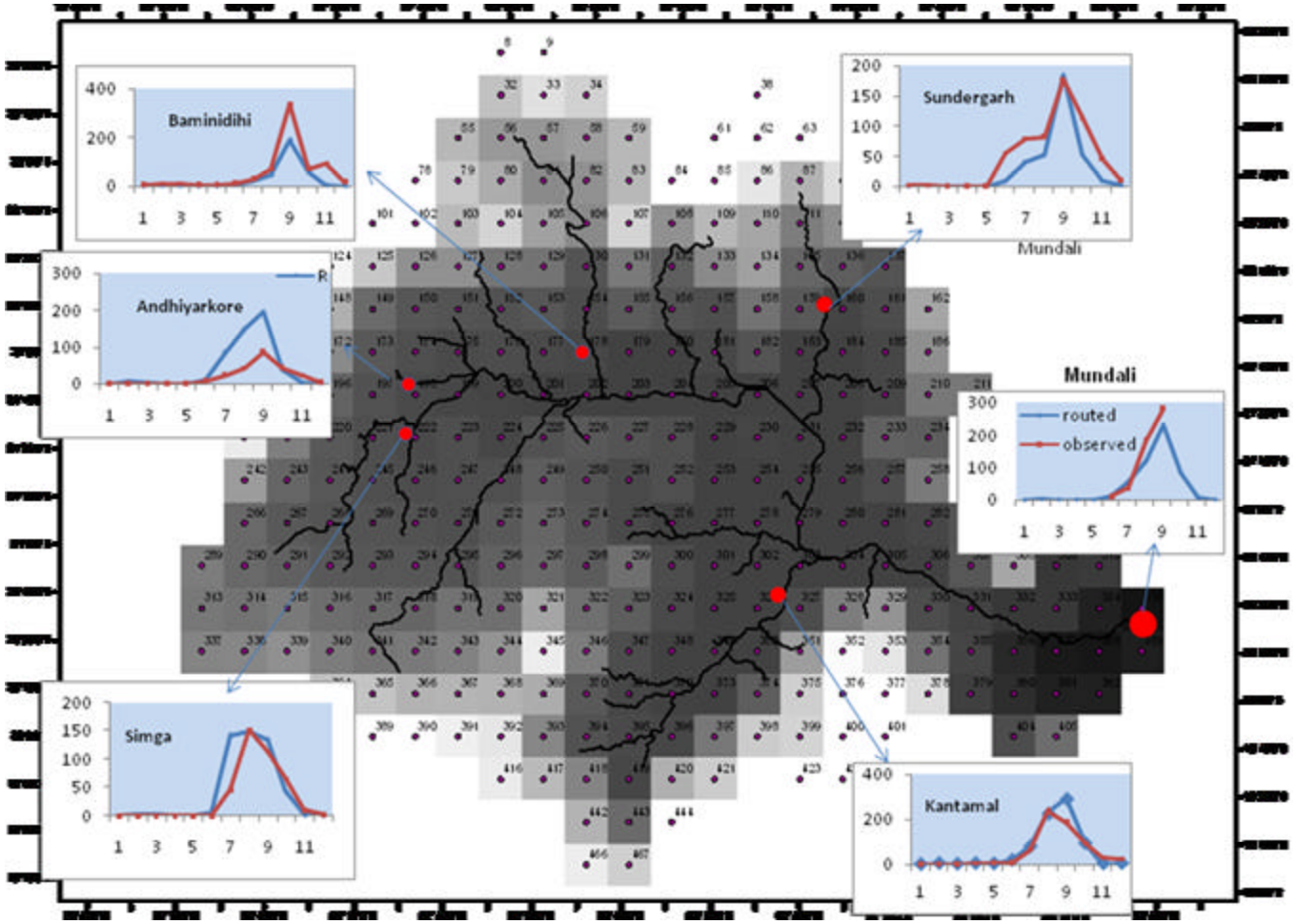

Fig 6.14 Monthly hydrographs at various outlets in the basin

6.3 Effect of landcover changes on streamflows

6.3.1 **Historical and current hydrological simulation using VIC model:**

Simulation was done for year 1972 and 1985 after calibration and validation of the VIC model for 2003. Only the vegetation cover and related parameters were changed in the simulations; the model meteorological forcings and soil parameters were kept same for both the current and historical scenarios. In this way, the effects of vegetation change on basin hydrology were isolated from the effects of climate variability.

6.3.2 **Trend of changes in streamflows:**

Streamflows for year 1972, 1985 and 2003 were compared to look for the changes that have taken place due to change in landcover in the Mahanadi river basin. Monthly discharges were found to be varying significantly as compared to daily flows. Fig 6.15 shows a scatter plot of monthly flows (mm) for 2003 and 1972, events above the slope line indicates an increase in river flow. A rise of 24.44 mm in the annual discharge is predicted at Mundali outlet of the Mahanadi basin from 1972 to 2003 (16.97 mm being in the period of 1972-85 and 7.47 mm in 1985-03) which is 4.53% of the flow in 1972. It may be concluded that a decrease in forest cover by 5.71% in the Mahanadi river basin has caused the river flow to increase by 4.53%. This is quite a significant amount in terms of volumetric rise (3514242122 m^3).

A rise of 32.14 mm was observed for the Kantamal sub-basin where a significant forest cover was lost for cultivation. The total forest cover in the Kantamal sub-basin was decreased to 39.23% in 2003 from 46.96% in 1972 (i.e. forest area was reduced by 7.73%). Simga and Sundergarh saw a rise in annual streamflow of 7.801 mm and 13.697 mm respectively. The forest cover in Simga sub-basin was reduced by 3.39% whereas in Sundergarh sub-basin it was 14.91% which is quite significant. Annual streamflow was increased by 10 mm at Baminidihi sub-basin owing to the reduction in forest cover by 5.92%. However, simulation was found to be poor for Andhiyarkore sub-basin. Table 6.9 summarizes the predicted incremental changes in runoff (mm) for each of the sub-basin by season (e.g. JFM refers to cumulative rise for January, February and March). In figure 6.16, monthly hydrographs for 1972 and 2003 are presented to see the changes that have taken place. A plot of relative percentage difference in runoff (from 1972 to 2003) over 1972 is also shown in the same figure. The rise in percent runoff was prominent during May, June, Oct and November months. The decrease in runoff from 1972 to 2003 may be due to reverse trend in landcover conversions and/or human activities.

In summary, a decrease in natural cover of forest over time has caused a significant rise in streamflows and particularly surface runoff. Removal of forest cover is known to increase streamflow as a result of reduced evapotranspiration. Base-flow is expected to decrease while surface runoff increases owing to the decrease in infiltration and hence groundwater recharge processes. Urban expansion and intensive cultivation will loosen the soil leading to soil loss (soil erosion) due to high flows. Urbanization also tends to decrease infiltration rates and increase extents of impervious surfaces, although the area over which such changes has occurred is a small fraction of the total basin area. The Variable Infiltration Capacity model, being physically based, distributed, macroscale model is particularly suitable for studying climate and landcover change scenarios and their implications on hydrological processes at regional and global scale over long time frames.

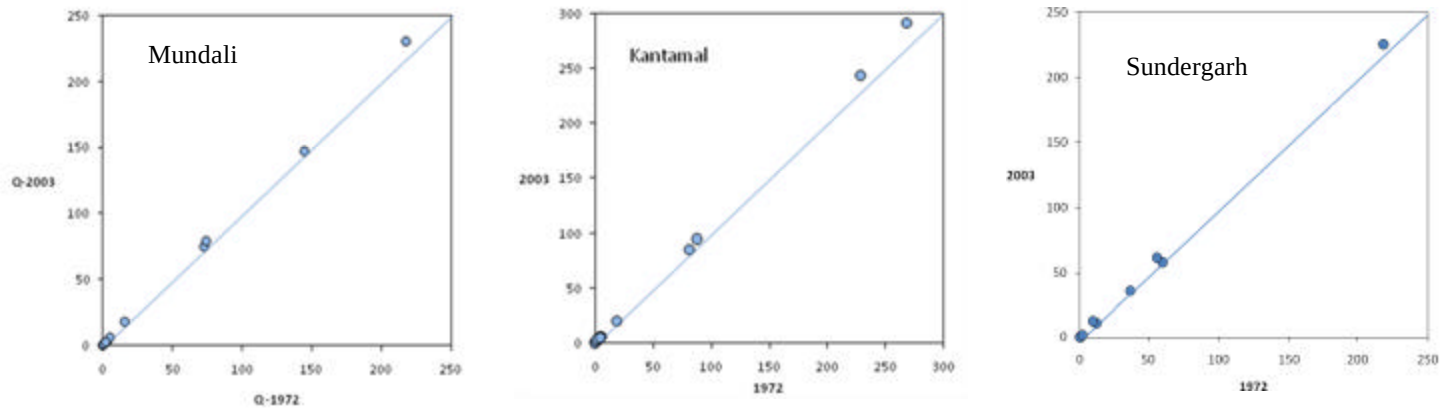

Fig.6.15 Comparison of streamflows for 1972-2003 at Mundali, Kantamal and Sundergarh

Stations	JFM	AMJ	JAS	OND	Annual	% increase	Vol. Increase (m^3)
Mundali	0.027	1.798	16.973	5.643	24.441	4.53	3514242122
Kantamal	0.137	1.901	22.348	7.757	32.144	4.54	699095928.3
Simga	0.177	0.474	3.35	3.8	7.801	1.51	139994254.8
Andhiyarkore	0.4	-1.42	-6.2	2.81	-4.42	-0.86	-8171253.325
Baminidih	0.03	0.72	3.54	5.79	10.07	3.06	111131057.3
Sundergarh	0.01	-0.78	5.35	9.12	13.7	3.47	88196780.89

Table 6.9 Changes in runoff by sub-basin and season (in mm)

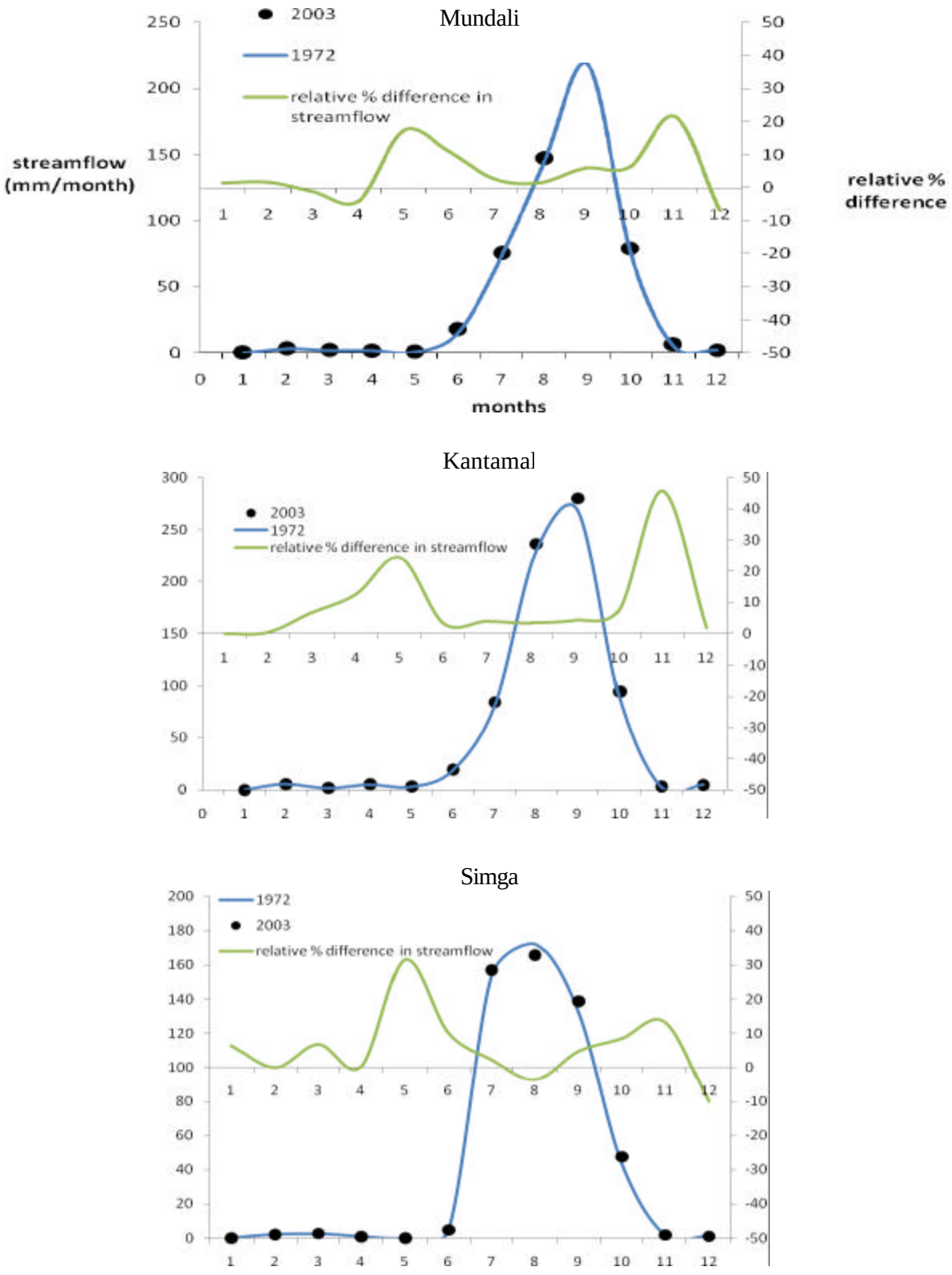

Fig 6.16 Monthly hydrographs of historic (1972) and current (2003) naturalized Streamflow for 3 stations, and relative percentage difference of runoff (contd..)

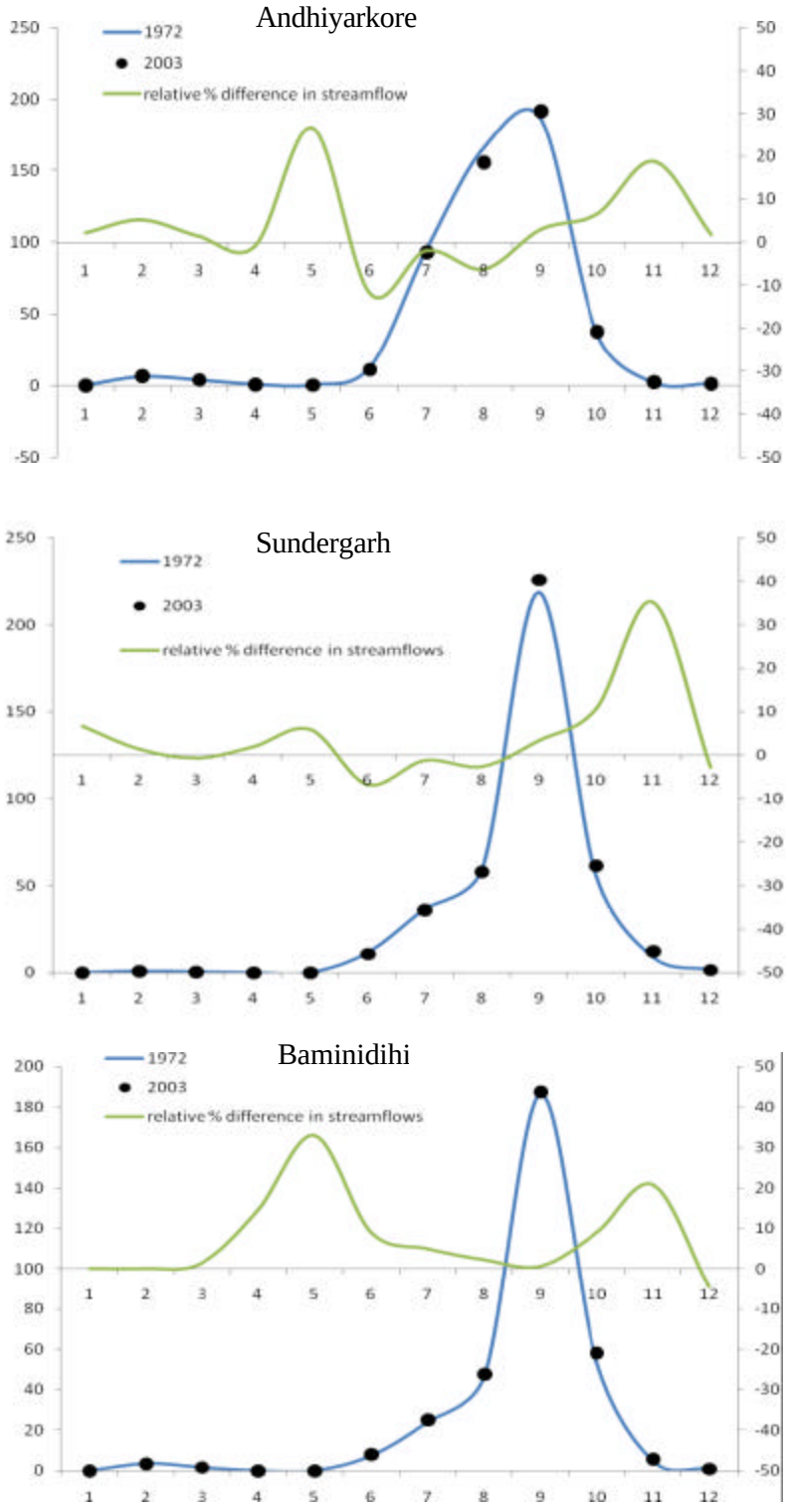

ig 6.16 Monthly hydrographs of historic (1972) and current (2003) naturalized Streamflow for 3 stations, and relative percentage difference of runoff

CHAPTER 7 – SUMMARY AND CONCLUSIONS

Land use and vegetative cover play an important role in watershed runoff and streamflow discharge patterns over time, including peak flows. Increased human interventions have caused rapid transitions in landcover, adversely affecting the watershed processes and hydrological cycle in the long run. Distributed hydrological modelling offers an efficient solution to evaluate the long term hydrological changes by allowing quantification of changes in streamflow patterns.

The Mahanadi river basin covering major portions of Chattisgarh and Orissa (India) has been repetitively facing the adverse hydro-meteorological conditions such as floods, droughts and cyclones etc. in the recent times. Frequent occurrence of these events indicates a shift in the hydrological response of the basin attributed to landcover changes. This study attempts to model the hydrology of Mahanadi river basin using physically based, distributed Variable Infiltration Capacity hydrological model and assess landcover change impacts on streamflows at various locations along the river.

A detailed remote sensing based landcover mapping of the basin for years 1972, 1985 and 2003 reveals following changes:

1. Total forest cover area has been reduced by 5.71% of the total area of the basin from 1972 to 2003. A reduction in barren land (0.64%) is followed by an increase in areas of surface water bodies (0.47%), built up land (0.22%), river bed (0.11%) and most prominently agriculture (5.55%). This implies that the total forest cover and barren land has reduced at the expense of increase in water body, river bed, agriculture and built up land in a span of 30 years.

2. Taking the internal conversion of various landcover classes into account, an overall trend from 1972 to 2003 was a change from forest and barren land to agriculture, built up and water bodies.

Performance of the Variable infiltration capacity macroscale hydrological model to simulate streamflows during calibration and validation can be summarized as follows:

1. Pre-calibration simulation and comparison of observed and simulated streamflow was done for year 2003. The coefficient of determination before calibration was found to be as 0.747, 0.327, 0.309, 0.428, 0.606, 0.495 for Mundali, Andhiyarkore, Baminidihi, Kantamal, Simga and Sundergarh sub-basins respectively.

2. The calibration of the model at Mundali outlet was performed for year 2003. Streamflow was found sensitive to variables like upper and lower soil layer depth, velocity of flow and vegetation parameters. Coefficient of determination (R^2) of 0.836, Nash-sutcliffe coefficient (Ns) of 0.821 and Relative error (Er) of 0.085 was obtained during daily simulation. The model performance was found better for monthly simulations with Ns of 0.89.

3. Model simulation was found good in Kantamal, Simga and Sundergarh sub-basins with Ns of more than 0.5. The reason being absence of large storage structures in sub-basins since VIC model simulates naturalized flow without any consideration for reservoirs.

Streamflows were simulated using VIC model for the year 1972, 1985 and 2003. Following conclusions can be drawn from the analysis carried for predicting changes over years:

1. An increase by 4.53% (24.44 mm) in the annual streamflow is predicted at Mundali outlet of the Mahanadi basin from 1972 to 2003. It may be concluded that a decrease in forest cover by 5.71% in the Mahanadi river basin has caused the river flow to increase by 4.53%. This is quite a significant amount in terms of volumetric rise (3514242122 m^3).

2. Kantamal sub-basin characterized by dense moist deciduous forest and intensive irrigated agriculture, has seen a rise by 4.54% (32.14 mm) where a significant forest cover in the upstream sub-basin was lost for cultivation. A rise of 3.06% and 3.47% was observed in Baminidihi and Sundergarh sub-basins.

3. The relative percentage increase in streamflow was found high in the months of May and November in all sub-basins. It may be concluded that the impact of landcover changes are most pronounced during low flows and that during high flows, role of landcover becomes comparatively less.

Scope of further improvements:

1. High temporal and spatial resolution of forcing data (precipitation and temperature) could lead to significant improvement in model performance since hydrological components are highly sensitive to the forcing input.

2. The observed data used to calibrate the model in this study is biased because the flow is affected by the storage structures like dams, reservoirs etc. along the river. Since VIC simulates naturalized flows, a regression analysis to remove the reservoir effects should be done to obtain a closer agreement between simulated and observed discharges.

3. Simulation can be performed for a period greater than the actual simulation period for analysis so that the initial hydrological conditions in the basin match with the actual ground conditions.

4. VIC model simulation in full energy balance mode should be attempted to better represent surface and atmospheric water and energy fluxes and fully utilize the potential of a physically based distributed modelling approach.

REFERENCES

Abdulla, F.A. and Lettenmaier, D.P., 1997. Development of regional parameter estimation equations for a macroscale hydrologic model. Journal of Hydrology, 197: 230-257.

Abdulla, F.A., Lettenmaier, D.P., Wood, E.F. and Smith, J.A., 1996. Application of a macroscale hydrologic model to estimate the water balance of the Arkansas-Red river basin. J.Geophys. Res., 101(D3): 7449-7459.

Asrar, G. and Dozier, J., 1994. EOS: Science Strategy for the Earth Observing System, Woodbury: American Institute of Physics.

Bosch, J.M. and Hewlett, J.D., 1982. A review of catchment experiments to determine the effects of vegetation changes on water yield and evapotranspiration. Journal of hydrology, 55: 3-23.

Bosch, J.M. and Hewlett, J.D., 1982. A review of catchment experiments to determine the effect of vegetation changes on water yield and evapotranspiration. J. Hydrology, 55: 3-23.

Bruijnzeel, L.A., 1990. Hydrology of moist forests and the effects of conversion: a state of knowledge review, UNESCO-Int. Inst. For Aerospace Survey and Earth Science, Publication of the Humid Tropics Programme, Free University, Amsterdam. 224.

Canadell, J., Jackson, R.B., Ehleringer, J.B. and Moorey, H.A., 1996. Maximum rooting depth of vegetation types at the global scale. Oecologia, 108(4): 1432-1939.

Cherkauer, K.A. and Lettenmaier, D.P., 1999. Hydrologic effects of frozen soils in the upper Mississippi River basin. J. Geophys. Res., 104(D16): 19,599-19,610.

Chow, V.T., Maidment, D.R. and Mays, L.W., 1988. Applied Hydrology. McGraw-Hill, New York.

Costa, M.H., Botta, A. and Cardille, J., 2004. Effects of large-scale change in land cover on the discharge of the Tocantins River, Amazonia. J. of Hydrolo.

Daniel, W.K. and Arlen, D.F., 1998. Evolution of Clark's unit graph method to spatially distributed runoff. Journal of Hydrologic Engineering, 3(1): 9-19.

Dunne, T. and Leopold, L.B., 1998. Water in Environmental Planning. W. H. Freeman and Company, New York, 687-694 pp.

Engman, E.T., 1996. Remote sensing applications to hydrology: future impact. Hydrological Sciences, 41: 637–647.

Entekhabi D., Asrar G., Betts A., Beven K.J., Bras R.L. and Duffy C.J.,1999 An Agenda for Land Surface Hydrology Research and a Call for the Second International Hydrological Decade. In, pp. 2043-2058. Bulletin of the American Meteorological Society

Fiorentino, M., 1996. Geographical Information Systems in Hydrology. Kluwer Academic Publishers.

Gleick, P., 2002. Environment and Security Water Conflict Chronology Version 2002, The World's Water - The Biennial Report on Freshwater Resources 2002. Island Press., Washington D.C., pp. 194-208.

Gosaim, A.K., Rao, S. and Basuray, D., 2006. Climate change impact assessment on hydrology of Indian river basins. Current Science, 90(3): 346-353.

Hamlet, A.F. and Lettenmaier, D.P., 1999. Columbia River Streamflow Forecasting Based on ENSO and PDO Climate Signals. ASCE J. of Water Res. Planning and Mgmt, 125(6): 333-341.

Hamlet, A.F. and Lettenmaier, D.P., 1999. Effects of Climate Change on Hydrology and Water Resources in the Columbia River Basin. Am. Water Res. Assoc, 35(6): 1597-1623.

Hamlet, A.F. and Lettenmaier, D.P., 2000. Long-Range Climate Forecasting and its Use for Water Management in the Pacific Northwest Region of North America. J. Hydroinformatics, 2(3): 163-182.

Hamlet, A.F., Huppert, D. and Lettenmaier, D.P., 2000. Economic Value of Climate/Streamflow Forecasts for Columbia River Non-Firm Energy Production,. ASCE J. W. Res. Planning and Mngmt.

Hibbert, A.R., 1967. Forest treatment effects on water yield, International Symposium for Hydrology, Pennysylvania, Pergamon: Oxford.

Hou, S., Liang, X., Chen, J. and Gong, P., 2004. An assessment of the VIC-3L hydrological model for the Yangtze River basin based on remote sensing: a case study of the Baohe River basin. Canadian Journal of Remote Sensing, 30(5): 840-853.

Jensen, J. R., 2000: Remote Sensing of the Environment. Prentice Hall Series in Geographic Information Science.

Lettenmaier, D.P., 2001. Present and Future of Modeling Global Environmental Change: Toward Integrated Modeling,. In: T.M. Eds. and H. Kida (Editors), Macroscale Hydrology: Challenges and Opportunities, pp. 111-136.

Leung, L.R., Hamlet, A.F., Lettenmaier, D.P. and A.Kumar, 1999. Simulations of the ENSO Hydroclimate Signals in the Pacific Northwest Columbia River Basin. Bull. Am. Met. Soc., 80(11): 2313-2329.

Liang, X., 1994. A Two-Layer Variable Infiltration Capacity Land Surface Representation for General Circulation Models. Water Resour. Series TR140, Univ. of Washington, Seattle.

Liang, X., Lattenmaier, D.P., Wood, E.F. and Burgess, S.J., 1994. A simple hydrologically based model of land surface, water, and energy flux for general circulation models. Journal of Geophysical Research, 99(D7): 14,415-14,428.

Liang, X., Lettenmaier, D.P. and Wood, E.F., 1996. One-dimensional Statistical Dynamic Representation of Subgrid Spatial Variability of Precipitation in the Two-Layer Variable Infiltration Capacity Model. J. Geophys. Res., 101(D16): 21,403-21,422.

Liang, X., Wood, E.F. and Lettenmaier, D.P., 1996. Surface soil moisture parameterization of the VIC-2L model: Evaluation and modifications. Global and Planetary Change, 13,: 195-206.

Liang, X., Wood, E.F. and Lettenmaier, D.P., 1999. Modeling ground heat flux in land surface parameterization schemes. J. Geophys. Res., 104(D8): 9581-9600.

Liang, X., Wood, E.F., Lohmann, D., Lettenmaier, D.P. and others, 1998. The Project for Intercomparison of Land-surface Parameterization Schemes (PILPS) Phase-2c Red-Arkansas River Basin Experiment: 2. Spatial and Temporal Analysis of Energy Fluxes. J. Global and Planetary Change: 19, 137-159.

Lohmann, D.E., Raschke, Nijssen, B. and Lettenmaier, D.P., 1998. Regional scale hydrology:II. Application of the VIC-2L model to the Weser river, Germany. Hydrological Sciences, 43(1): 143-158.

Maidment, D.R., 1992. Handbook of Hydrology. McGraw-Hill, USA.

Matheussen, B., Kirschbaum, R.L., Goodman, I.A. and O'Donnell, G.M., 2000. Effects of land cover change on streamflow in the interior Columbia River Basin (USA and Canada). Hydrological Processes, 14: 867-885.

Mattheussen, B., Kirschbaum, R.L., Goodman, I.A., O'Donnell, G.M. and D.P.Lettenmaier, 2000. Effects of land cover change on streamflow in the interior Columbia river basin (USA and Canada). Hydrol. Process, 14: 867-885.

Maurer, E.P., O'Donnell, G.M., Lettenmaier, D.P. and Roads, J.O., 2001. Evaluation of the Land Surface Water Budget in NCEP/NCAR and NCEP/DOE Reanalyses using an Off-line Hydrologic Model. J. Geophys. Res., 106(D16): 17,841-17,862.

Maurer, E.P., O'Donnell, G.M., Lettenmaier, D.P. and Roads, J.O., 2001. Evaluation of NCEP/NCAR Reanalysis Water and Energy Budgets using Macroscale Hydrologic Simulations, In: Land Surface Hydrology, Meteorology, and Climate: Observations and Modeling, AGU series in Water Science and Applications. 137-158.

Muszik, I., 1996. Lumped Modeling and GIS in Flood Prediction. Geographical Information Systems in Hydrology. Kluwer Academic Publishers.

Neitsch, S.L., Arnold, J.G., Kiniry, J.R., Srinivasan and Williams, J.R., 2000. Soil and water assessment tool users manual ver: 2000, Grassland, Soil and Water Research Laboratory, Agricultural Research Service and Blackland Research Center, Texas Agricultural Experiment Station, Temple, TX.

Nijssen, B.N., Lettenmaier, D.P., Liang, X., Wetzel, S.W. and Wood, E.F., 1997. Streamflow simulation for continental-scale river basins. Water Resour. Res, 33(4): 711-724.

Nijssen, B.N., O'Donnell, G.M., Lettenmaier, D.P. and Wood, E.F., 2001. Predicting the discharge of global rivers. J. Clim., 14.

Nijssen, B.N., Schnur, R. and Lettenmaier, D.P., 2001. Global retrospective estimation of soil moisture using the VIC land surface model. J. Clim., 14: 1790-1808.

Postel, S., 1999. Pillar of Sand, Can the Irrigation Miracle Last?, Worldwatch Institute: New York.

Rajeevan, M., Bhate, J., Kale, J.D. and Lal, B. High resolution daily gridded rainfall data for the Indian region: Analysis of break and active monsoon spells. India Meteorological Department, New Delhi.

Rao, P.G., 1993. Climatic changes and trends over a major river basin in India. Climate Research, 2: 215-223.

Refsgaard, J.C. and Abbott, M.B., 1996. Distributed Hydrological Modelling.

Reisner, M., 1986. Cadillac Desert, The American West and its Disappearing Water. Viking Penguin Inc.:, New York.

Ritchie, J.C. and Rango, A., 1996. Remote sensing applications to hydrology:introduction. Hydrological Sciences, 41: 429–431.

Sahin, V. and Hall, M.J., 1996. The effects of afforestation and deforestation on water yields. J. Hydrology, 178,: 293-309.

Sandholt I., Anderson J., Dybkjaer G., Nyborg L., Lo M., Rasmussen K., Refsgaard J.C., Jensen K. and Toure A., 2003. Integration of earth observation data in distributed hydrological models: the Senegal River basin. Canadian Journal of Remote Sensing, 29: 701-710.

Sherman, L.K., 1932. Streamflow from rainfall by the unit graph method, Engineering News Record.

Shruthi, B. V., 2006: Modelling Hydrological Regime in Diverse Land-use at Mesoscale, Water Resource Department, Andhra University.

Singh, V.P., 1996. Lumped Modeling and GIS in Flood Prediction. Kluwer Academic Publishers.

Stednick, J.D., 1996. Monitoring the effects of timber harvest on annual water yield. Journal of hydrology, 176: 79-95.

Troch, P.A., Paniconi, C. and McLaughlin, D., 2003. Catchment-scale hydrological modeling and data assimilation. Advances in Water Resources, 26: 131–135.

Twine, T.E., Kucharik, C.J. and Foley, J.A., 2004. Effects of land cover chnage on the energy and water balance of the Mississippi River basin. Journal of Hydrometeorology, 5(4): 640-655.

Vanbrunt, D., 2002. Modelling Streamflow Flow using GIS, North Carolina State University.

Vieux, B., 2001: Distributed Hydrologic Modelling using GIS. Kluwer Academic Publishers

Wang, G. and Eltahir, E.A.B., 2000. Ecosystem Dynamics and the Sahel Drought. GRL, 27: 795-798.

Wood, E.F., Lettenmaier, D., Liang, X., Nijssen, B. and Wetzel., S.W., 1997. Hydrological modeling of continental-scale basins. Annu. Rev. Earth Planet. Sci: 25, 279-300.

Appendix I: Roughness length of different vegetation types (m)

	January	February	March	April	May	June	July	August	September	October	November	December
1. Evergreen Needleleaf Forest	1.11	1.10	1.09	1.08	1.08	1.07	1.07	1.08	1.08	1.09	1.10	1.11
2. Evergreen Broadleaf Forest	2.65	2.65	2.65	2.65	2.65	2.65	2.65	2.65	2.65	2.65	2.65	2.65
3. Deciduous Needleleaf Forest	1.11	1.10	1.09	1.08	1.08	1.07	1.07	1.08	1.08	1.09	1.10	1.11
4. Deciduous Broadleaf Forest	0.52	0.52	0.67	0.91	1.03	1.04	1.04	1.04	1.04	0.92	0.67	0.52
5. Mixed Cover	0.82	0.81	0.88	1.00	1.05	1.06	1.06	1.06	1.06	1.00	0.88	0.82
6. Woodland	0.76	0.76	0.78	0.83	0.85	0.84	0.85	0.85	0.85	0.83	0.79	0.76
7. Wooded Grassland	0.35	0.35	0.37	0.41	0.42	0.42	0.42	0.42	0.43	0.41	0.37	0.35
8. Closed Shrubland	0.06	0.06	0.06	0.05	0.05	0.05	0.05	0.06	0.06	0.06	0.06	0.06
9. Open Shrubland	0.04	0.04	0.04	0.03	0.03	0.03	0.03	0.04	0.04	0.04	0.04	0.04
10. Grassland	0.08	0.08	0.08	0.08	0.08	0.08	0.08	0.08	0.08	0.08	0.08	0.08
11. Cropland	0.08	0.08	0.08	0.08	0.08	0.08	0.08	0.08	0.08	0.08	0.08	0.08
12. Bare Ground	0.01	0.01	0.01	0.01	0.01	0.01	0.01	0.01	0.01	0.01	0.01	0.01
13. Urban and Built-Up	0.19	0.19	0.21	0.23	0.25	0.25	0.25	0.25	0.25	0.24	0.21	0.19

(Source: Land Data Assimilation Scheme (LDAS) data set, http://ldas.gsfc.nasa.gov/LDAS8th/MAPPED.VEG/)

Appendix II: Displacement Height of different vegetation types (m)

	January	February	March	April	May	June	July	August	September	October	November	December
1. Evergreen Needleleaf Forest	13.76	13.80	13.86	13.88	13.90	13.93	13.91	13.89	13.88	13.86	13.80	13.76
2. Evergreen Broadleaf Forest	27.37	27.37	27.37	27.37	27.37	27.37	27.37	27.37	27.37	27.37	27.37	27.37
3. Deciduous Needleleaf Forest	13.76	13.80	13.86	13.88	13.90	13.93	13.91	13.89	13.88	13.86	13.80	13.76
4. Deciduous Broadleaf Forest	13.66	13.66	14.62	15.70	16.33	16.62	16.66	16.60	16.41	15.73	14.62	13.66
5. Mixed Cover	13.71	13.73	14.24	14.79	15.12	15.28	15.29	15.25	15.15	14.80	14.21	13.71
6. Woodland	10.76	10.78	11.02	11.26	11.41	11.50	11.50	11.47	11.42	11.26	10.99	10.76
7. Wooded Grassland	5.00	5.01	5.17	5.35	5.46	5.54	5.56	5.54	5.48	5.36	5.16	5.00
8. Closed Shrubland	0.24	0.24	0.24	0.23	0.24	0.26	0.27	0.30	0.28	0.26	0.25	0.24
9. Open Shrubland	0.28	0.28	0.26	0.24	0.24	0.24	0.24	0.30	0.31	0.30	0.29	0.28
10. Grassland	0.22	0.23	0.23	0.24	0.26	0.30	0.33	0.31	0.27	0.24	0.23	0.23
11. Cropland	0.22	0.23	0.23	0.24	0.26	0.30	0.33	0.31	0.27	0.24	0.23	0.23
12. Bare Ground	0.00	0.00	0.00	0.00	0.00	0.00	0.00	0.00	0.00	0.00	0.00	0.00
13. Urban and Built-Up	2.61	2.62	2.73	2.85	2.93	2.99	3.02	3.01	2.95	2.86	2.73	2.62

(Source: Land Data Assimilation Scheme (LDAS) data set, http://ldas.gsfc.nasa.gov/LDAS8th/MAPPED.VEG/)

Appendix III: Canopy height and Root length of different vegetation types

Vegetation type	Height of canopy (m)	Rooting depth (m)
1. Evergreen Needle leaf Forest	17.00	1
2. Evergreen Broadleaf Forest	35.00	1.25
3. Deciduous Needle leaf Forest	15.50	1
4. Deciduous Broadleaf Forest	20.00	1.25
5. Mixed Cover	19.25	1.125
6. Woodland	14.34	0.997475
7. Wooded Grassland	7.04	0.872075
8. Closed Shrub land	0.60	0.650795
9. Open Shrub land	0.51	0.577705
10. Grassland	0.57	0.75
11. Cropland	0.55	0.75
12. Bare Ground	0.20	0.55
13. Urban and Built-Up	6.02	0.79722

(Source: Land Data Assimilation Scheme (LDAS) data set, http://ldas.gsfc.nasa.gov/LDAS8th/MAPPED.VEG/)

Appendix IV: Example of an output flux file

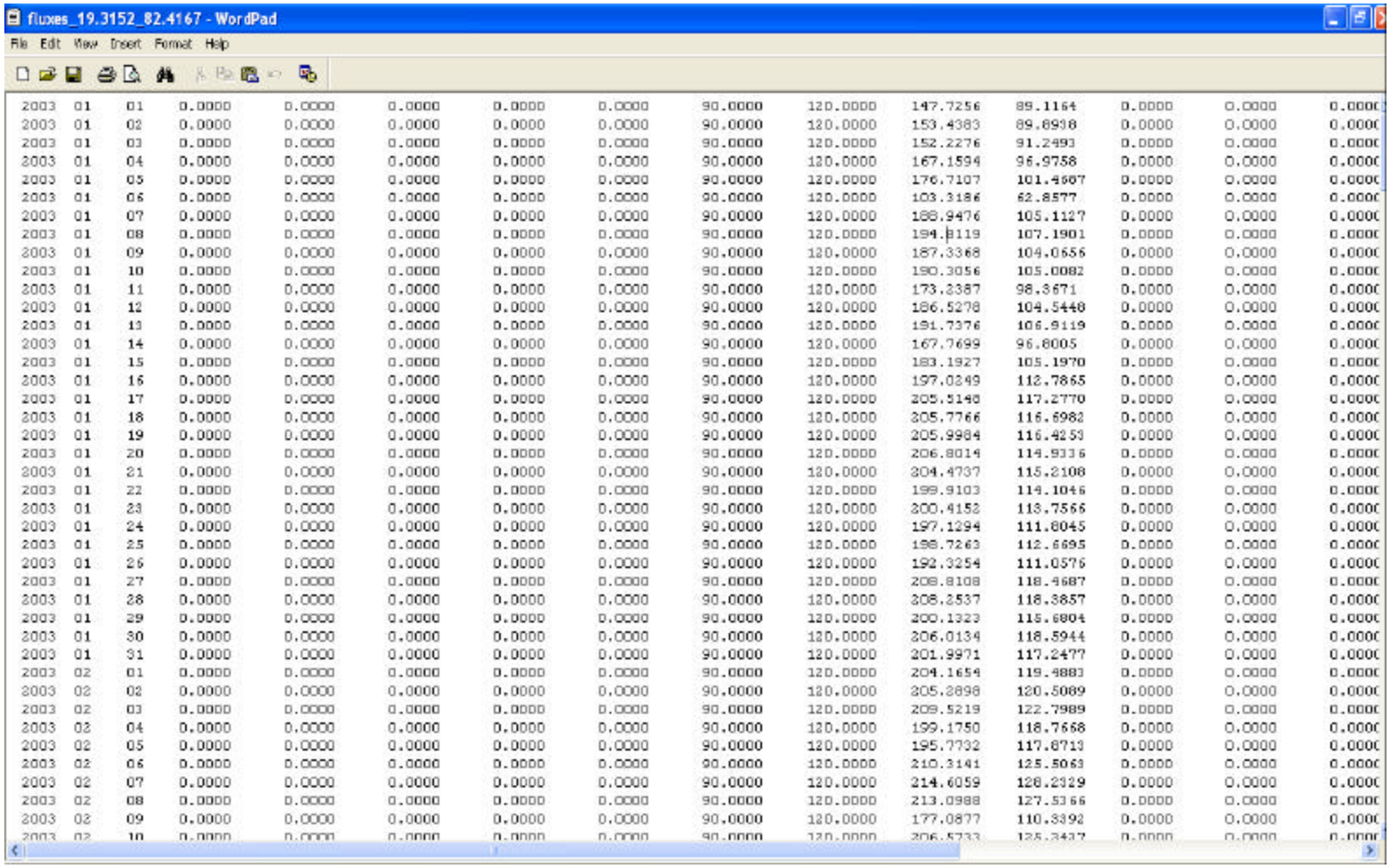

2003	01	01	0.0000	0.0000	0.0000	0.0000	0.0000	90.0000	120.0000	147.7256	89.1164	0.0000	0.0000	0.0000
2003	01	02	0.0000	0.0000	0.0000	0.0000	0.0000	90.0000	120.0000	153.4383	89.8938	0.0000	0.0000	0.0000
2003	01	03	0.0000	0.0000	0.0000	0.0000	0.0000	90.0000	120.0000	152.2276	91.2493	0.0000	0.0000	0.0000
2003	01	04	0.0000	0.0000	0.0000	0.0000	0.0000	90.0000	120.0000	167.1594	96.9758	0.0000	0.0000	0.0000
2003	01	05	0.0000	0.0000	0.0000	0.0000	0.0000	90.0000	120.0000	176.7107	101.4607	0.0000	0.0000	0.0000
2003	01	06	0.0000	0.0000	0.0000	0.0000	0.0000	90.0000	120.0000	103.3186	62.8577	0.0000	0.0000	0.0000
2003	01	07	0.0000	0.0000	0.0000	0.0000	0.0000	90.0000	120.0000	188.9476	105.1127	0.0000	0.0000	0.0000
2003	01	08	0.0000	0.0000	0.0000	0.0000	0.0000	90.0000	120.0000	194.8119	107.1901	0.0000	0.0000	0.0000
2003	01	09	0.0000	0.0000	0.0000	0.0000	0.0000	90.0000	120.0000	187.3368	104.0656	0.0000	0.0000	0.0000
2003	01	10	0.0000	0.0000	0.0000	0.0000	0.0000	90.0000	120.0000	190.3056	105.0082	0.0000	0.0000	0.0000
2003	01	11	0.0000	0.0000	0.0000	0.0000	0.0000	90.0000	120.0000	173.3387	98.3671	0.0000	0.0000	0.0000
2003	01	12	0.0000	0.0000	0.0000	0.0000	0.0000	90.0000	120.0000	186.5278	104.5448	0.0000	0.0000	0.0000
2003	01	13	0.0000	0.0000	0.0000	0.0000	0.0000	90.0000	120.0000	191.7376	106.9119	0.0000	0.0000	0.0000
2003	01	14	0.0000	0.0000	0.0000	0.0000	0.0000	90.0000	120.0000	167.7699	96.8005	0.0000	0.0000	0.0000
2003	01	15	0.0000	0.0000	0.0000	0.0000	0.0000	90.0000	120.0000	183.1927	105.1970	0.0000	0.0000	0.0000
2003	01	16	0.0000	0.0000	0.0000	0.0000	0.0000	90.0000	120.0000	197.0249	112.7865	0.0000	0.0000	0.0000
2003	01	17	0.0000	0.0000	0.0000	0.0000	0.0000	90.0000	120.0000	205.5148	117.2770	0.0000	0.0000	0.0000
2003	01	18	0.0000	0.0000	0.0000	0.0000	0.0000	90.0000	120.0000	205.7766	116.6982	0.0000	0.0000	0.0000
2003	01	19	0.0000	0.0000	0.0000	0.0000	0.0000	90.0000	120.0000	205.9984	116.4253	0.0000	0.0000	0.0000
2003	01	20	0.0000	0.0000	0.0000	0.0000	0.0000	90.0000	120.0000	206.8014	114.9336	0.0000	0.0000	0.0000
2003	01	21	0.0000	0.0000	0.0000	0.0000	0.0000	90.0000	120.0000	204.4737	115.2108	0.0000	0.0000	0.0000
2003	01	22	0.0000	0.0000	0.0000	0.0000	0.0000	90.0000	120.0000	199.9103	114.1046	0.0000	0.0000	0.0000
2003	01	23	0.0000	0.0000	0.0000	0.0000	0.0000	90.0000	120.0000	200.4152	113.7566	0.0000	0.0000	0.0000
2003	01	24	0.0000	0.0000	0.0000	0.0000	0.0000	90.0000	120.0000	197.1294	111.8045	0.0000	0.0000	0.0000
2003	01	25	0.0000	0.0000	0.0000	0.0000	0.0000	90.0000	120.0000	198.7263	112.6695	0.0000	0.0000	0.0000
2003	01	26	0.0000	0.0000	0.0000	0.0000	0.0000	90.0000	120.0000	192.3254	111.0576	0.0000	0.0000	0.0000
2003	01	27	0.0000	0.0000	0.0000	0.0000	0.0000	90.0000	120.0000	208.8108	118.4687	0.0000	0.0000	0.0000
2003	01	28	0.0000	0.0000	0.0000	0.0000	0.0000	90.0000	120.0000	208.2537	118.3857	0.0000	0.0000	0.0000
2003	01	29	0.0000	0.0000	0.0000	0.0000	0.0000	90.0000	120.0000	200.1323	115.6804	0.0000	0.0000	0.0000
2003	01	30	0.0000	0.0000	0.0000	0.0000	0.0000	90.0000	120.0000	206.0134	118.5944	0.0000	0.0000	0.0000
2003	01	31	0.0000	0.0000	0.0000	0.0000	0.0000	90.0000	120.0000	201.9971	117.2477	0.0000	0.0000	0.0000
2003	02	01	0.0000	0.0000	0.0000	0.0000	0.0000	90.0000	120.0000	204.1654	119.4883	0.0000	0.0000	0.0000
2003	02	02	0.0000	0.0000	0.0000	0.0000	0.0000	90.0000	120.0000	205.2898	120.5089	0.0000	0.0000	0.0000
2003	02	03	0.0000	0.0000	0.0000	0.0000	0.0000	90.0000	120.0000	209.5219	122.7989	0.0000	0.0000	0.0000
2003	02	04	0.0000	0.0000	0.0000	0.0000	0.0000	90.0000	120.0000	199.1750	118.7668	0.0000	0.0000	0.0000
2003	02	05	0.0000	0.0000	0.0000	0.0000	0.0000	90.0000	120.0000	195.7732	117.8713	0.0000	0.0000	0.0000
2003	02	06	0.0000	0.0000	0.0000	0.0000	0.0000	90.0000	120.0000	210.3141	125.5063	0.0000	0.0000	0.0000
2003	02	07	0.0000	0.0000	0.0000	0.0000	0.0000	90.0000	120.0000	214.6059	128.2329	0.0000	0.0000	0.0000
2003	02	08	0.0000	0.0000	0.0000	0.0000	0.0000	90.0000	120.0000	213.0988	127.5166	0.0000	0.0000	0.0000
2003	02	09	0.0000	0.0000	0.0000	0.0000	0.0000	90.0000	120.0000	177.0877	110.3392	0.0000	0.0000	0.0000
2003	02	10	0.0000	0.0000	0.0000	0.0000	0.0000	90.0000	120.0000	206.5733	126.3437	0.0000	0.0000	0.0000

Appendix V: Example Forcing file

data_19.3152_82.4167 - Notepad

File Edit Format View Help

0.0	26.25	14.75
0.0	23.92	12.14
0.0	26.53	14.53
0.0	25.75	11.81
0.0	28.42	12.03
0.0	17.64	11.03
0.0	27.53	9.31
0.0	28.14	7.64
0.0	28.03	10.53
0.0	28.53	10.14
0.0	28.42	14.14
0.0	28.42	11.53
0.0	28.53	10.31
0.0	24.92	12.31
0.0	23.75	9.03
0.0	25.64	7.31
0.0	26.31	4.25
0.0	28.03	5.53
0.0	29.31	6.53
0.0	33.53	8.03
0.0	30.64	9.14
0.0	29.75	10.92
0.0	29.92	11.31
0.0	31.31	13.75
0.0	31.53	13.75
0.0	30.75	14.92
0.0	32.14	11.31
0.0	31.92	11.92
0.0	30.53	13.75
0.0	31.31	13.03
0.0	30.92	14.03

Appendix VI: Vegetation parameter file

vegpar - Notepad

File Edit Format View Help

8	3		
2	0.632487	4	1
21	0.127264	1	1
38	0.240249	3.5	1
9	5		
1	0.002370	0.02	1
2	0.401166	4	1
21	0.287485	1	1
38	0.308539	3.5	1
129	0.000440	0.03	1
32	6		
1	0.003975	0.02	1
2	0.071180	4	1
18	0.002635	0.02	1
21	0.569601	1	1
38	0.348215	3.5	1
129	0.004394	0.05	1

Appendix VII: Soil parameter file

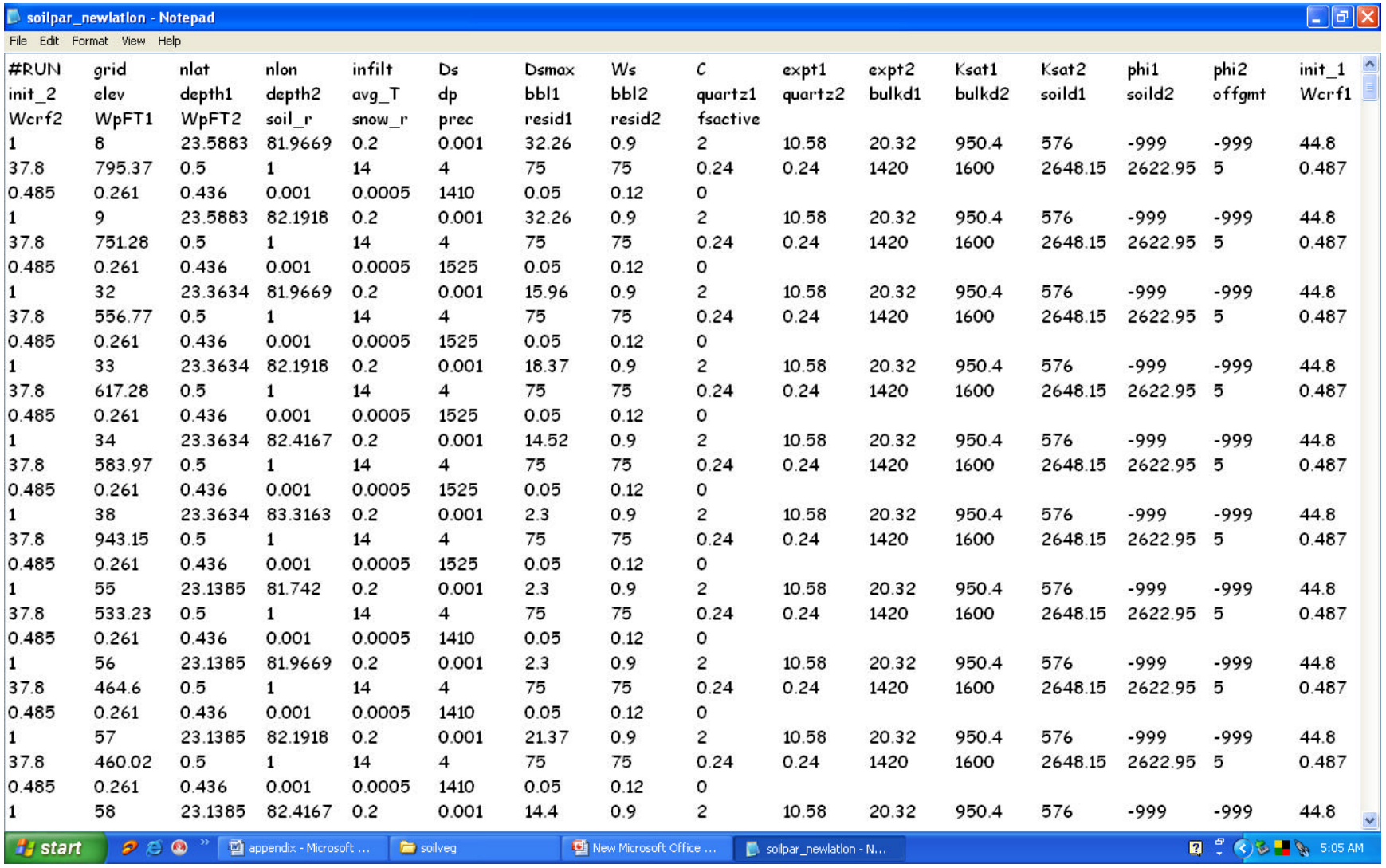

soilpar_newlatlon - Notepad

File Edit Format View Help

#RUN	grid	nlat	nlon	infilt	Ds	Dsmax	Ws	C	expt1	expt2	Ksat1	Ksat2	phi1	phi2	init_1
init_2	elev	depth1	depth2	avg_T	dp	bbl1	bbl2	quartz1	quartz2	bulkd1	bulkd2	soild1	soild2	offgmt	Wcrf1
Wcrf2	WpFT1	WpFT2	soil_r	snow_r	prec	resid1	resid2	fsactive							
1	8	23.5883	81.9669	0.2	0.001	32.26	0.9	2	10.58	20.32	950.4	576	-999	-999	44.8
37.8	795.37	0.5	1	14	4	75	75	0.24	0.24	1420	1600	2648.15	2622.95	5	0.487
0.485	0.261	0.436	0.001	0.0005	1410	0.05	0.12	0							
1	9	23.5883	82.1918	0.2	0.001	32.26	0.9	2	10.58	20.32	950.4	576	-999	-999	44.8
37.8	751.28	0.5	1	14	4	75	75	0.24	0.24	1420	1600	2648.15	2622.95	5	0.487
0.485	0.261	0.436	0.001	0.0005	1525	0.05	0.12	0							
1	32	23.3634	81.9669	0.2	0.001	15.96	0.9	2	10.58	20.32	950.4	576	-999	-999	44.8
37.8	556.77	0.5	1	14	4	75	75	0.24	0.24	1420	1600	2648.15	2622.95	5	0.487
0.485	0.261	0.436	0.001	0.0005	1525	0.05	0.12	0							
1	33	23.3634	82.1918	0.2	0.001	18.37	0.9	2	10.58	20.32	950.4	576	-999	-999	44.8
37.8	617.28	0.5	1	14	4	75	75	0.24	0.24	1420	1600	2648.15	2622.95	5	0.487
0.485	0.261	0.436	0.001	0.0005	1525	0.05	0.12	0							
1	34	23.3634	82.4167	0.2	0.001	14.52	0.9	2	10.58	20.32	950.4	576	-999	-999	44.8
37.8	583.97	0.5	1	14	4	75	75	0.24	0.24	1420	1600	2648.15	2622.95	5	0.487
0.485	0.261	0.436	0.001	0.0005	1525	0.05	0.12	0							
1	38	23.3634	83.3163	0.2	0.001	2.3	0.9	2	10.58	20.32	950.4	576	-999	-999	44.8
37.8	943.15	0.5	1	14	4	75	75	0.24	0.24	1420	1600	2648.15	2622.95	5	0.487
0.485	0.261	0.436	0.001	0.0005	1525	0.05	0.12	0							
1	55	23.1385	81.742	0.2	0.001	2.3	0.9	2	10.58	20.32	950.4	576	-999	-999	44.8
37.8	533.23	0.5	1	14	4	75	75	0.24	0.24	1420	1600	2648.15	2622.95	5	0.487
0.485	0.261	0.436	0.001	0.0005	1410	0.05	0.12	0							
1	56	23.1385	81.9669	0.2	0.001	2.3	0.9	2	10.58	20.32	950.4	576	-999	-999	44.8
37.8	464.6	0.5	1	14	4	75	75	0.24	0.24	1420	1600	2648.15	2622.95	5	0.487
0.485	0.261	0.436	0.001	0.0005	1410	0.05	0.12	0							
1	57	23.1385	82.1918	0.2	0.001	21.37	0.9	2	10.58	20.32	950.4	576	-999	-999	44.8
37.8	460.02	0.5	1	14	4	75	75	0.24	0.24	1420	1600	2648.15	2622.95	5	0.487
0.485	0.261	0.436	0.001	0.0005	1410	0.05	0.12	0							
1	58	23.1385	82.4167	0.2	0.001	14.4	0.9	2	10.58	20.32	950.4	576	-999	-999	44.8

start appendix - Microsoft ... soilveg New Microsoft Office ... soilpar_newlatlon - N... 5:05 AM

Appendix VIII: Vegetation library file

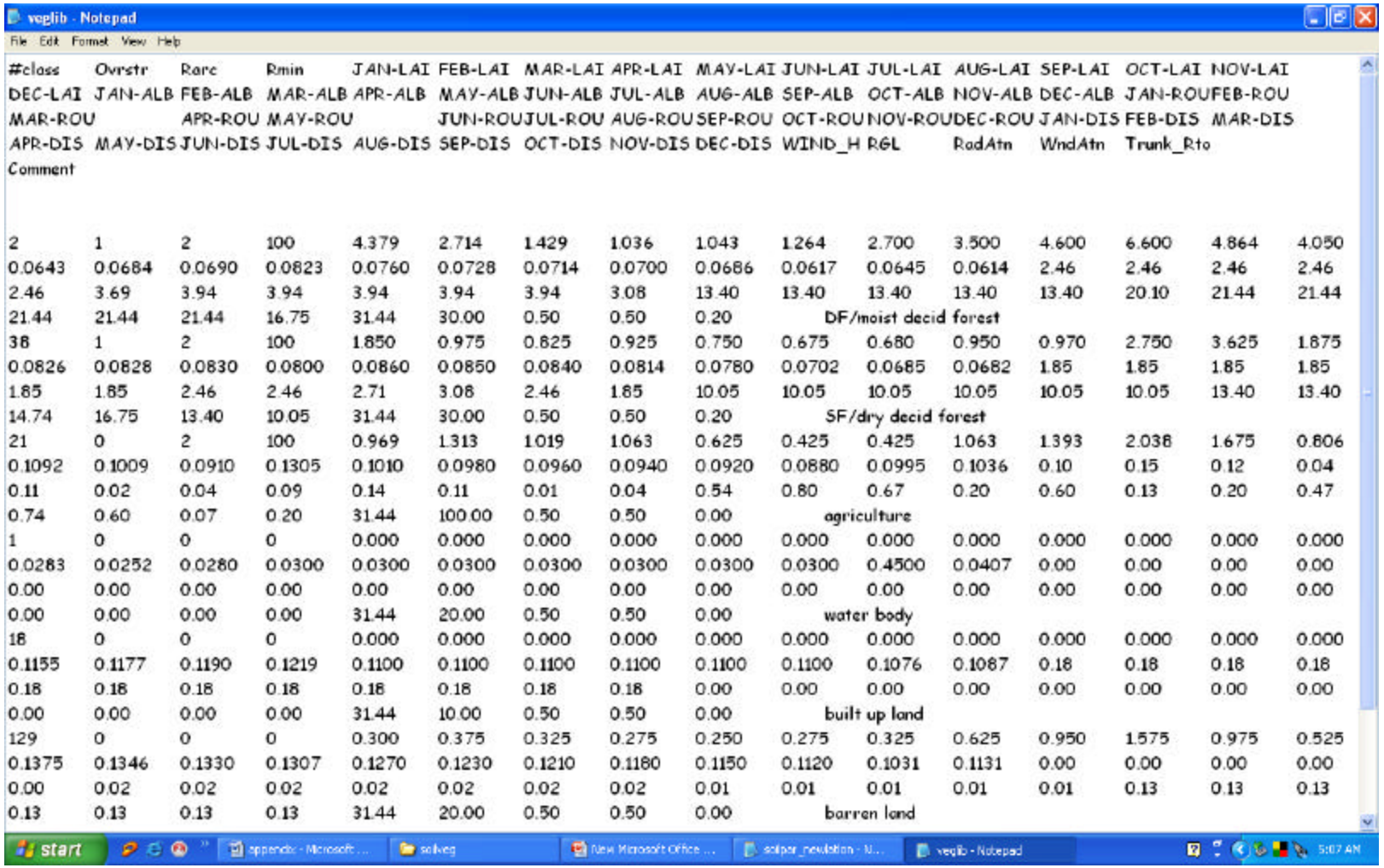

veglib - Notepad

File Edit Format View Help

#class	Ovrstr	Rarc	Rmin	JAN-LAI	FEB-LAI	MAR-LAI	APR-LAI	MAY-LAI	JUN-LAI	JUL-LAI	AUG-LAI	SEP-LAI	OCT-LAI	NOV-LAI	
DEC-LAI	JAN-ALB	FEB-ALB	MAR-ALB	APR-ALB	MAY-ALB	JUN-ALB	JUL-ALB	AUG-ALB	SEP-ALB	OCT-ALB	NOV-ALB	DEC-ALB	JAN-ROU	FEB-ROU	
MAR-ROU		APR-ROU	MAY-ROU		JUN-ROU	JUL-ROU	AUG-ROU	SEP-ROU	OCT-ROU	NOV-ROU	DEC-ROU	JAN-DIS	FEB-DIS	MAR-DIS	
APR-DIS	MAY-DIS	JUN-DIS	JUL-DIS	AUG-DIS	SEP-DIS	OCT-DIS	NOV-DIS	DEC-DIS	WIND_H	RGL	RadAtn	WndAtn	Trunk_Rto		
Comment															
2	1	2	100	4.379	2.714	1.429	1.036	1.043	1.264	2.700	3.500	4.600	6.600	4.864	4.050
0.0643	0.0684	0.0690	0.0823	0.0760	0.0728	0.0714	0.0700	0.0686	0.0617	0.0645	0.0614	2.46	2.46	2.46	2.46
2.46	3.69	3.94	3.94	3.94	3.94	3.94	3.08	13.40	13.40	13.40	13.40	13.40	20.10	21.44	21.44
21.44	21.44	21.44	16.75	31.44	30.00	0.50	0.50	0.20	DF/moist decid forest						
38	1	2	100	1.850	0.975	0.825	0.925	0.750	0.675	0.680	0.950	0.970	2.750	3.625	1.875
0.0826	0.0828	0.0830	0.0800	0.0860	0.0850	0.0840	0.0814	0.0780	0.0702	0.0685	0.0682	1.85	1.85	1.85	1.85
1.85	1.85	2.46	2.46	2.71	3.08	2.46	1.85	10.05	10.05	10.05	10.05	10.05	10.05	13.40	13.40
14.74	16.75	13.40	10.05	31.44	30.00	0.50	0.50	0.20	SF/dry decid forest						
21	0	2	100	0.969	1.313	1.019	1.063	0.625	0.425	0.425	1.063	1.393	2.038	1.675	0.806
0.1092	0.1009	0.0910	0.1305	0.1010	0.0980	0.0960	0.0940	0.0920	0.0880	0.0995	0.1036	0.10	0.15	0.12	0.04
0.11	0.02	0.04	0.09	0.14	0.11	0.01	0.04	0.54	0.80	0.67	0.20	0.60	0.13	0.20	0.47
0.74	0.60	0.07	0.20	31.44	100.00	0.50	0.50	0.00	agriculture						
1	0	0	0	0.000	0.000	0.000	0.000	0.000	0.000	0.000	0.000	0.000	0.000	0.000	0.000
0.0283	0.0252	0.0280	0.0300	0.0300	0.0300	0.0300	0.0300	0.0300	0.0300	0.4500	0.0407	0.00	0.00	0.00	0.00
0.00	0.00	0.00	0.00	0.00	0.00	0.00	0.00	0.00	0.00	0.00	0.00	0.00	0.00	0.00	0.00
0.00	0.00	0.00	0.00	31.44	20.00	0.50	0.50	0.00	water body						
18	0	0	0	0.000	0.000	0.000	0.000	0.000	0.000	0.000	0.000	0.000	0.000	0.000	0.000
0.1155	0.1177	0.1190	0.1219	0.1100	0.1100	0.1100	0.1100	0.1100	0.1100	0.1076	0.1087	0.18	0.18	0.18	0.18
0.18	0.18	0.18	0.18	0.18	0.18	0.18	0.18	0.00	0.00	0.00	0.00	0.00	0.00	0.00	0.00
0.00	0.00	0.00	0.00	31.44	10.00	0.50	0.50	0.00	built up land						
129	0	0	0	0.300	0.375	0.325	0.275	0.250	0.275	0.325	0.625	0.950	1.575	0.975	0.525
0.1375	0.1346	0.1330	0.1307	0.1270	0.1230	0.1210	0.1180	0.1150	0.1120	0.1031	0.1131	0.00	0.00	0.00	0.00
0.00	0.02	0.02	0.02	0.02	0.02	0.02	0.02	0.01	0.01	0.01	0.01	0.01	0.13	0.13	0.13
0.13	0.13	0.13	0.13	31.44	20.00	0.50	0.50	0.00	barren land						

start appendix - Microsoft ... solveg New Microsoft Office ... soilpar_revolution - N... veglib - Notepad 5:07 AM

Appendix IX: Routing output (monthly and daily streamflows at Simga station) in mm.